

Crown Architecture, Wood Stiffness and the Pipe Model Theory for White Spruce [*Picea glauca* (Moench) Voss] and Aspen (*Populus tremuloides* Michx.)

by

Derek Felix Sattler

A thesis submitted in partial fulfillment of the requirements for the degree of

Doctor of Philosophy

in

Forest Biology & Management

Department of Renewable Resources
University of Alberta

© Derek Felix Sattler, 2015

Abstract

In forestry, the wood fibre supply chain describes the integration of harvesting operations, raw material transformation and end-product marketing. The forest industry may achieve an overall greater return on investment by developing a supply chain which incorporates measures of wood quality. The main goal of this thesis was to develop components of a decision support tool that may be used by forest managers to achieved wood quality based objectives for white spruce [*Picea glauca* (Moench)] and aspen (*Populus tremuloides* Michx.). The first component presented in this thesis is a model for the prediction of pith to bark wood stiffness. For both spruce and aspen, wood stiffness was found to develop in closer association with cambial age than tree size. The results carry implications concerning the role of the stem and the adaptation to mechanical and hydraulic demands. Based on variables included in the models, silvicultural activities that alter slenderness and radial growth rate in spruce are likely to have the greatest impact on wood stiffness. Conversely, there appears to be little opportunity for silvicultural activities to influence wood stiffness in aspen. The second component presented in this thesis is a set of models for the prediction of the number of branches, branch diameter and branch angle per unit crown length for spruce. Relative or absolute depth into the crown were significant variables in all the models, reflecting the influence of varying light transmittance on crown architecture. While tree-level variables such as crown length and tree slenderness featured in all the branch models, no indices of stand-level species composition or competition were found to directly influence the branch characteristics, other than tree social position. Overall, the models suggest that crown architecture is predominantly influenced by “neighbourhood” conditions. An

additional set of branch models were developed to identify the tree-level characteristics which influence the recovery of first grade select lumber from harvested trees. The practical application of these models may be achieved by integrating them into Crobas, a process-based tree growth simulator which uses principles related to functional balance and the pipe model theory. Tests concerning key assumptions of Crobas indicated that (i) there is indeed a constant allometric relationship between foliage mass and crown length for both spruce and aspen, and (ii) the constant ratio of foliage mass to sapwood area at crown base held reasonably well for spruce. The results, however, were less encouraging for aspen. Further efforts to validate Crobas are, therefore, recommended for white spruce. For aspen, modifications to the pipe model relationship should be sought before further validation exercises are performed. Since all components of this study examined data from unmanaged stands, the results provide a baseline reference point upon which to compare measurements from managed stands.

Preface

This thesis is my original work. I was responsible for the sampling design and either completed or oversaw the collection of all measurements used in this thesis. I completed all the analyses and authored all the written text presented in this thesis. The contributions I received from my supervisor (Dr. Philip G Comeau) were in the form of comments and edits to drafts of chapters 2, 3 and 4 of this thesis. Comments and edits to drafts of chapters 2 and 3 were also provided by Dr. Alexis Achim. The final structure of the chapters 2, 3 and 4 were also shaped by the comments from anonymous reviewers received during the peer-review process when the articles were submitted to scientific journals for publication.

A version of chapter 2 has been published as: Sattler, D.F., Comeau, P. G., and Achim, A. 2014. Within-tree patterns of wood stiffness for white spruce (*Picea glauca*) and trembling aspen (*Populus tremuloides*). *Canadian Journal of Forest Research* **44**: 162–171. [dx.doi.org/10.1139/cjfr-2013-0150](https://doi.org/10.1139/cjfr-2013-0150)

A version of chapter 3 has been published as: Sattler, D.F., Comeau, P. G., and Achim, A. 2014. Branch models for white spruce (*Picea glauca* (Moench) Voss) in naturally regenerated stands. *Forest Ecology and Management* **325**: 74–89. doi:10.1016/j.foreco.2014.03.051

A version of chapter 4 has been accepted for publication: Sattler, D.F., and Comeau, P.G. (*In press*). Crown allometry and application of the *Pipe Model Theory* to white spruce (*Picea glauca* (Moench) Voss) and aspen (*Populus tremuloides* Michx.). *Canadian Journal of Forest Research*.

Data collected for this thesis (presented in chapters 2 and 3) and text describing the sampling methods were used in following publication of which I am a co-author: Power, H., LeMay, V., Berninger, F., Sattler, D. and Kneeshaw, D. 2012. Differences in crown characteristics between black (*Picea mariana*) and white spruce (*Picea glauca*). *Canadian Journal of Forest Research* **42**: 1733-1743. 10.1139/x2012-106

Acknowledgements

I would like to thank my supervisor, Dr. Philip G. Comeau as well as my co-supervisor Dr. Alexis Achim. Thank you for your suggestions, comments, support and patience. I am also grateful for the advice provided by the members of my thesis committee. The work presented in this paper was completed while I was a member of the Forest Value Network / Projet Forêt Valeur, which was formed through a strategic network grant from Natural Sciences and Engineering Research Council of Canada (NSERC). I wish to gratefully acknowledge the NSERC and those responsible for the original network proposal submitted to NSERC. The exchange of ideas with others in this network was instrumental in how this thesis evolved into its present form. I wish to offer an enormous “thanks!” to the numerous field and lab assistants who contributed to the collection of data used in the analyses. I wish to thank the staff at Centre de recherche sur les matériaux renouvelables at Université Laval, Québec, where a significant portion of the work within this thesis was completed. En fin. Rut, on l’a réussi. Quelle expérience. J’ai tellement hâte à vivre tous les défis qui viendront. Es mi Guapa!

Table of Contents

Abstract.....	i
Preface.....	iv
Acknowledgements	vi
Table of Contents	vii
List of Tables	xii
List of Figures.....	xvi
Chapter 1: Introduction	1
1.1 Why this study was completed	1
1.2 Thesis objectives.....	6
1.3 White spruce, aspen and the importance of a baseline	7
1.4 Wood stiffness and its components.....	11
1.5 Wood stiffness and tree function	13
1.6 Branching characteristics and wood quality	15
1.7 Crobas and the pipe model theory	17
References	20
Chapter 2: Within-tree patterns of wood stiffness for white spruce (<i>Picea glauca</i> [Moench] Voss) and trembling aspen (<i>Populus tremuloides</i> Michx.).....	29

2.1	Introduction.....	29
2.2	Material and methods.....	32
2.2.1	Site description and sample preparation	32
2.2.2	Covariates for analyses	37
2.2.3	Model screening.....	39
2.2.4	Cambial age or tree size?	40
2.2.5	Models for pith to bark wood stiffness	42
2.3	Results.....	43
2.3.1	Cambial age or tree size?	43
2.3.2	Final mixed effect models.....	44
2.4	Discussion.....	50
2.4.1	Cambial age or tree size?	50
2.4.2	Final models for pith to bark wood stiffness	52
2.5	Conclusions.....	55
	References.....	56
	Chapter 3: Branch models for white spruce (<i>Picea glauca</i> (Moench) Voss) in naturally regenerated stands	62
3.1	Introduction.....	62
3.2	Material and methods.....	66

3.2.1	Site description and measurements.....	66
3.2.2	Model building.....	69
3.3	Results.....	74
3.3.1	Number of branches per stem section.....	74
3.3.2	Diameter of the largest branch per stem section.....	81
3.3.3	Diameter of branches smaller than the largest.....	85
3.3.4	Branch angle	88
3.4	Discussion.....	93
3.4.1	Number of branches per section	93
3.4.2	Diameter of the largest branch per section	96
3.4.3	Branch diameter other than the largest branch	97
3.4.4	Branch angle	97
3.4.5	Model applications and conclusions	98
	References.....	101
	Chapter 4: Crown allometry and application of the <i>Pipe Model Theory</i> to white spruce (<i>Picea glauca</i> (Moench) Voss) and aspen (<i>Populus tremuloides</i> Michx.).....	107
4.1	Introduction.....	107
4.2	Material and methods.....	110
4.2.1	Site description.....	110

4.2.2	Field and laboratory measurements	111
4.2.3	Scaling up from branch to tree.....	112
4.2.4	Whole crown allometry.....	114
4.2.5	Within-crown allometry.....	114
4.2.6	Whole-crown foliage mass from pipe model theory.....	115
4.2.7	Within-crown foliage mass from pipe model theory	116
4.3	Results.....	117
4.3.1	Foliage mass and crown length: whole crown allometry.....	117
4.3.2	Foliage mass and crown length: within-crown allometry.....	119
4.3.3	Pipe model ratio: whole-crown allometry.....	123
4.3.4	Pipe model ratio: within-crown allometry	125
4.4	Discussion.....	129
4.4.1	Foliage mass – crown length allometry	129
4.4.2	Within-crown scaling between foliage mass and crown length.....	132
4.4.3	Whole crown foliage mass from pipe model theory	133
4.4.4	Within-crown foliage mass from pipe model theory	135
4.5	Conclusions.....	138
References		139

Chapter 5: Conclusion and recommendations	145
Bibliography	151

List of Tables

Table 1 Estimated stand basal area ($\text{m}^2 \cdot \text{ha}^{-1}$) and number of trees per hectare (no. of trees $\cdot \text{ha}^{-1}$) calculated from fixed radius plots established around sample trees, with the corresponding proportions of white spruce (sw) and trembling aspen (aw).....	33
Table 2 Mean values for cambial age at breast height, diameter at breast height (DBH; cm) and height (HT; m) of trees sampled for wood stiffness (minimum and maximum values in parentheses).....	35
Table 3 Total number of logs and small clear samples collected from each log section.....	36
Table 4 List of covariates used in the analyses and associated descriptions.	39
Table 5 Estimated fixed-effects (standard deviation in parentheses) and associated random effects (with 95% confidence intervals) from Equations 3 and 4. <i>P</i> -values for fixed effects are generated from Wald-type tests.	46
Table 6 Summary statistics for diameter at breast height (DBH), crown length (Cl), height to live crown (Htlcrn), and slenderness (Slc). Values are averages for the plot. Minimum and maximum values are in braces { }.	68
Table 7 Summary statistics for branch diameter, maximum branch diameter (mm), number of branches ($\geq 5\text{mm}$) per 1m section and branch angle for branches	

≥ 5 mm diameter. Values are averages for the plot. Values in braces {} represent the minimum and maximum.....69

Table 8 Description of tree and stand-level variables tested in the branch models. Natural log transformations of the variables were also tested and are denoted in the text with the prefix ‘ln’.....71

Table 9 Estimated fixed effect parameters with standard errors and significance tests (p-value) for z-values for Equation 9 (No. branches ≥ 5 mm; *NBrTot*). Standard deviations of the random intercept for the plot and tree-level and estimated overdispersion parameter are listed with the error statistics from the fixed effects component (RMSE = root mean square error).76

Table 10 Estimated fixed effect parameters with standard errors and significance tests (p-value) for z-values for Equation 10 (No. branches ≥ 12.5 mm; *NoBrNoIGrd*). Standard deviations of the random intercept for the plot and tree-level and estimated overdispersion parameter are listed with the error statistics from the fixed effects component (RMSE = root mean square error).....79

Table 11 Estimated fixed effect parameters with standard errors for Equation 11 (*MaxBrD*), standard deviations of the random effects (Plot, Tree and Residuals) and error statistics from the fixed effects component (RMSE = root mean square error).83

Table 12 Estimated fixed effect parameters with standard errors and significance tests (p-value) for z-values for Equation 12 (*RelBrD*). Standard deviations of the random

intercept for the plot, tree, and section-level are listed with the error statistics from the fixed effects component (RMSE = root mean square error).....	86
Table 13 Estimated fixed effect parameters with standard errors for Equation 13 (<i>BrAngTot</i>). Standard deviations of the random components (Plot, Tree, Section and Residuals) are listed with the error statistics for the fixed effects component (RMSE = root mean square error)	90
Table 14 Estimated fixed effect parameters with standard errors for Equation 14 (<i>BrAngNoIGrd</i>). Standard deviations of the random components (Plot, Tree, Section and Residuals) are listed with the error statistics for the fixed effects component (RMSE = root mean square error).	91
Table 15 Means (with standard deviation in parentheses) by diameter class (Diam class) of tree-level variables for the sampled spruce and aspen trees.....	112
Table 16 Symbols and associated description of variables used for the analyses.	113
Table 17 Estimated parameters (standard error, SE, in parentheses) and fit statistics from the constant and variable allometric models (CAR and VAR; Equation 16 and 17 in text) fitted to spruce and aspen data. For each species, the CAR and VAR models were fitted as a function of crown length (Cl; m).	118
Table 18 Parameter estimates (standard error, SE, in parentheses) for Equation 18, describing the relationship between within-crown Wf_k and Cl_k (k =crown quarter section 1, 2, 3, 4) for spruce and aspen.....	120

Table 19 Results of equivalence tests on prediction of W_f from the fitted pipe model (Equation 19) and from published DBH and Height-based equations [Spruce = Manning (1984); Aspen = Alemdag (1984)]. Equivalence tests of predictions from the fitted pipe model are for the full dataset (all DBH classes) and by individual DBH classes (diam class 1 to 5 for spruce and diam class 1 to 4 for aspen).....125

Table 20 Estimated parameters (with standard errors, SE, in parentheses) for the relationship of the within-crown pipe model ratio (R_{p_k} = foliage mass/sapwood area at crown quarter section k) as a function of distance from stump (H_k) and as a function of relative depth from crown apex (R_{dinc}) (see Equation 21).127

List of Figures

- Figure 1 Approximate location of sample plots. All plots were within the Central Mixedwood Natural Subregion, which lies within the Boreal Forest Natural Region of Alberta, Canada. The Dry Mixedwood Natural Subregion is also indicated as mixed stands of aspen-white spruce are common within this area.....10
- Figure 2 Pith to bark trends (solid lines) of MOE plotted against ring number from pith for white spruce. Trends are plotted by log section (CB = crown base, DBH = 1.3m, MB = mid-point between DBH and crown base, MC = mid crown). Circles represent observed values.....38
- Figure 3 Pith to bark trends (solid lines) of MOE plotted against ring number from pith for aspen. Trends are plotted by log section (CB = crown base, DBH = 1.3m, MB = mid-point between DBH and crown base, MC = mid crown). Circles represent observed values.38
- Figure 4 Relationship between the estimated random effect (empirical best linear unbiased predictor = EBLUP) for the rate parameter in Equation. 2 and the mean juvenile ring width for white spruce and aspen. Relationships are shown for the EBLUPs for individual trees generated using rings from pith (circles with solid regression line) or distance from pith (triangles with dashed regression line) in Equation 2.44

Figure 5 Plots of observed versus model predicted values of MOE (GPa) (solid line is the 1:1 relationship), and normalized residuals versus model predicted values of MOE (GPa) (solid line is loess function; dashed line is zero bias).47

Figure 6 Plot showing model predicted MOE (GPa) from the fixed effects component of the model for white spruce. Numbers at the top represent a sample plot. Circles are observed values of MOE.....48

Figure 7 Plot showing model predicted MOE (GPa) from the fixed effects component of the model for aspen. Numbers at the top represent a sample plot. Circles are observed values of MOE.49

Figure 8 Model predictions of MOE (GPa) for different levels of relative height (spruce and aspen), slenderness (spruce only), and rings/mm (spruce only) while holding other covariates constant. Simulated levels represent the minimum, 1st quartile, mean, 3rd quartile and maximum values observed for the respective covariates.....50

Figure 9 Frequency plots for branch characteristics. Graphs were generated from 15 plots, 64 trees and 874 1m sections.75

Figure 10 Caterpillar plots showing distribution of plot and tree level random effects for Equation 9 (No. branches \geq 5mm; *NBrTot*).76

Figure 11 Fitted values from the fixed effect component of Equation 9 (No. branches \geq 5mm; *NBrTot*) versus observed values (top) and boxplot showing the range for the predicted number of branches \geq 5mm across relative distance into the crown.77

Figure 12 Caterpillar plots showing distribution of plot and tree level random effects for Equation 10 (No. branches $\geq 12.5\text{mm}$; <i>NBrNoIGrd</i>).	80
Figure 13 Fitted values from the fixed effect component of Equation 10 (No. branches $\geq 12.5\text{mm}$; <i>NBrNoIGrd</i>) versus observed values (top) and boxplot showing the range for the predicted number of branches $\geq 12.5\text{mm}$ across relative distance into the crown.	80
Figure 14 Simulated predictions for the number of branches $\geq 5\text{mm}$ and (left panel) and the number of branches $\geq 12.5\text{mm}$ at different levels of the covariates included in the respective models.....	81
Figure 15 Distribution of plot and tree level random effects for Equation 11 (<i>MaxBrD</i>)......	83
Figure 16 Fitted values from Equation 11 (<i>MaxBrD</i>) versus observed values for maximum branch diameter (top) and boxplot showing the range for the predicted maximum branch diameter across relative distance into the crown.	84
Figure 17 Simulated predictions for maximum branch diameter for different levels of the covariates used in the model.....	85
Figure 18 Distribution of plot, tree and section random effects for Equation 12 (<i>RelBrD</i>). The y-axis for section random effects (i.e., a list of Plot+tree+section) is omitted....	87
Figure 19 Fitted values from the fixed effect component of Equation 12 versus observed values for branch diameters (top), and boxplot showing the range for the predicted branch diameter across relative distance into the crown.	87

Figure 20 Simulated predictions from Equation 12 (<i>RelBrD</i>) for different levels of the covariates used in the model.....	88
Figure 21 Distribution of plot, tree and section random effects from Equation 13 (<i>BrAngTot</i>). Those for Equation 14 (<i>BrAngNoIGrd</i>) are not shown, but are similar to those seen here.....	90
Figure 22 Fitted values from the fixed effect component of Equation 13 versus observed values for branch angle (branch dimeters $\geq 5\text{mm}$) (top), and boxplot showing the range for the predicted branch angle across relative distance into the crown.	91
Figure 23 Fitted values from the fixed effect component of Equation 14 versus observed values for branch angle (branch diameters $\geq 12.5\text{mm}$), and boxplot showing the range for the predicted branch angles (diameters $\geq 12.5\text{mm}$) across relative distance into the crown.	92
Figure 24 Simulated predictions from Equations 13 and 14 showing branch angles for different levels of branch rank.....	93
Figure 25 Whole-crown allometry between foliage mass (Kg) and crown length (m) for white spruce (a) and aspen (b). Lines are predictions from the fitted constant (black lines) and variable (grey lines) allometric equations (Equation 16 and 17, respectively).....	119
Figure 26 Within-crown scaling between foliage mass (Kg) and crown length (m) for quarter sections of the crown (Equation 18). Top panel is for spruce, bottom panel is for aspen.	121

Figure 27 Pearson residuals from the relationship between foliage mass and crown length in white spruce by crown quarter section (Equation 18) plotted against basal area of larger trees (m^2ha^{-1} ; Bal). 122

Figure 28 Pearson residuals from the relationship between foliage mass and crown length in aspen by crown quarter section (Equation 18) plotted against basal area of larger trees (m^2ha^{-1} ; Bal)..... 123

Figure 29 Pearson residuals from Equation 21 fitted to the white spruce data. Top panels show residuals from Equation 21 fitted using distance from stump (H_k ; m) while bottom panels show residuals from Equation 21 fitted using relative distance from tree apex ($Rdinc$)..... 128

Figure 30 Pearson residuals from Equation 21 fitted to the aspen data. Top panels show residuals from Equation 21 fitted using distance from stump (H_k ; m) while bottom panels show residuals from Equation 21 fitted using relative distance from tree apex ($Rdinc$)..... 129

Chapter 1: Introduction

1.1 Why this study was completed

Within Canada, the wood products industry has relied on an abundant supply of wood fibre to meet market demands. This volume-based economy has, in turn, placed an enormous amount of pressure on forest managers to increase growth rates in managed stands. However, by focusing on the volume of wood fibre that can be supplied, the Canadian forest industry is underachieving in terms of the potential economic returns on its investments. There are, in fact, two consequences to a volume-focused forest industry. First, there is general consensus that increased rates of tree growth have an overall negative impact on the quality of wood fibres. Empirically, this has been demonstrated for several wood properties, including density in white spruce (*Picea glauca* [Moench] Voss) (Middleton and Munro 2002) and stiffness in black spruce (*Picea mariana* [Mill.] BSP) (Zhang et al. 2002). Therefore, by striving to increase growth rates, the industry is limiting the possible range of end use products that can be derived from the forest. Second, in the absence of information pertaining to the quality of wood fibres, the forest industry is liable to assign the same price per unit to timber of “low” quality as it is to timber of “high” quality. In other words, if the quality of wood fibres are largely ignored, then an accurate valuation of harvested timber cannot be completed. It has been shown that when wood fibre production is measured not only in terms of volume, but also in terms of the quality, there are clear economic benefits for the forest industry (Acuna and Murphy 2007; Reid et al. 2009; Amishev and Murphy 2009; Lyhykainen et al. 2009).

It follows that a re-structuring of the wood fibre value chain is necessary in order for the Canadian forest industry to remain competitive in the global market. While there are many facets

to the wood fibre chain, a critical component lies in how forests are managed. There is strong evidence that the silvicultural systems employed by forest managers offer an effective means by which specific wood-quality based objectives can be achieved (Antony et al. 2012; Rais et al. 2014). However, for many of the commercially important tree species in Canada, it remains unclear how key wood properties are affected by factors such as stand density, species composition, growth rate or cambial age. Therefore, if the Canadian forest industry is to shift towards wood-quality based objectives, this knowledge gap needs to be filled.

An important step in filling this gap is the development of models which can predict wood properties in standing trees. Predictions from these models can, in turn, be used to assess wood properties prior to harvest and aid in determining the quality of wood with respect to the intended end product. Many such models have already been developed and are in use in other timber producing countries. Examples range from models which predict the frequency of branch knots to models which predict the microstructure of tracheids. The earliest models were designed to provide predictions of a given trait at the whole-tree level; that is, an average value per tree for a given wood property. Examples include the prediction of maximum branch size in Norway spruce (*Picea abies* [L.] Karst.) (Colin and Houllier 1991) and average wood stiffness in radiata pine (*Pinus radiata* D. Don) (Waghorn et al. 2007). The modelling approach most often used has been to relate the wood property of interest to easily measured tree and stand level variables. Through this approach, silvicultural activities which alter the independent variables in the models are linked to the wood properties being predicted.

While wood property models which predict a single average value per tree are useful, they are limited in terms of the advantages to silviculturalists due to large variation within the stem

(Zobel and van Buijtenen 1989). For several of the most important wood properties, within-tree variation is much larger than the variation between trees or between stands. This includes variation in the radial (i.e., from pith to bark) and longitudinal (i.e., from tree base to tree top) direction with respect to the main stem of the tree. A clear illustration of the former is the increase towards an asymptote in wood stiffness which has been observed for several species. Wolcott et al. (1987), for example, noted a 22% increase in wood stiffness between the inner core and the outer mature wood in red spruce (*Picea rubens*). Likewise, Schneider et al. (2008) noted that within tree variation in wood stiffness was greater than between tree wood stiffness for Jack pine (*Pinus banksiana* Lamb.). Therefore, economically, there is more to be gained from knowledge pertaining to within-tree properties than properties at the whole tree level. Though less common than their whole-tree counterparts, models for the prediction of within-tree wood traits have also been developed for several tree species. Unfortunately, the utility of these models to the forest industry has been plagued by different factors. One challenge has been to find equation forms that are flexible enough to represent the complex within-tree trends, yet stable enough that the parameters can be generalized to a wider population. The recent use of data-driven modelling techniques, such as generalized additive models, to predict within-tree wood properties is one example on the extreme end of model flexibility (Pokharel et al. 2014). However, in the absence of sufficient data, such models have limited application.

Another challenge has been to link within-tree trends to external stand and tree level factors. Unlike models which predict an average value per tree, finding easily measurable variables from which predictions of within tree traits can be obtained has not been as straight forward. This is because by modelling within-tree trends, we are modelling a dynamic process. Consequently,

independent variables used in the models must also be dynamic; that is, measured over time. Unfortunately, this principle is not always respected (for example, see Antony et al. 2012). Largely, this is a result of the scarce availability of dynamic measures of tree and stand variables. Despite these data limitations, recent advancements in the modelling of within-tree traits has been made by framing the development of internal wood properties within the context of the evolutionary advantages they provide (Lachenbruch et al. 2011). Through this approach, we have begun to formulate stronger arguments as to why a given internal wood trait should be modeled as a function of, say, cambial age and not distance from pith. Nevertheless, there remains a considerable amount of work to be done if such models are to be available for commercial use in Canada.

In order for the models described above to have an impact on the forest value chain, they must be integrated into decision support tools. As their name suggests, decision support tools are designed to help forest managers formulate strategic plans to meet their objectives. Growth and yield simulators are one of the more commonly used decision support tools. Within Canada, growth and yield simulators have been developed and calibrated to nearly all of the broad physiographic regions where there is active large-scale commercial harvesting. These simulators allow forest managers to plan for future harvests and determine the optimum harvesting systems for a given stand. Because of their modular construction, it is possible to add models that predict wood properties to these simulators. The introduction of such models is relatively straightforward if the models make use of independent variables already employed within the simulator. By including these models within decision support tools, forest managers can identify the best silvicultural strategies to achieve specific wood quality objectives. An early example of such a

system was presented by Houllier et al. (1995) for use on Norway spruce in France. In Finland, an example is the PipeQual simulator (Mäkelä and Mäkinen 2003). This latter simulator has been shown to have potential application for the Canadian forest industry (Schneider et al. 2008; Shcherbinina 2012). PipeQual was created through merging process-based tree growth model Crobas (Mäkelä 1997) and various models which predicted wood properties. Part of the interest in PipeQual stems for its use of Crobas, which in theory, provides an element of transportability to the model. This is because tree growth within Crobas follows functional-structural relationships which have been shown to be relatively constant across various plant communities (Shinokazi et al. 1964; Mäkelä 1986). Within Canada, the closest approximation to the PipeQual simulator is the tree and stand simulator (TASS) (Mitchell 1975) used in British Columbia. Elsewhere within Canada, the merger of wood property models and tree growth simulators is limited. Expanding the use of wood property models through their integration into decision support tools is, therefore, a key challenge facing the Canadian forest industry.

It is clear from the foregoing discussion that the impetus for this study originates from both a practical and theoretical stand-point. Practical, in the sense that the models presented in this thesis were developed with the intention that they be integrated into decision support systems and, in turn, used by forest managers to achieve wood quality objectives. However, for these models to be robust, they needed to be based on sound theoretical principles. Therefore, this thesis also had the goal to further develop the theoretical principles that currently underpin our understanding of how certain wood properties are formed and why certain structural relationships within trees are maintained.

1.2 Thesis objectives

The main objectives of this thesis were to:

1. Develop a model for the prediction of within tree radial variation in wood stiffness for white spruce and aspen (Chapter 2);
2. Develop models for the prediction of branch frequency, branch basal area, maximum branch size and branch frequency (Chapter 3);
3. Describe the allometric relationship between foliage mass and crown length at the level of the whole crown and contrast it to scaling within the crown (Chapter 4);
4. Evaluate the applicability of the pipe model relationship used by Crobas to describe whole crown foliage mass and within crown foliage mass (Chapter 4).

In addressing these objectives, the general research questions which were examined are:

1. Is tree size or age the main developmental trait influencing radial patterns of wood stiffness in white spruce and aspen and what factors cause deviations in these patterns? (Chapter 2)
2. What are the tree and stand-level factors influencing branch architecture in white spruce? (Chapter 3)
3. Are the structural assumptions of the Crobas model appropriate for use on white spruce and aspen within the context of a strategic-level decision support tool? (Chapter 4)

4. Do within-crown allometric relationships follow those observed at the whole-crown level? (Chapter 4)

The research chapters of this thesis (i.e., Chapters 2, 3 and 4) are organized according to a journal-article format. All research chapters presented in this thesis, or a modification thereof, have been published in peer reviewed journals. The following section provides a brief overview of some the key technical and theoretical aspects related to the specific objectives of this thesis. Finally, chapter 5 presents the overall conclusions that may be drawn from this study.

1.3 White spruce, aspen and the importance of a baseline

This study focused on white spruce (*Picea glauca* (Moench) Voss) and aspen (*Populus tremuloides* Michx.). Within North America, the distribution of both species is transcontinental. In particular, aspen is recognized as the most widely distributed tree species on the continent (Perala 1990). In Alberta, stands of white spruce and aspen may be found in several of the province's ecological subregions (Natural Regions Committee 2006). The term 'mixedwoods' has widely been used to describe the forests where these species co-occur. Their co-occurrence is one of the defining characteristics of both the Central and Dry Mixedwood subregions, which lie within the Boreal Forest Natural Region (Natural Subregions Committee 2006). It is within the Central Mixedwood that sampling for this study took place (Figure 1). Within this subregion, white spruce and aspen are commonly found on upland sites that are of medium soil nutrient and mesic soil moisture regime. Such stands are known as the '*Reference site*'.

The silvics of both species have been well studied within the western Canada and are documented by Heger (1971), Navratil and Bella (1988), Peterson and Peterson (1992) and Grossnickle (2000) among others. Briefly, aspen is a shade-intolerant deciduous tree species that

largely regenerates through the development of root suckers (i.e., vegetative regeneration). On ‘*Reference sites*’, it is often a pioneer species following disturbance and can regenerate in high number to form pure, single-species stands. The lower branches in aspen crowns are shed rapidly, particularly when stand densities are high. In contrast to aspen, white spruce usually regenerates through seed. White spruce is shade tolerant and is commonly found in the understory of stands where aspen has formed the main canopy. White spruce is a long-lived species whose branches are slow to be shed. It gradually begins to form the main canopy as aspen die out, which generally occurs when spruce are between 80 and 120 year of age at breast height (Grossnickle 2000).

In terms of commercial harvest, white spruce and aspen are both important species for the forest products industry in Alberta (ASRD 2014). However, white spruce carries greater economic importance given the high value of its timber. Although harvested spruce may be used in the manufacture of pulp and paper products, the majority of harvested volume is transformed into lumber (ASRD 2014). Aspen, on the other hand, is mainly used by the pulp and paper industry. However, a growing proportion is being directed toward the production of oriented strand board (OSB) and laminated veneer lumber (Ondro 1991; FPInnovations 2009). In Alberta, the harvest of white spruce and aspen is generally done using a clear-cut system. Following harvest, it is generally recommended that spruce be planted at a density between 1200 and 1600 stems per hectare (Kabzems et al. 2007). When spruce is the intended crop species, efforts to control aspen regeneration can be intense and include manual brushing and application of herbicide. There is no commercial thinning or pruning of white spruce in Alberta.

Currently, there is no information on how wood properties in white spruce and aspen differ between naturally regenerated stands and those regenerated following harvest. Indeed, few studies of this type have been performed in Canada. Zhang et al. (2002), however, noted that wood stiffness in plantation grown black spruce was on average 28% lower than wood obtained from natural stands. The study by Zhang et al. (2002) highlights the importance of establishing a baseline reference point for wood attributes used in the assessment of wood quality. Without such information, there is little way of knowing if management activities improve or degrade a given property. The work presented in this thesis is, therefore, of considerable importance to the forest products industry as it focuses on establishing a baseline reference point for several wood attributes for white spruce and aspen. To this end, all samples were collected from naturally regenerated stands in which no other silvicultural treatments had been applied.

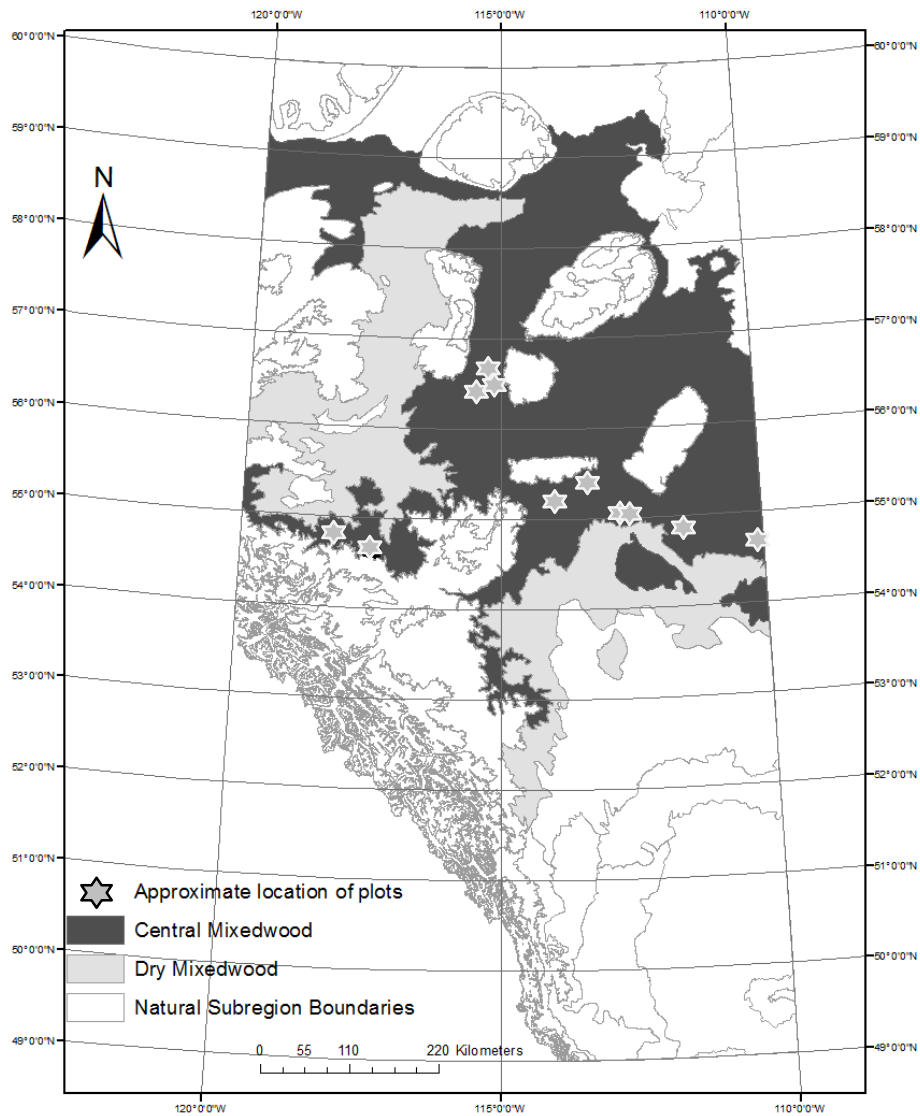


Figure 1 Approximate location of sample plots. All plots were within the Central Mixedwood Natural Subregion, which lies within the Boreal Forest Natural Region of Alberta, Canada. The Dry Mixedwood Natural Subregion is also indicated as mixed stands of aspen-white spruce are common within this area.

1.4 Wood stiffness and its components

When subjected to external forces, wood will bend. Upon removal of these forces, wood will return to its original state if the force applied was below a given threshold. This ability to resist deformation combined with its low weight is one of the main advantages of wood in terms of its use in construction. To define this elastic property, specific measures have been derived (Forest Products Laboratory 2010). Modulus of elasticity (MOE) is among the more commonly used metrics to describe the elastic properties of wood (Niklas and Spatz 2010). Measurement of MOE can be along the longitudinal, radial or tangential axis of the stem. However, by far the most frequently used measurement of MOE is along the longitudinal axis which may be denoted as MOE_L . Unless specified otherwise herein, the term wood stiffness is used to refer to MOE_L .

A direct measure of wood stiffness is achieved using static bending tests. Specifically, a load (measured in N) is applied to a wood sample. The strain, or deflection (measured in mm^2), of the wood sample is then measured. When the relationship between the applied load and the strain is linear, the removal of the load will result in the sample specimen returning to its original state. The ratio between load and strain within this zone where the relationship is linear is the measure of wood stiffness. To obtain within-tree measurements of wood stiffness, static bending tests can be performed on samples taken along a radial or longitudinal gradient. Specific gravity, moisture content and deformities in the wood fibre grain (for example, knots) are all factors that are known to influence wood stiffness (Liang and Feng 2007; Forest Products Laboratory 2010) and must be taken into account when performing static bending tests. Indirect measure of wood stiffness is also possible. At the whole tree level, this can be obtained using principles of acoustic velocity, a process that is well documented by Mochan et al. (2009). At the ring-level, wood

stiffness can be inferred from measurements of microfibril angle and specific gravity collected using x-ray diffraction, for example, via Silviscan (Evans and Ilic 2001).

At the cellular level, there appear to be several factors which determine wood stiffness. Among these, a strong determinant appears to be the microfibril angle (Cave and Walker 1994; Megraw et al. 1999), which is negatively correlated with wood stiffness. Microfibril angle, as a wood property, is defined by the angle of microfibrils with respect to the longitudinal axis of the cell (Panshin and de Zeeuw, 1980). In particular, the orientation of microfibrils in the thickest portion of the cell wall (i.e., the S₂ layer) determine the physical properties of the cell. Microfibrils within the S₂ layer are composed primarily of cellulose, followed by lignin and hemicellulose. For several species including, Scots pine (*Pinus sylvestris* L.) (Auty et al. 2013) and radiata pine (Moore et al. 2014), the orientation of microfibrils has been shown to be positively correlated with radial growth rate. It has been suggested that the increased production of hormones, such as auxins, play a role in determining how the micro-crystalline structure of the microfibrils are arranged (Downes et al. 2009). However, the underlying process that links growth rate and microfibril angle remains speculative (Walker 2006).

A second factor that appears to have an influence on wood stiffness is wood specific gravity (Rosner et al. 2008). Like microfibril angle, wood density has been shown to be affected by auxins. As auxin concentrations increase, there is an increase in lumen size and a reduction in cell wall thickness noticeable within earlywood cells (Panshin and de Zeeuw 1980). This change in cell structure results in a corresponding decrease in specific gravity. It is thought that these changes to the structure of the cell contribute to a weakening of the flexural properties of wood

(Archer 1987). However, like microfibril angle, the precise mechanisms linking specific gravity, growth rate and wood stiffness remain speculative.

1.5 Wood stiffness and tree function

Despite the complex relationships that occur at the cellular level, models predicting pith to bark trends in wood stiffness have been able to explain a relatively large proportion of the total variation (Leban and Haines 1999, Auty and Achim 2008). This is in contrast to models for pith to bark trends in specific gravity, where R^2 values of less 40% are common (cf. Peng and Stewart 2013). From an empirical standpoint, the results for wood stiffness are encouraging. However, a major decision that is often overlooked when developing these models is the choice of radial metric to use. That is, should the radial development of wood stiffness be modelled as a function of cambial age (i.e., rings from pith) or as a function of distance from pith? Care must be taken when making this decision as each metric implies a different set of adaptive evolutionary responses. For example, if radial development of wood stiffness is more closely associated with distance from pith, then regardless of growth rate, a maximum wood stiffness will be attained once the tree reaches a given size. Conversely, if wood stiffness develops in close association with cambial age, then this implies that the maximum stiffness will be attained at a distance progressively further from the pith as radial growth rate increases. Gartner (1995) describes two possible underlying adaptive mechanisms that could explain such trends, namely, mechanical and hydraulic constraints.

It is suggested that when mechanical stability is of high relative importance, it will infer more of a size-related influence on the radial pattern of wood stiffness (Lachenbruch et al. 2011). For example, for trees exposed to high winds, there would be an evolutionary advantage to attaining

a maximum wood stiffness once a given size is reached rather than once the tree has reached a certain age. When hydraulic constraints are of high priority (e.g., evapotranspirative demands are high), then the argument follows that the development of wood stiffness should closely follow cambial age. This argument follows from the observation that tree pathway redundancy reduces the frequency of embolism for certain species (Zimmermann 1983; Tyree et al. 1994). Within deciduous species, redundancy can be achieved through an increased number of growth rings within a given area, placing more vessels in closer contact (Hargrave et al. 1994; Lachenbruch et al. 2011). Furthermore, an increase in the number of growth rings within a given area confers an advantage as it increases the diversity of cell types (i.e., vessels and fibres) within the given area, thereby providing greater protection against embolism.

Finding evidence in support of these arguments has proven difficult, however. This is largely due to the presence of confounding factors. Crown size, stand density and the relative position of trees within the stand are all factors that interact with the mechanical and hydraulic demands placed on trees. The inability to take into account these interactive effects has led to a sometimes questionable association between wood stiffness and various tree and stand-level variables. For example, neglecting the exponential relationship between stem diameter and bending moment can lead to a false impression that radial growth rate has a significant effect on wood stiffness. However, isolating these factors within a forest is challenging, at best. Alternatively, insight can be gained by contrasting measurements of wood stiffness from tree species which exhibit different growth patterns but which occupy the same growing space. A clear example of this are the mixed stands of white spruce and aspen that characterize the western boreal forest of Canada.

1.6 Branching characteristics and wood quality

The interest in describing branching patterns has grown within recent decades. Historically, this research has largely been driven by the desire to improve predictions of tree growth. More recently, however, the motives have been driven by wood quality objectives (Mäkinen et al. 2009). The size, frequency and orientation of knots within a tree are all factors that affect the quality of sawn-wood products. This is mainly due to the way knots affect the normal orientation of wood fibres. By causing a deviation in the normal wood grain, the overall mechanical properties of wood are reduced (Boatright and Garrett 1979). Branch angle plays a role in that the surface area of knots within sawn lumber will be greater if branches maintain a small angle relative to the stem. Not only has this been shown to reduce the mechanical properties wood, but it also severely affects the visual appearance of wood. These effects on the overall appearance and mechanical properties of wood are reflected in the current system of lumber grading used within Canada (NLGA 2003), which is largely based on a visual inspection of knots.

Since lumber grading is tied to external knot characteristics, there are considerable economic gains to be achieved by increasing our knowledge of the factors controlling branching patterns. Indeed, several studies have examined the effects of stand density management, fertilizer treatment and species composition on various branch properties. Groot and Schneider (2011), for example, found that white spruce maximum branch diameter was more sensitive to competition than other commercially important conifers in the Canadian boreal forest. For Norway spruce, Mäkinen et al. (2001) noted that while fertilization had the desirable effect of increased tree growth rates, it had the less desirable effect of increasing branch diameters. It was suggested that this negative effect could, in part, be offset through increased planting density.

The results of these studies have revealed that certain branch characteristics are under strong environmental control, others under strong genetic control, while others lie somewhere in between. These findings highlight the fact that, although managing stands to control branching patterns have the potential to provide economic gains, the practice also poses significant economic risk. This point is illustrated with the characteristic of branch frequency in white spruce and Norway spruce. Merrill and Mohn (1985) note that branch frequency in white spruce is under low genetic control. Conversely, Steffenrem et al. (2008) report that whorl frequency is under strong genetic control in Norway spruce. Thus, in the case of Norway spruce, it would make little economic sense to invest in silvicultural treatments which attempt to regulate whorl frequency. Conversely, similar efforts to control branching in white spruce are likely to pay greater dividends. Silvicultural treatments aimed at manipulating branching characteristics carry an economic risk when they are applied without sufficient forehand knowledge of environmental or genetic controls.

The problems faced when developing models of branch characteristics are similar to those for the prediction of internal wood properties. In particular, there is the persistent issue of using static measures of tree and stand level characteristics to predict the dynamic process of branch formation and growth. Recently, Trincado and Burkhart (2009) provided a stochastic model of branch initiation, growth and death for use in loblolly pine (*Pinus taeda* L.) which used data from destructively sampled trees. While their study advanced the field of branch modelling, the costs to undertake such a study would be prohibitive for many species. In lieu of this, branch models have focused on providing a description of the crown at a given point in time. Within most of Canada, the development and practical application of branch models is in its infancy.

Although considerable work has gone into developing and integrating branch models into TASS, there are few other examples. The models presented here and other ongoing work seek to fill this gap.

1.7 Crobas and the pipe model theory

Crobas is a carbon balance model of tree growth that is based on principles related to pipe model theory (Shinozaki et al. 1964) and functional balance (Davidson 1969). A detailed description of the Crobas model is provided by Mäkelä (1997). Briefly, however, the Crobas model works at the level of the individual tree, although predictions are provided for the average tree within a stand. Within Crobas, the acquisition of carbon is a function of the tree's photosynthetic ability which is determined by the tree's foliage mass and a constant which specifies the species-specific rate of photosynthesis. Foliage mass, is assumed to follow an allometric relationship with crown length. This assumption is supported by empirical findings from both deciduous (Ilomäki et al. 2003) and coniferous (Kantola and Mäkelä 2004) tree species. To allocate carbon within a tree, Crobas combines the principle of functional balance and the pipe model theory. The principle of functional balance describes the balance between leaf activity and activity of fine roots (Landsberg and Sands 2010). In terms of tree function, these two sites represent where carbon and nutrients are obtained. Within Crobas, this principle is used as the basis for the constant ratio that is assumed to exist between fine root and foliage mass.

The principle of functional balance also postulates that carbon and nutrients are allocated within trees in a manner which optimizes tree growth given a set of environmental constraints (e.g., under drought conditions). However, the allocation of carbon and nutrients to different units of the tree (e.g., branches, stem, foliage, roots) tends to proceed in a manner which maintains

certain structural relationships. From a theoretical standpoint, structural relationships that are maintained over time imply a high level of importance in terms of tree function.

Among the structural relationships that exist between different units of the tree, the ratio between sapwood area at crown base and foliage mass and the relationship between foliage mass and crown length are relatively constant (Mäkelä and Sievänen 1992; Mäkelä and Vanninen 1998). The functional-structural explanation for the latter relationship is that it represents the optimal balance between photosynthetic capacity and the cost of maintaining the components required to support the crown. With regards to the ratio between sapwood area at crown base and foliage mass, the relationship is based on the supply of water and nutrients to living foliage, but also implies an importance in terms of mechanical support. To account for the taper of ‘pipes’ within the living crown, modifications to this relationship have been adopted (Mäkelä 1997). Specifically, the within-crown ratio between sapwood area and foliage mass has been adjusted to vary as a function of whorl age. Within Crobas, the allocation of carbon to different units of the tree proceeds in a manner which maintains both of these relationships.

The constant sapwood area – foliage mass relationship is an adaptation of the original pipe model described by Shinozaki et al. (1964). The original model was formulated following empirical observation that the ratio between the cross-sectional area of a plant stem at a given point and the foliage mass above that point remained constant. It was then proposed that tree form may be described if trees were viewed as an assemblage of pipes which connect roots to leaves. Active pipes transport nutrients and water to living foliage while disused pipes form as branches are shed and give taper to the stem. The original model, however, makes no specific reference to sapwood. Based on further empirical observations (Waring et al. 1982; Nikinmaa

1992), Mäkelä (1986) adapted the original theory and specified that a constant relationship exists between the cross-sectional area of sapwood at the base of the live crown and foliage mass. This modification implies that high priority is given to the maintenance of hydraulic function since sapwood area is associated with water transport. However, the association between sapwood area and hydraulic function has been called in to question given that sapwood permeability and hydraulic path length are not explicitly considered. Consequently, it has been suggested that changes in permeability and path length may influence the pipe model ratio (Mencuccini and Grace 1996).

The platform on which the Crobas simulator operates has continued to evolve in association with the demands of the Finish forest industry. In particular, Crobas has been joined to other sub-models which estimate tree attributes used in assessing wood quality. Importantly, many of these sub-models have also been derived using pipe model theory. Mäkelä (2002), for example, describes the derivation of stem taper and the vertical distribution of branch basal area using pipe model theory. By basing these models on functional-structural relationships, the Crobas model lends itself for use outside of the region to which it was initially calibrated. Indeed, it was this feature of Crobas which stimulated interest in evaluating its applicability to white spruce and aspen stands within the Canadian Boreal Forest.

References

- Acuna, M.A., and Murphy, G.E. 2007. Estimating relative log prices of Douglas-fir through a financial analysis of the effects of wood density on lumber recovery and pulp yield. *For. Prod. J.* **57**: 60-65.
- Alberta Environment and Sustainable Resource Development (ASRD). 2014. Sustainable forest management facts and statistics: Annual allowable cut. ISBN 978-1-4601-1944-0 ISSN 2368-4844. Fall 2014, Environment and Sustainable Resourced Development. <http://esrd.alberta.ca/lands-forests/forest-management/forest-management-facts-statistics/default.aspx> Accessed May 2015.
- Amishev, D., and Murphy, G.E. 2009. Estimating breakeven prices for Douglas-fir veneer quality logs from stiffness graded stands using acoustic tools. *For. Prod. J.* **59**: 45-52.
- Antony, F., Schimleck, L.R., Jordan, L., Daniels, R.F., and Clark, A., III. 2012. Modeling the effect of initial planting density on within tree variation of stiffness in loblolly pine. *Ann. For. Sci.* **69**: 641-650.
- Archer, R.R. 1987. On the Origin of Growth Stresses in Trees .1. Micro Mechanics of the Developing Cambial Cell-Wall. *Wood Sci. Technol.* **21**: 139-154.
- Auty, D., and Achim, A. 2008. The relationship between standing tree acoustic assessment and timber quality in Scots pine and the practical implications for assessing timber quality from naturally regenerated stands. *Forestry* **81**: 475-487.
- Auty, D., Gardiner, B.A., Achim, A., Moore, J.R., and Cameron, A.D. 2013. Models for predicting microfibril angle variation in Scots pine. *Ann. For. Sci.* **70**: 209-218.

- Boatright, S. W. J. and Garrett, G. G. 1979. The effects of knots on the fracture strength of wood - I. A review of methods of assessment. *Holzforschung* 33-3, pp. 58-72.
- Cave, I.D., and Walker, J.C.F. 1994. Stiffness of Wood in Fast-Grown Plantation Softwoods - the Influence of Microfibril Angle. *For. Prod. J.* **44**: 43-48.
- Colin, F., and Houllier, F. 1991. Branchiness of Norway Spruce in North-Eastern France - Modeling Vertical Trends in Maximum Nodal Branch Size. *Ann. Sci. For.* **48**: 679-693.
- Davidson, R.L. 1969. Effect of root/leaf temperature differentials on root/shoot ratios in some pasture grasses and clover. *Annals of Botany* **33**: 561-569.
- Downes, G.M., Drew, D., Battaglia, M., and Schulze, D. 2009. Measuring and modelling stem growth and wood formation: An overview. *Dendrochronologia* **27**: 147-157.
- Evans, R., and Ilic, J. 2001. Rapid prediction of wood stiffness from microfibril, angle and density. *For. Prod. J.* **51**: 53-57.
- Forest Products Laboratory. 2010. Wood handbook—Wood as an engineering material. General Technical Report FPL-GTR-190. Madison, WI: U.S. Department of Agriculture, Forest Service, Forest Products Laboratory. 508 p.
- FPIinnovations 2009. Wood market statistics including pulp and paper in Alberta. 2009 Edition. Compiled by Rhonda Lindenbach-Gibson and James Poon, for FPIinnovations, Point-Claire, QC and Vancouver, BC.
- Gartner, B.L. 1995. Patterns of xylem variation within a tree and their hydraulic and mechanical consequences. In B. L. Gartner, ed. *Plant Stems: Physiology and Functional Morphology*, pp. 125-149. Academic Press, San Diego, CA.

- Groot, A., and Schneider, R. 2011. Predicting maximum branch diameter from crown dimensions, stand characteristics and tree species. *For. Chron.* **87**: 542-551.
- Grossnickle SC. 2000. *Ecophysiology of northern spruce species: the performance of planted seedlings*. Ottawa: NRC Research Press.
- Hargrave, K., Kolb, K., Ewers, F., and Davis, S. 1994. Conduit Diameter and Drought-Induced Embolism in *Salvia-Mellifera* Greene (Labiatae). *New Phytol.* **126**: 695-705.
- Heger, L. 1971. Site-index/soil relationships for white spruce in Alberta Mixedwoods. Canadian Forestry Service, Information Report FMR-X-32, Project 31. Forest Management Institute, Ottawa, ON. 15 p.
- Houllier, F., Leban, J.M., and Colin, F. 1995. Linking Growth Modeling to Timber Quality Assessment for Norway Spruce. *For. Ecol. Manage.* **74**: 91-102.
- Ilomäki, S., Nikinmaa, E., and Mäkelä, A. 2003. Crown rise due to competition drives biomass allocation in silver birch. *Can. J. of For. Res.* **33**: 2395-2404.
- Kabzems, R., A.L. Nemeč, and C. Farnden. 2007. Growing trembling aspen and white spruce intimate mixtures: Early results (13–17 years) and future projections. *BC Journal of Ecosystems and Management* 8(1):1–14.
- Kantola, A., and Mäkelä, A. 2004. Crown development in Norway spruce [*Picea abies* (L.) Karst.]. *Trees-Structure and Function* **18**: 408-421.
- Lachenbruch, B., Moore, J.R., and Evans, R. 2011. Radial Variation in Wood Structure and Function in Woody Plants, and Hypotheses for Its Occurrence.

- Landsberg, J.J., and Sands, P. 2010. *Physiological Ecology of Forest Production: Principles, Processes and Models*; Academic Press (Elsevier): New York, NY, USA, 2010.
- Leban, J.M., and Haines, D.W. 1999. The modulus of elasticity of hybrid larch predicted by density, rings per centimeter, and age. *Wood Fiber Sci.* **31**: 394-402.
- Liang Shan-qing, and Fu Feng. 2007. Comparative study on three dynamic modulus of elasticity and static modulus of elasticity for Lodgepole pine lumber. *Journal of Forestry Research (Harbin)* **18**: 309-312.
- Lyhykainen, H.T., Mäkinen, H., Mäkelä, A., Pastila, S., Heikkila, A., and Usenius, A. 2009. Predicting lumber grade and by-product yields for Scots pine trees. *For. Ecol. Manage.* **258**: 146-158.
- Mäkelä, A. 2002. Derivation of stem taper from the pipe theory in a carbon balance framework. *Tree Physiol.* **22**: 891-905.
- Mäkelä, A. 1997. A carbon balance model of growth and self-pruning in trees based on structural relationships. *For. Sci.* **43**: 7-24.
- Mäkelä, A. 1986. Implications of the Pipe Model-Theory on Dry-Matter Partitioning and Height Growth in Trees. *J. Theor. Biol.* **123**: 103-120.
- Mäkelä, A., and Mäkinen, H. 2003. Generating 3D sawlogs with a process-based growth model. *For. Ecol. Manage.* **184**: 337-354.
- Mäkelä, A., and Vanninen, P. 1998. Impacts of size and competition on tree form and distribution of aboveground biomass in Scots pine. *Can. J. of For. Res.* **28**: 216-227.

- Mäkelä, A., and Sievänen, R. 1992. Height Growth Strategies in Open-Grown Trees. *J. Theor. Biol.* **159**: 443-467.
- Mäkinen, H., Saranpää, P., and Linder, S. 2001. Effect of nutrient optimization on branch characteristics in *Picea abies* (L.) Karst. *Scand. J. For. Res.* **16**: 354-362.
- Mäkinen, H., Mäkelä, A., and Hynynen, J. 2009. Predicting Wood and Branch Properties of Norway Spruce as a Part of a Stand Growth Simulation System. U S Forest Service Pacific Northwest Research Station General Technical Report PNW-GTR 15-21.
- Megraw, RA, Bremer, D, Leaf, G, & Roers, J. 1999. Stiffness in Loblolly Pine as a Function of Ring Position and Height, and its Relationship to Microfibril Angle and Specific Gravity (IUFRO Workshop S5.01.04, La Londe-Les-Meures, pp. 341–349)
- Mencuccini, M., and Grace, J. 1996. Developmental patterns of above-ground hydraulic conductance in a Scots pine (*Pinus sylvestris* L) age sequence. *Plant Cell and Environment* **19**: 939-948.
- Merrill, R., and Mohn, C. 1985. Heritability and Genetic Correlations for Stem Diameter and Branch Characteristics in White Spruce. *Can. J. For Res.* **15**: 494-497.
- Middleton, G. R. and Munro, B. D. 2002. Wood density of Alberta white spruce - Implications for silvicultural practices. Forintek Canada Corp. Vancouver, BC. 66p.
- Mitchell, K. 1975. Dynamics and Simulated Yield of Douglas-Fir. *For. Sci.* 1-39.
- Mochan, S., Connolly, T. and Moore, J. 2009. Using Acoustic Tools in Forestry and the Wood Supply Chain. Edinburgh: Forestry Commission, Sep. 2009. Technical Note. 6 p.

- Natural Regions Committee 2006. Natural Regions and Subregions of Alberta. Compiled by D.J. Downing and W.W. Pettapiece. Government of Alberta. Pub. No. T/852.
- Navratil, S. and Bella, I. E. 1988. Regeneration, development and density management in aspen stands. Northern Forestry Centre, Forestry Canada, 5320 - 122 st., Edmonton, Alberta, T6H 3S5
- Nikinmaa, E. 1992. Analyses of the growth of Scots pine: Matching structure with function. Acta For. Fenn. **235**: 1-68.
- Niklas, K.J., and Spatz, H. 2010. Worldwide Correlations of Mechanical Properties and Green Wood Density. Am. J. Bot. **97**: 1587-1594.
- NLGA 2003. Standard grading rules for Canadian lumber. National Lumber Grades Authority, New Westminster, British Columbia, Canada
- Ondro, W.J. 1991. Present trends and future prospects for poplar utilization in Alberta. For. Chron. **67**: 271-274
- Panshin, A.J., de Zeeuw, C., 1980. Textbook of Wood Technology. McGraw-Hill Book Company, New York.
- Peng, M., and Stewart, J.D. 2013. Development, validation, and application of a model of intra- and inter-tree variability of wood density for lodgepole pine in western Canada. Can. J. For. Res. **43**: 1172-1180.
- Perala, D. A. 1990. *Populus tremuloides*. Michx. Quaking aspen. Pp. 555-569, IN: R.M. Burns and B.H. Honkala. Silvics of North America. Volume 2. Hardwoods. USDA Forest Service Agric. Handbook 654, Washington, D.C.

http://willow.ncfes.umn.edu/silvics_manual/Volume_2/populus/tremuloides.htm

Accessed May 2015.

- Peterson, E.B. and Peterson, N.M. 1992. Ecology, management, and use of aspen and balsam poplar in the prairie provinces, Canada. For. Can., Northwest Reg., North. For. Cent., Edmonton, Alberta. Spec. Rep. 1.
- Pokharel, B., Dech, J.P., Groot, A., and Pitt, D. 2014. Ecosite-based predictive modeling of black spruce (*Picea mariana*) wood quality attributes in boreal Ontario. Can. J. For. Res. **44**: 465-475.
- Rais, A., Poschenrieder, W., Pretzsch, H., and van de Kuilen, J.G. 2014. Influence of initial plant density on sawn timber properties for Douglas-fir (*Pseudotsuga menziesii* (Mirb.) Franco). Ann. For. Sci. **71**: 617-626.
- Reid, D.E.B., Young, S., Tong, Q., Zhang, S.Y., and Morris, D.M. 2009. Lumber grade yield, and value of plantation-grown black spruce from 3 stands in northwestern Ontario. For. Chron. **85**: 609-617.
- Rosner, S., Klein, A., Muller, U., and Karlsson, B. 2008. Tradeoffs between hydraulic and mechanical stress responses of mature Norway spruce trunk wood. Tree Physiol. **28**: 1179-1188.
- Schneider, R., Zhang, S.Y., Swift, D.E., Begin, J., and Lussier, J. 2008. Predicting selected wood properties of jack pine following commercial thinning. Can. J. For. Res. **38**: 2030-2043.
- Shcherbinina, A. 2012. Validation of the jack pine version of Crobas-Pipequal. Master thesis, University of British Columbia, Vancouver, Canada.

- Shinozaki, K.K., Yoda, K., Hozumi, K., and Kira, T. 1964. A quantitative analysis of plant form — the pipe model theory. 1. Basic analyses. *Jpn. J. Ecol.* **14**: 97–105.
- Steffenrem, A., Lindland, F., and Skroppa, T. 2008. Genetic and environmental variation of internodal and whorl branch formation in a progeny trial of *Picea abies*. *Scand. J. For. Res.* **23**: 290-298.
- Trincado, G., and Burkhart, H.E. 2009. A framework for modeling the dynamics of first-order branches and spatial distribution of knots in loblolly pine trees. *Can. J. For. Res. -Rev. Can. Rech. For.* **39**: 566-579.
- Tyree, M.T., Davis, S.D., and Cochard, H. 1994. Biophysical Perspectives of Xylem Evolution - is there a Tradeoff of Hydraulic Efficiency for Vulnerability to Dysfunction. *Iawa Journal* **15**: 335-360.
- Waghorn, M.J., Watt, M.S., and Mason, E.G. 2007. Influence of tree morphology, genetics, and initial stand density on outerwood modulus of elasticity of 17-year-old *Pinus radiata* RID C-3813-2009. *For. Ecol. Manage.* **244**: 86-92.
- Walker, J.C.F. 2006. Primary wood processing: principles and practice.
- Waring, R.H., Schroeder, P.E., and Oren, R. 1982. Application of the Pipe Model-Theory to Predict Canopy Leaf-Area. *Can. J. For. Res.* **12**: 556-560.
- Wolcott, M.P., Shepard, R.K., and Shottafer, J.E. 1987. Age and thinning effects on wood properties of red spruce (*Picea rubens* Sarg.). Technical Bulletin - Maine Agricultural Experiment Station iv + 17 pp.-iv + 17 pp.

Zhang, S.Y., Chauret, G., Ren, H.Q.Q., and Desjardins, R. 2002. Impact of initial spacing on plantation black spruce lumber grade yield, bending properties, and MSR yield. *Wood Fiber Sci.* **34**: 460-475.

Zimmermann, M.H. 1983. *Xylem structure and the ascent of sap*. Berlin; Springer-Verlag.uthor,
A. 2010. Title, publication details, in style permitted by your discipline.

Chapter 2: Within-tree patterns of wood stiffness for white spruce (*Picea glauca* [Moench] Voss) and trembling aspen (*Populus tremuloides* Michx.)

2.1 Introduction

Wood stiffness, defined by modulus of elasticity (MOE), is a property that shows large variation from pith to bark for several tree species. This is true for both white spruce (*Picea glauca* [Moench] Voss) (Lenz et al. 2010) and *Populus* species (Yu et al. 2008) such as aspen (*Populus tremuloides* Michx.). In terms of biomechanical function, the manner in which wood stiffness develops from pith to bark has been tied to both the mechanical and hydraulic functions of the main stem (Gartner 1995; Alvarez 2005; van Gelder et al. 2006). For the wood products industry, variations in the pith to bark patterns for wood stiffness have an effect on the quality of lumber products (Kliger et al. 1998). Furthermore, silvicultural activities have been shown to influence pith to bark patterns of stiffness through changes in radial growth rate and tree slenderness (Antony et al. 2012), among other factors. Therefore, models which predict wood stiffness from pith to bark are of considerable importance. While wood stiffness has been previously examined for white spruce (Kuprevicius et al. 2013), studies on aspen are sparse. Moreover, models for the purpose of prediction are lacking for both species.

The pith to bark development of wood stiffness can be viewed as a function of either cambial age (rings from pith; RFP) or tree size (distance from pith; DFP). An important step in model development is the choice of which of these two metrics to use. While the choice is usually based on statistical merit, there are implications concerning the biomechanical function of the tree.

Lachenbruch et al. (2011), for example, suggests that the development of a wood property in close association with cambial age is indication that hydraulic constraints have priority over mechanical constraints. Conversely, a wood property whose radial pattern is closely associated with tree size suggests that mechanical constraints may have greater relative importance.

Biomechanical arguments aside, a review of recently published papers describing pith to bark patterns of wood stiffness in coniferous species revealed that cambial age is the most commonly used metric (Leban and Haines 1999; Auty and Achim 2008; Lenz et al. 2010). Wood traits which are correlated with wood stiffness, such as microfibril angle (Cowdrey and Preston 1966; Evans and Ilic 2001; Ricardo et al. 2012), modulus of rupture (Castéra et al. 1996; Liu et al. 2007), and specific gravity (Evans and Ilic, 2001) were also most often modeled using cambial age (Alteyrac et al. 2006; Schneider et al. 2008; Auty et al. 2013). Models for specific gravity in lodgepole pine (*Pinus contorta* Douglas ex Loudon) (Peng and Stewart 2013) and microfibril angle in sugi trees (*Cryptomeria japonica* D. Don) (Kubo and Koyama 1993) were among the few examples where tree size was used to model the pith to bark trends for a given wood property. For deciduous species, models for pith to bark trends in wood stiffness are scarce and there appears to be no consensus as to which metric should be used (Lachenbruch et al. 2011). However, Matyas and Peszlen (1997) used cambial age to model various wood quality traits for hybrid poplar clones (*Populus × euroamericana* (Dode) Guinier). For two species of eucalyptus (*Eucalyptus globulus* and *E. grandis*), Kojima et al. (2009) found that fibre length was best modelled as a function of cambial age. Conversely, they found that fibre length was best modeled using tree size for two species of acacia (*Acacia mangium* and *A. auriculiformis*).

For a given species, the choice of metric used when modeling pith to bark wood stiffness or other wood property has not been consistent. This has likely led to some confusion. Lundgren (2004), for example, used both cambial age and tree size to model radial patterns of wood stiffness and microfibril angle in Norway spruce (*Picea abies* [L.] Karst.), but dropped cambial age when modeling specific gravity. For loblolly pine (*Pinus taeda* L.), Antony et al. (2012) used tree size as the base variable upon which to build a model for pith to bark wood stiffness. However, for the same species, pith to bark patterns for microfibril angle were modeled using cambial age (Jordan et al. 2006). From these examples, it is clear that a greater focus needs to be placed on the selection of either cambial age or tree size.

Regardless of radial metric, existing models for pith to bark wood stiffness have used tree or ring-level variables to help explain some of the variability. Tree slenderness and radial growth rate (e.g., mean ring width) are two variables which have previously been shown to explain a significant amount of variability in pith to bark wood stiffness (Leban and Haines 1999; Antony et al. 2012). It is speculated that the main pathway linking ring width to wood stiffness is through changes in microfibril angle (Lasserre et al. 2009). In the case of tree slenderness, it is argued that in order to maintain mechanical stability, slender trees require greater wood stiffness (Waghorn et al. 2007). Using ring width or a measure of mean ring width in models for pith to bark wood stiffness is straightforward. For tree slenderness, it is preferable that the measure represent the state of the tree at the time wood is formed. Because past measures of tree slenderness are not always available, tree slenderness at the time of sampling is sometimes used in place (for example, see Antony et al. 2012). However, this assumes that the tree's slenderness coefficient has remained constant throughout its development.

For the current study, the objectives were: (1) to determine which metric (cambial age or tree size) is most closely associated with the pith to bark development of wood stiffness and (2) to develop a predictive model for pith to bark wood stiffness. With regards to the latter objective, the model was also used to test the influence of radial growth rate, slenderness and vertical position within the stem on wood stiffness. Data for this study came from measurements collected on white spruce and aspen within the central mixedwood boreal forest of Alberta, Canada. Such data is of considerable interest to the forest products industry as it provides a baseline reference point upon which to compare measurements of wood stiffness from plantation-grown trees.

2.2 Material and methods

2.2.1 Site description and sample preparation

Measurements of wood stiffness were obtained from 64 white spruce trees located within 15 permanent sample plots (PSPs) (Alberta Sustainable Resource Development; ASRD 2005) and 27 trembling aspen trees from 9 PSPs. The trees were felled between 2009 and 2011. The PSPs were selected to provide: (1) a range of basal area ($\text{m}^2 \text{ha}^{-1}$) (Table 1), (2) a range of species composition (measured as a percent of total stand basal area), and (3) a range in mean cambial age at breast height for trees in the main canopy (mean age for the stands ranged from 52 to 153 years). All PSPs were situated in unmanaged stands. Since sampling involved the removal of large stem sections from felled trees, the proximity to roads influenced the final selection of PSPs. All PSPs were located in the central mixedwood natural subregion of the Alberta boreal mixedwood forest (Beckingham and Archibald 1996). Vegetation at all sites were indicative of the modal soil moisture and nutrient regime for the region, which Beckingham and Archibald

(1996) describe as moderately well-drained orthic gray luvisolic soils. As such, site productivity was estimated to be similar across the sampled PSPs. The plots ranged in terms of overstory species composition from pure trembling aspen, to nearly pure white spruce.

Table 1 Estimated stand basal area ($\text{m}^2\cdot\text{ha}^{-1}$) and number of trees per hectare (no. of trees $\cdot\text{ha}^{-1}$) calculated from fixed radius plots established around sample trees, with the corresponding proportions of white spruce (sw) and trembling aspen (aw).

Plot	Basal area, m^2ha^{-1}	Proportion of total basal area that is:		No. trees ha^{-1}	Proportion of no. trees ha^{-1} total that is:	
		sw	aw		sw	aw
52	41.4 (14.3)	0.45	0.30	633.1 (283.9)	0.63	0.22
54	32.8 (16.6)	0.00	0.99	537.3 (314.5)	0.00	0.95
267	48.2 (6.2)	0.49	0.40	487.8 (123.3)	0.66	0.23
368	31.4 (5.8)	0.49	0.49	1887.0 (186.5)	0.37	0.61
379	45.3 (13.3)	0.82	0.09	910.53 (238.6)	0.57	0.05
383	38.9 (20.2)	0.61	0.22	309.9 (155.6)	0.61	0.23
386	38.2 (12.3)	0.74	0.19	1134.2 (437.7)	0.80	0.15
400	42.6 (11.2)	0.00	0.93	939.7 (194.8)	0.00	0.90
401	40.5 (11.1)	0.31	0.59	1156.8 (397.2)	0.32	0.46
430	34.6 (7.1)	0.18	0.82	1679.7 (442.9)	0.15	0.85
432	31.8 (7.5)	0.00	0.95	2551.7 (264.7)	0.00	0.94
433	30.2 (4.1)	0.00	0.91	2161.5 (364.9)	0.00	0.90
434	36.6 (10.8)	0.35	0.63	1346.2 (335.5)	0.50	0.49
435	36.9 (8.2)	0.15	0.84	1613.3 (473.5)	0.18	0.81
436	39.0 (11.1)	0.07	0.89	1161.3 (297.9)	0.11	0.80
440	48.4 (12.4)	0.92	0.08	512.3 (74.9)	0.90	0.10
444	49.7 (14.7)	0.63	0.34	683.1 (175.0)	0.73	0.24
645	29.1 (3.6)	0.47	0.51	939.7 (352.4)	0.28	0.67
648	25.7 (10.4)	0.91	0.03	871.2 (359.0)	0.79	0.04

Note: Stand basal area and number of trees per hectare values are given as means followed by standard deviations (SD) in parentheses.

Selected trees were located a minimum of 30 m and a maximum of 100 m from the edge of the PSPs and were free of any major visible defects. However, trees with minor stem deformities were occasionally sampled when this was the prevailing condition within the stand. When white spruce and trembling aspen co-occurred in a PSP, a minimum of two trees per species were selected and were either in a dominant or co-dominant position relative to their conspecifics. This was verified by first measuring DBH (diameter at breast height; cm) and comparing it to the range of DBH between by the 3rd and 4th quartile obtained from the most recent inventory of the PSP. Furthermore, selected trees were a minimum of 20m from each other. Trees with a noticeable lean were avoided. Within some of the plots, decay within trembling aspen trees prevented the collection of samples leading to an unequal number of PSPs from which white spruce and trembling aspen were collected. The DBH of the selected trees were measured prior to felling, while total tree height was measured once the trees were on the ground (Table 2). Logs measuring 60 cm in length were then cut from the main stem, with the top ends of the log sections located at breast height (BH), the mid-point between the base of the tree and the base of the live crown (MB) and at crown base (CB). For white spruce an additional section was taken at the mid-point between the base of the crown and the crown apex (MC). When the distance between the top of the log section at BH and the base of the log section at CB measured less than 3 m, the section located at MB was not collected. Before cutting the samples, the height from the base of the tree to the top of each log section was recorded.

Table 2 Mean values for cambial age at breast height, diameter at breast height (DBH; cm) and height (HT; m) of trees sampled for wood stiffness (minimum and maximum values in parentheses).

White spruce					Trembling aspen			
Plot	n	Age	mean DBH	mean HT	n	Age	mean DBH	mean HT
52	5	105	28.9 (23.3-38.6)	24.1 (15.1-28.7)	2	112	35.9 (34-37.8)	27.8 (25.4-30.2)
54	0				4	111	30.1 (27.5-32.1)	28.2 (27-28.9)
267	6	131	39.8 (32.4-43.7)	31.8 (28.4-33.3)	0			
368	4	59	17.7 (13.8-25.5)	15.3 (13.2-18.8)	3	79	14.2 (13-15.9)	16.4 (15.3-18.2)
379	4	148	35.9 (30.3-41.2)	30.2 (27.1-32.3)	0			
383	3	93	39.1 (31.3-44.1)	29.1 (24.9-32.1)	0			
386	6	95	21.2 (18.0-29.0)	19.6 (16.8-24.0)	0			
400	0				5	60	27.8 (24.8-32.7)	26.6 (24.3-27.9)
401	5	55	22.9 (20.7-25.2)	17.3 (16.6-18.2)	2	66	27.4 (26-28.8)	22.1 (21.3-23)
430	3	52	17.0 (13.7-21.4)	15.0 (11.3-17.2)	0			
432	0				4	47	14.6 (13.4-17.5)	18.7 (16.9-20.8)
433	0				5	46	15.3 (13.5-17.7)	18.5 (16.6-20.7)
434	4	62	20.8 (15.8-23.2)	17.1 (15.7-19.3)	0			
435	3	441	15.0 (14.5-16.1)	14.8 (13.3-15.9)	0			
436	4	421	17.2 (14.8-21.6)	13.4 (11.0-15.5)	0			
440	4	132	37.8 (30.5-43.8)	31.2 (28.9-34.7)	0			
444	6	162	33.7 (22.1-45.2)	27.2 (23.8-30.8)	0			
645	3	55	28.5 (25.7-31.9)	20.6 (18.3-22.2)	2	81	17.4 (17-17.8)	18.7 (18.6-18.8)
648	4	122	24.7 (21.7-28.1)	21.0 (19.8-22.1)	0			

To maintain consistency during sample preparation, all sampled logs were cut along the longitudinal axis oriented in the north-south direction, leaving a 5 cm wide pith-to-bark section. The north-south direction was chosen since winds within the study area are predominantly easterly, and therefore, may induce the formation of reaction wood along the east-west direction. The planks were then stored in a conditioning chamber for 8 weeks where the relative humidity and temperature were maintained at 65% and 21°C, resulting in a nominal pre-test moisture content of 12%. Small clear specimens (knot-free test pieces measuring 1cm (radial axis) x 1cm

(tangential axis) x 15cm (longitudinal axis)) were cut from each log, allowing a minimum of 3 mm between each specimen and the number of annual rings and the distance (mm) from the pith to the ring at the centre of each specimen recorded. This yielded a total of 1527 small clear specimens for white spruce and 422 specimens for trembling aspen (Table 3). Log sections which yielded fewer than 3 small clear specimens were not included in the analyses. This occurred most often on sections collected from trembling aspen trees, either because the log diameters were too small or because the presence of heart-rot severely reduced the amount of defect-free wood. Wood stiffness was measured by subjecting the small clear specimens to a static three-point bending test using a MTS test machine which operated with a 5kN load cell. The small clear specimens were placed on two metal supports that were spaced at a distance of 140 mm. Following American Society for Testing and Materials (ASTM) D143 standards (1994), the load was applied on the tangential surface nearest the pith at a rate of 2 mm per second.

Table 3 Total number of logs and small clear samples collected from each log section.

Log Section	White spruce		Trembling aspen	
	Logs	Small clears	Logs	Small clears
BH	64	505	27	153
MB	46	362	24	148
CB	61	382	24	111
MC	59	278		

Note: BH = 1.3 m; MB, midpoint between base of live crown and base of stump; CB, base of live crown; and MC, midpoint between base of live crown and tree top.

2.2.2 Covariates for analyses

Measures of radial growth rate used in the analyses were: (1) overall mean ring width (OMRW; mm/year) and its reciprocal (ORPM; rings/mm), and (2) mean juvenile ring width (MJRW; mm/year) and its reciprocal (JRPM; rings/mm). The overall mean ring width for a given log section was obtained by dividing the distance from pith from the outer-most small clear sample by the number of rings from pith for the same sample. For mean juvenile ring width, the distance from pith for the small clear sample nearest the transition from juvenile wood to mature wood was divided by the number of rings from pith for the same sample. For BH log sections, the transition zone was estimated to be at ring 40. For all other log sections, the transition zone was estimated to be at ring 20. These estimates were based on a preliminary examination of the pith to bark trends for wood stiffness (Figures 2 and 3), which were corroborated by reports from the literature (Wang and Micko 1984; Middleton and Munro 2002).

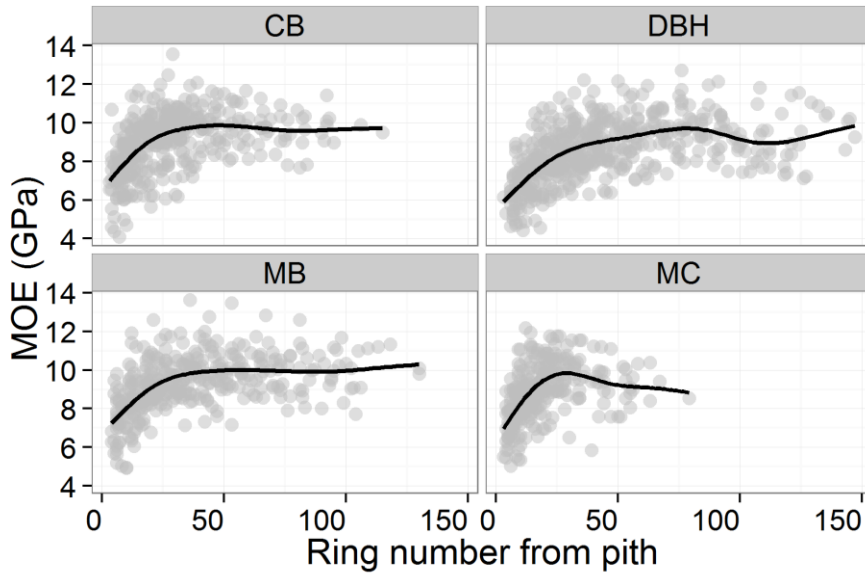


Figure 2 Pith to bark trends (solid lines) of MOE plotted against ring number from pith for white spruce. Trends are plotted by log section (CB = crown base, DBH = 1.3m, MB = mid-point between DBH and crown base, MC = mid crown). Circles represent observed values.

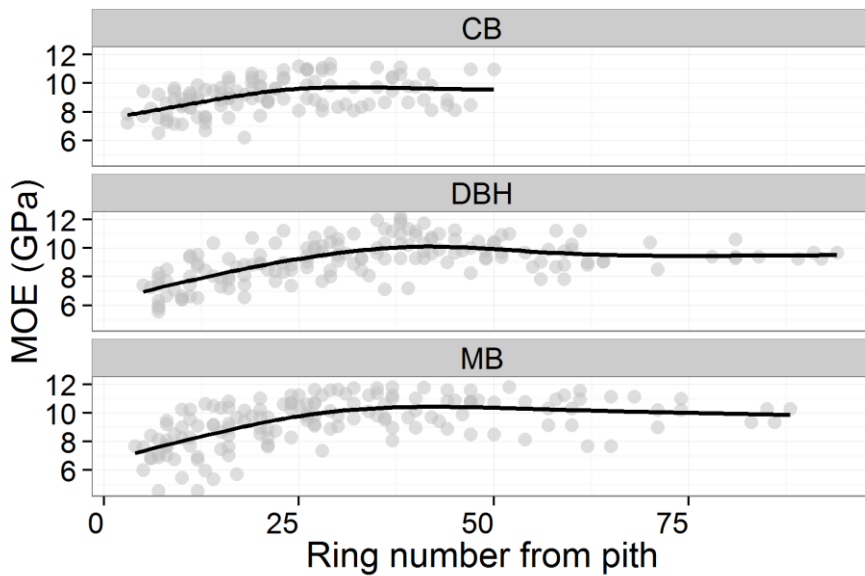


Figure 3 Pith to bark trends (solid lines) of MOE plotted against ring number from pith for aspen. Trends are plotted by log section (CB = crown base, DBH = 1.3m, MB = mid-point between DBH and crown base, MC = mid crown). Circles represent observed values.

Estimates of past tree slenderness (HHDR) were obtained following stem reconstruction. Specifically, height-age curves were created by plotting the height of each log sample against the ontogenetic age of the sample. Using the height-age curves, past height was estimated using the graphical method of stem reconstruction described by Dyer and Bailer (1987), though it is acknowledged that this approach tends to underestimate tree heights (Carmean 1972; Dyer and Bailer 1987; Machado et al. 2010). Past DBH was calculated from the distance from pith to every 5th ring on the BH section. Unfortunately, the distance from pith to every 5th ring was not recorded for aspen. Therefore, no estimates of past tree slenderness were available for this species. For both spruce and aspen, the vertical location of each log section relative to total tree height (RELHT) was also a covariate used in the analyses. A summary of the covariate symbols used in the analyses is provided in Table 4.

Table 4 List of covariates used in the analyses and associated descriptions.

Variable Symbol	Description
RFP	Cambial age, measured as the number of rings from pith
DFP	Tree size, measured as distance from the pith (cm)
RELHT	Height of log section relative to total tree height
OMRW	Mean ring width for the log section (mm/yr)
MJRW	Mean ring width for juvenile wood (mm/yr)
ORPM	1/OMRW
JRPM	1/MJRW
HHDR	Historical height-to-diameter ratio

2.2.3 Model screening

An initial screening phase was used to select an equation form appropriate to describe pith to bark wood stiffness in spruce and aspen. The screening phase consisted of comparing three

equations based on the Bayesian information criterion (BIC). The equations screened provided a different level of flexibility in the shape of the fitted regression. Two of the equations had previously been used to model radial patterns of wood stiffness and are described by Leban and Haines (1999) and Auty and Achim (2008). A third equation, the Mitscherlich equation, is described by Briggs 1925. There was no prior evidence of use of this equation for the purpose of modeling pith to bark wood stiffness. The base form of the Mitscherlich equation used during screening was:

$$\text{[Eq. 1]} \quad \text{MOE} = \text{MOE}_{max} (1 - \exp(-\exp(\gamma)(x - \text{offset})))$$

where MOE is as previously defined, MOE_{max} represents the asymptote of wood stiffness and γ is the rate of increase in wood stiffness towards the asymptote. Equation 1 contains a single base covariate, x , which may be offset from the intercept (through the *offset* parameter). Likewise, the equations of Leban and Haines (1999) and Auty and Achim (2008) were formulated to contain a single base covariate. For each species, the equations were fitted twice; once where the base covariate was the cambial age and once where the base covariate was the distance from pith. For simplification, the screening phase used only data from BH samples. For both spruce and aspen, Equation 1 was selected for further model development as it provided the lowest BIC values regardless of which base covariate was used.

2.2.4 Cambial age or tree size?

Following screening, it was necessary to determine if cambial age or tree size should be used as the base covariate. For this, Equation 1 was re-written to include a tree-level random effect on the rate parameter:

$$[\text{Eq. 2}] \text{MOE}_{sp,x,jl} = \left(\beta_{sp,0,x} \right) \left(1 - e^{\left(- \exp \left(\beta_{sp,1,x} + b_{sp,1,x,j} \right) \left(x_{sp,jl} + \beta_{sp,2,x} \right) \right)} \right) + \varepsilon_{sp,x,jl}$$

where $\beta_{sp,0,x}$, $\beta_{sp,1,x}$ and $\beta_{sp,2,x}$ are the fixed effect parameters for the asymptote, rate and offset, respectively. The subscript sp denotes the species (sw for spruce, or aw for aspen) and j denotes the tree to which the model was adjusted. The tree-level random effect, $b_{sp,1,x,j}$, was assumed to be normally distributed as $b_j \sim N(0, \Psi_1)$, where Ψ_1 is the variance-covariance matrix of the random effect. A positive definite diagonal variance-covariance matrix was used to model the random structure. The within-group errors were assumed independent and identically normally distributed ($\varepsilon_{jl} \sim N(0, \sigma^2)$) and were assumed to be independent of the random effects.

As was previously done, Equation 2 was fitted once using cambial age (subscript $x = \text{RFP}$) and once using distance from pith (subscript $x = \text{DFP}$). When $x = \text{RFP}$, subscript l is the l th ring from pith within tree j . When $x = \text{DFP}$, l is the l th centimeter from pith within tree j . The models were fitted using maximum likelihood parameter estimation methods.

Beginning with Equation 2 fitted using distance from pith, estimates of $b_{sp,1,DFP,j}$ (i.e., the empirical best linear unbiased predictor; EBLUP) were regressed on the mean juvenile ring width. A non-significant relationship was used to support the assertion that, regardless of growth rate, all trees share a similar rate of increase in wood stiffness and achieved maximum wood stiffness at the same distance from pith. Conversely, a significant negative relationship was used to support the assertion that the rate of increase in wood stiffness changes with growth rate. Therefore, the maximum wood stiffness of a tree is not tied to a specific tree size.

A similar and complementary set of arguments were formulated for the results of Equation 2 fitted using cambial age. Specifically, a non-significant relationship between b_{sp,l,RFP_j} and mean juvenile ring width was used as evidence that pith to bark patterns of wood stiffness are tied more closely to cambial age. This is because, regardless of tree size, the rate of increase in wood stiffness is the same, implying that maximum wood stiffness would be achieved at a specific cambial age. Conversely, a significant negative relationship would support the assertion that pith to bark development of wood stiffness is not tied to cambial age.

2.2.5 Models for pith to bark wood stiffness

The species-specific models for pith to bark wood stiffness were finalized following the selection of the base covariate. The final models for spruce and aspen were obtained after testing the addition of random effects for section (k), tree (j) and plot (i) to both the asymptotic and rate parameters in Equation 2. As before, the random effects were assumed to be normally distributed. Variance-covariance matrices associated with the plot ($\psi_{sp,i}$), tree ($\psi_{sp,ij}$) and section ($\psi_{sp,ijk}$) random effects were modeled using a diagonal structure which assumed independence among the different grouping levels. A more general but parameter intensive positive-definite variance-covariance matrix was also tested but failed to significantly improve the models. In addition, within-group independence of random effects were assumed. Finally, residual errors for the models were assumed to be independent for different i, j, k and independent of the random effects. Correlation among individual measurements within a tree were dealt with by using a mixed autoregressive moving average correlation structure, which is an appropriate structure for unequally spaced observations (Pinheiro and Bates 2000).

The inclusion of covariates for slenderness (spruce only), mean radial growth rate and relative position in the stem to the models came after each was systematically tested as an additive effect on the asymptote and rate parameters. The importance of the covariates were assessed using Wald-type significance tests and evaluated at the probability level of $\alpha = 0.05$. A random effect was dropped if its 95% confidence limits overlapped with zero or if its standard deviation was small (<5%) relative to the associated fixed effect parameter (Pinheiro and Bates 2000). Fit statistics used to evaluate the models were root mean square error (RMSE), RMSE in percent and the adjusted- R^2 which was calculated following the equations provided by Groot and Schneider (2011). All mixed-effect models were fit using maximum likelihood methods within the nlme package in R (R Core Team 2012; Pinheiro et al. 2013).

2.3 Results

2.3.1 Cambial age or tree size?

For both spruce and aspen, fit statistics for Equation 2 were slightly better for cambial age (spruce: RMSE = 1.03, $R^2 = 0.55$; aspen: RMSE = 0.98m, $R^2 = 0.58$) than for tree size (spruce: RMSE = 1.13, $R^2 = 0.46$; aspen: RMSE = 2.77, $R^2 = 0.40$). With tree size (i.e., DFP) as the base covariate in the model for spruce, there was a significant negative relationship between the estimated tree-level random effect (i.e., the empirical best linear unbiased predictor; EBLUP) ($b_{sw,l,DFP,j}$) and mean juvenile ring width (adjusted $R^2 = 0.25$, p-value < 0.05) (Figure 4). With cambial age as the base covariate, no relationship was observed between the random effect ($b_{sw,l,RFP,j}$) and mean juvenile ring width (adjusted- $R^2 = 0.01$, p-value>0.05), which corroborated with the result obtained using tree size. For aspen, the results were similar. Using tree size, the random effect ($b_{aw,l,DFP,j}$) was negatively related to mean juvenile ring width (adjusted $R^2 = 0.15$,

p-value < 0.05). In accordance, no relationship was noted between the random effect ($b_{aw,1,RFP,j}$) and mean juvenile ring width when the model was fitted using cambial age as the base covariate.

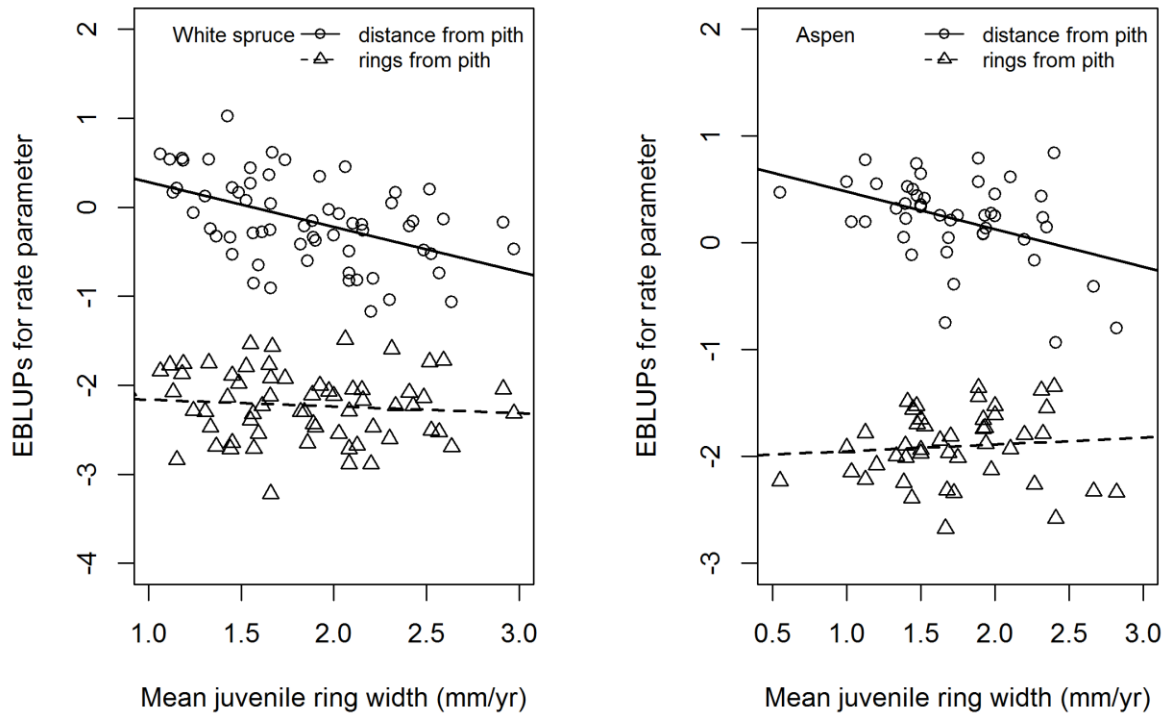


Figure 4 Relationship between the estimated random effect (empirical best linear unbiased predictor = EBLUP) for the rate parameter in Equation. 2 and the mean juvenile ring width for white spruce and aspen. Relationships are shown for the EBLUPs for individual trees generated using rings from pith (circles with solid regression line) or distance from pith (triangles with dashed regression line) in Equation 2.

2.3.2 Final mixed effect models

Using cambial age, the final model for pith to bark wood stiffness for spruce was:

[Eq. 3]

$$\text{MOE}_{sw,ijkl} = \left(\beta_{sw,0} + b_{sw,0,i} + b_{sw,0,ij} + b_{sw,0,ijk} + \beta_{sw,1}^{\text{HHDR}}_{ijk} + \beta_{sw,2}^{\text{ORPM}}_{ijk} \right) \left(1 - e^{-\left(\beta_{sw,3} + b_{sw,3,j} + \beta_{sw,4}^{\text{RELHT}}_{ijk} \left(\text{RFP}_{ijkl} + \beta_{sw,5} \right) \right)} \right) + \varepsilon_{sw,ijkl}$$

while that for aspen was:

[Eq. 4]

$$\text{MOE}_{aw,ijl} = \left(\beta_{aw,0} + b_{aw,0,j} \right) \left(1 - e^{-\left(\beta_{aw,1} + b_{aw,1,i} + b_{aw,1,ij} + \beta_{aw,2}^{\text{RELHT}}_{ijk} \left(\text{RFP}_{ijkl} + \beta_{aw,3} \right) \right)} \right) + \varepsilon_{aw,ijl}$$

where $\text{MOE}_{sp,ijkl}$ is the estimated wood stiffness on the l th ring from pith, in the k th section, in the j th tree within the i th plot for either spruce ($sp = sw$) or aspen ($sp = aw$). The $b_{sw,0}$ and $b_{sw,3}$ and the $b_{aw,0}$ and $b_{aw,1}$ are the random effects for the asymptote and rate parameters in Equations 3 and 4, respectively. All other variables are as previously defined. Covariates in the final models were significant according to Wald-type tests (Table 5). Plots of observed versus fitted values (conditioned on the random effects) showed good agreement across all values of wood stiffness for both spruce and aspen. Plots of the normalized residuals against fitted values showed no obvious systematic biases for either spruce or aspen (Figure 5). For spruce, the correlation between the asymptote and the rate parameters conditioned on the fixed and random effects revealed a small, positive relationship ($r=0.13$). For aspen, the relationship was found to be negative ($r=-0.24$).

Table 5 Estimated fixed-effects (standard deviation in parentheses) and associated random effects (with 95% confidence intervals) from Equations 3 and 4. *P*-values for fixed effects are generated from Wald-type tests.

White Spruce			Trembling aspen		
Fixed Effects	Estimated coefficient	<i>P</i> -value	Fixed Effects	Estimated coefficient	<i>P</i> -value
$\beta_{sw,0}$ (asymptote)	8.12 (0.411)	<0.001	$\beta_{aw,0}$ (asymptote)	10.23 (0.20)	<0.001
$\beta_{sw,1}$ (HHDR)	1.15 (0.305)	<0.001	$\beta_{aw,1}$ (rate)	-2.64 (0.14)	<0.001
$\beta_{sw,2}$ (ORPM)	1.00 (0.511)	0.048	$\beta_{aw,2}$ (RELHT)	0.328 (0.10)	<0.003
$\beta_{sw,3}$ (rate)	-2.63 (0.061)	<0.001	$\beta_{aw,3}$ (offset)	-9.62 (2.01)	<0.001
$\beta_{sw,4}$ (RELHT)	0.98 (0.086)	<0.001			
$\beta_{sw,5}$ (offset)	-6.62 (0.725)	<0.001			

White Spruce			Trembling aspen		
Random Effects	Estimated Std dev.	95% CI	Random Effects	Estimated Std dev.	95% CI
$\sigma_{b_{sw,0i}}$	0.61	0.38-0.96	$\sigma_{b_{aw,0j}}$	0.74	0.49-1.13
$\sigma_{b_{sw,0ij}}$	0.40	0.25-0.65	$\sigma_{b_{aw,1i}}$	0.13	0.06-0.31
$\sigma_{b_{sw,0ijk}}$	0.36	0.15-87	$\sigma_{b_{aw,1ij}}$	0.12	0.05-0.29
$\sigma_{b_{sw,3j}}$	0.20	0.14-0.26	$\sigma_{\varepsilon_{aw,jl}}$	0.91	0.80-1.02
$\sigma_{\varepsilon_{sw,ijkl}}$	0.89	0.78-1.02			

Note: HHDR, historical height-to-diameter ratio; ORPM, overall rings·mm⁻¹; RELHT, relative vertical height. White spruce (sw), n = 1527, i = 15 plots, j = 64 trees, k = 229 sections; trembling aspen (aw), n = 422, i = 8 plots, j = 27 trees.

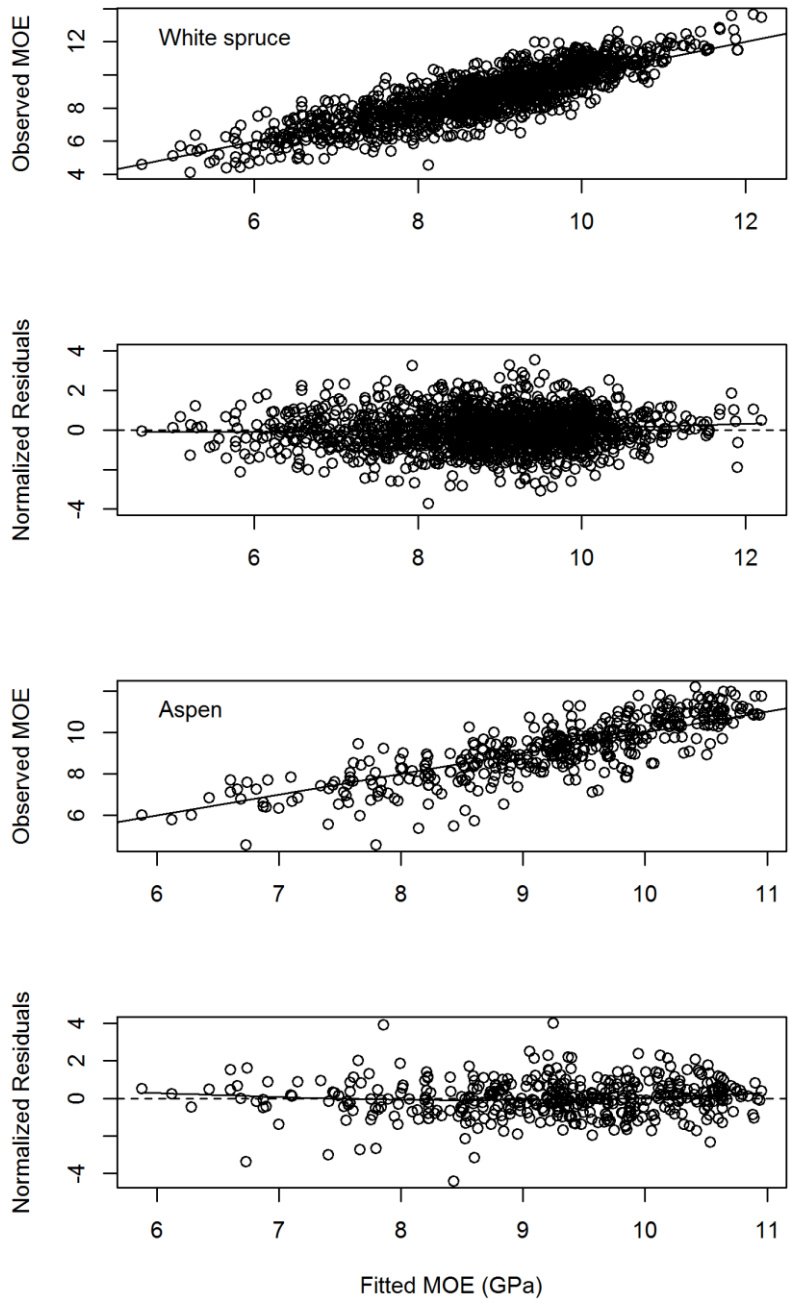


Figure 5 Plots of observed versus model predicted values of MOE (GPa) (solid line is the 1:1 relationship), and normalized residuals versus model predicted values of MOE (GPa) (solid line is loess function; dashed line is zero bias).

For spruce, predictions of pith to bark wood stiffness from the fixed effects component of the model (Figure 6) explained 39% of the variability, while RMSE and RMSE in percent was 1.17 and 13%, respectively. The random effects for plot, tree and section explained an additional 10%, 15% and 4% respectively (total adjusted- R^2 for fixed + random effects = 67%). For aspen, model predictions from the fixed-effects (Figure 7) explained 34% of the variability, while the RMSE and RMSE in percent was 1.15 and 12%, respectively. Plot and tree level random effects explained an additional 5% and 25%, respectively (total adjusted- R^2 for fixed + random effects = 64%). Any variability between sections in aspen were accounted for by the covariate for relative height (RELHT), thus, section level random effects were not included.

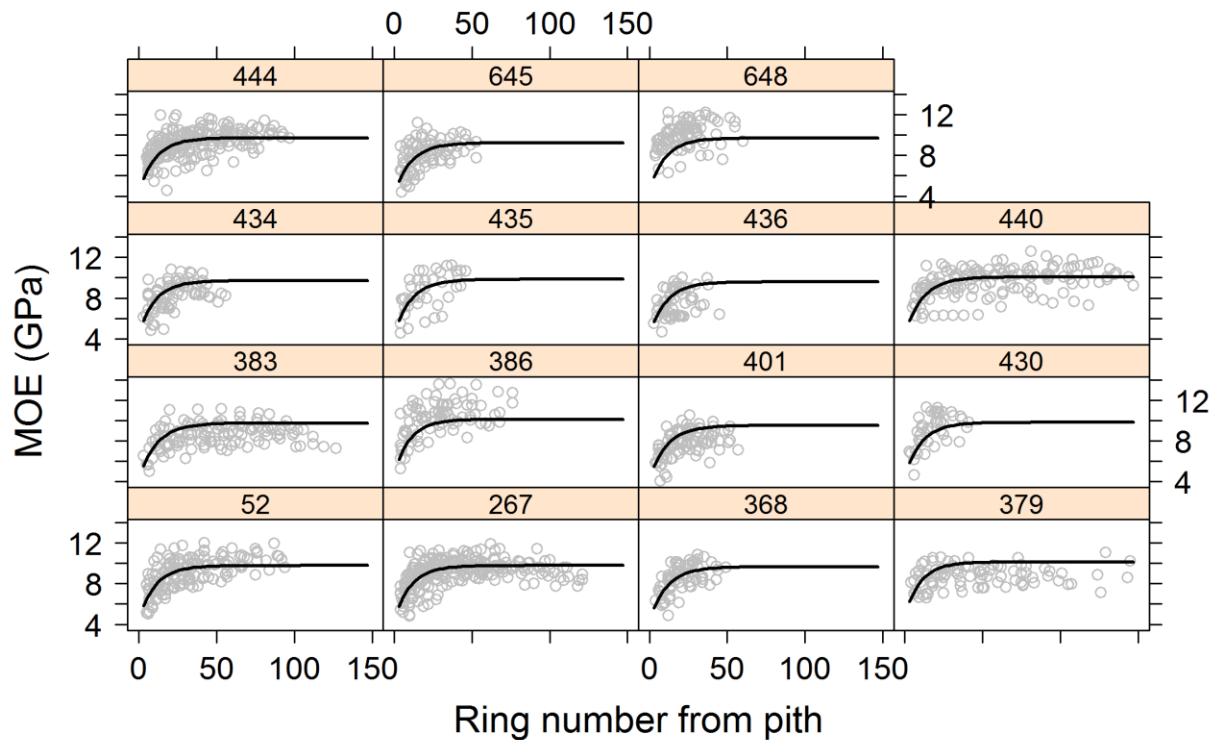


Figure 6 Plot showing model predicted MOE (GPa) from the fixed effects component of the model for white spruce. Numbers at the top represent a sample plot. Circles are observed values of MOE.

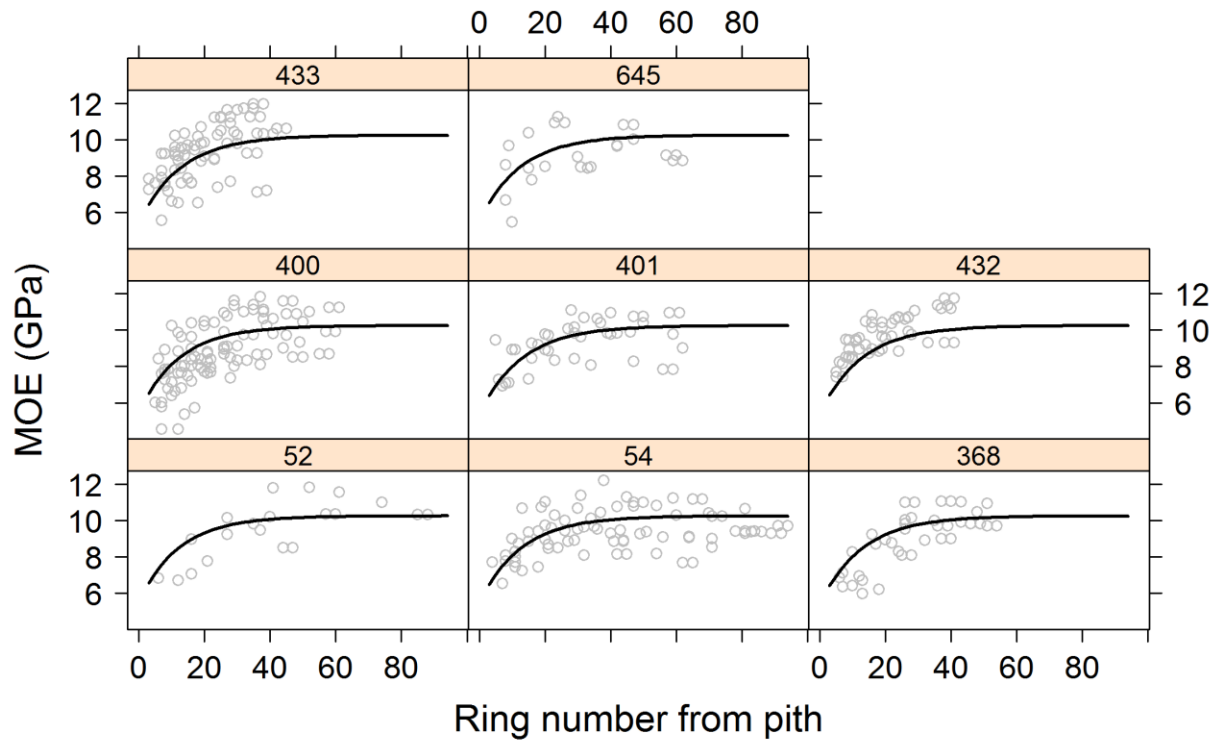


Figure 7 Plot showing model predicted MOE (GPa) from the fixed effects component of the model for aspen. Numbers at the top represent a sample plot. Circles are observed values of MOE.

For both spruce and aspen, the coefficient for relative height indicated that higher rates of increase in wood stiffness occurred with increasing height within the tree (Figure 8). For spruce, an increase in tree slenderness (HHDR) and a decrease mean radial growth rate (i.e., increasing ORPM) both resulted in an increase in wood stiffness in the mature wood zone (Figure 8). The relative effect of either covariate on wood stiffness appeared similar.

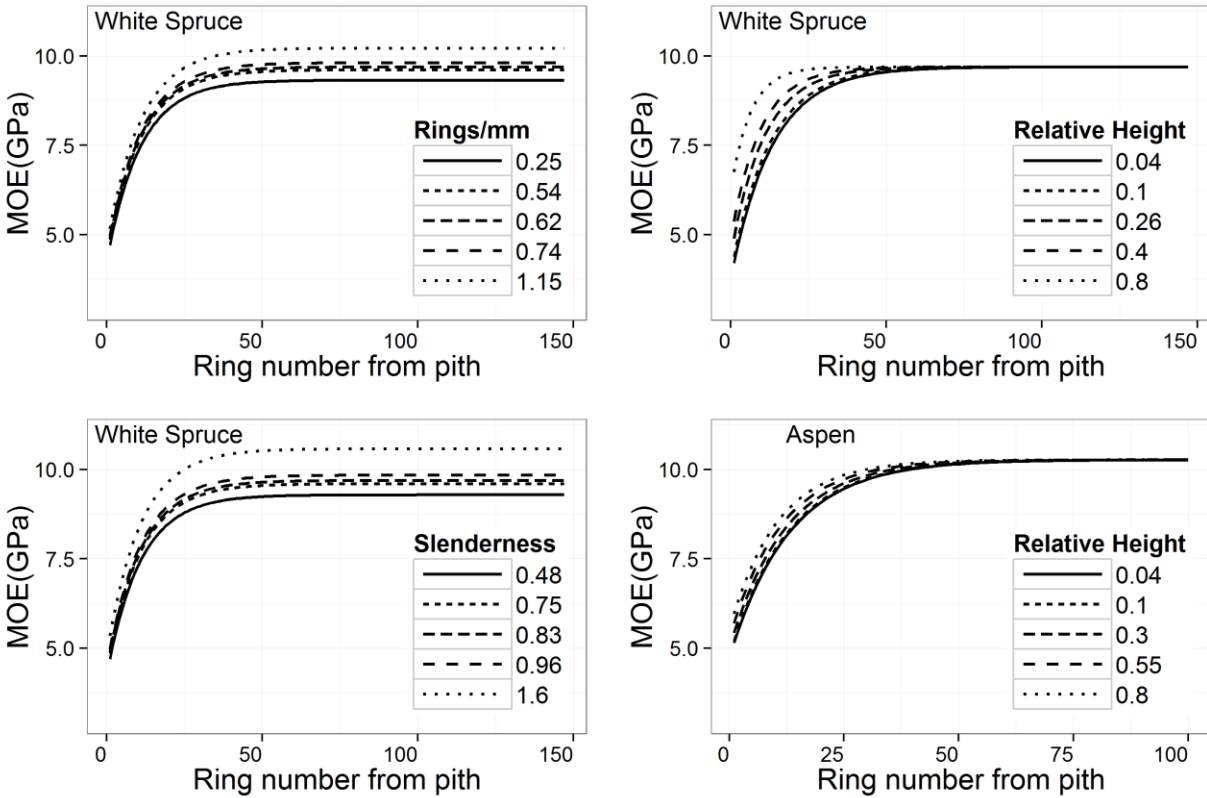


Figure 8 Model predictions of MOE (GPa) for different levels of relative height (spruce and aspen), slenderness (spruce only), and rings/mm (spruce only) while holding other covariates constant. Simulated levels represent the minimum, 1st quartile, mean, 3rd quartile and maximum values observed for the respective covariates.

2.4 Discussion

2.4.1 Cambial age or tree size?

The decision to model pith to bark wood stiffness as a function of cambial age or tree size carries with it considerable biomechanical implications (Lachenbruch et al. 2011). Unfortunately, the reasoning behind the selection of one covariate over the other has rarely been discussed in the literature. For future studies of pith to bark wood stiffness or other wood property, it is

recommended that, at minimum, the statistical merit of each covariate be presented. When possible, decisions based on statistical merit should be further supplemented with evidence of hydraulic or mechanical constraints which favour the selection of one covariate over the other.

The approach used here was a modification of that used by Kojima et al (2009), where radial patterns of fibre length were examined for various hardwood species. The current study modified this approach by examining the relationship of the rate-governing parameter against a continuous variable, rather than arbitrarily defined tree diameter classes as was done by Kojima et al (2009). For the current study, basic fit statistics from the initial model for pith to bark wood stiffness (i.e., Equation 2) indicated that cambial age was a superior variable to tree size for both spruce and aspen. However, for both species, the improvement in model performance was not overly convincing. Greater support for the use of cambial age came following an examination of the tree-level random effects against the mean juvenile radial growth rate. The results of the latter analysis showed that for two trees of a similar age but different size, the rate of increase in wood stiffness from pith to bark will be lower for the larger of the two trees.

The result suggest that the adaptive pressures acting on spruce and aspen seem to have resulted in a preferential association between wood stiffness and cambial age for both species. This is somewhat surprising given the stark contrast in growth strategies employed by the two species. While not measured for this study, it seems likely that as result of their different growth strategies, hydraulic and mechanical constraints experienced by spruce and aspen are also quite different. Quantifying these constraints for spruce and aspen is necessary if a biomechanical explanation for the current set of findings is desired.

2.4.2 Final models for pith to bark wood stiffness

The finding that the rate of increase from pith to bark in wood stiffness was lower near the base of the tree than near the top of the tree for spruce and aspen is in line with the findings from previous studies. Both Watt et al. (2011) and Antony et al. (2012) suggested that the underlying cause for the observed trend was the faster rate of decrease in microfibril angle for stem sections near the tree apex. For aspen, the trends in wood stiffness may also be related to fibre length. Fibre length has been shown to be positively correlated with mechanical properties in *populus* clones (DeBell et al. 2002), while Koubaa et al. (1998) noted that for hybrid aspen, fibre length within the first 8 annual rings increased with increasing height within the tree. Additionally, Gartner et al. (1997) found that the ratio of fibres to vessels increased with increasing height within red alder (*Alnus rubra* Bong.). This, in turn, would result in greater wood stiffness near the apex of the tree.

Despite the previous studies on wood stiffness, the advantages conferred by having a higher rate of increase in wood stiffness near the tree apex than near the base of the stem remain speculative. One argument is that it is an adaptive response to the presence of knots. Knots compromise the mechanical properties of wood (Samson and Blanchet, 1992). Since knot frequency increases with increasing position within the tree for both spruce and aspen, there is likely a need to offset the risk of stem breakage by forming wood with increased stiffness. Such a response may partially explain the current set of observed trends. Indeed, a similar suggestion was posed with respect to observed increases in modulus of rupture with increasing height for white spruce (Middleton and Munro, 2002). However, for aspen, a similar hypothesis has not been put forth.

Clearly, further work is need to examine the link between vertical trends in the radial patterns of wood stiffness and the evolutionary advantages that this may confer.

Including a dynamic measure of tree slenderness in the final models for wood stiffness is unique in the sense that previous models for wood stiffness tested tree slenderness at the time of sampling. Models which use this latter approach assume that tree slenderness does not change over time. For spruce and aspen in unmanaged mixedwood stands, this is unlikely given the complex and changing growing conditions. The approach used to calculate past tree slenderness was made possible due the sampling of logs at different heights within the tree. Furthermore, it was important that both distance and ring number from pith be demarcated at regular intervals. Failure to do so for the aspen trees sampled was a shortcoming.

The results for spruce indicate that more slender trees will have greater wood stiffness within the mature wood zone. This is in agreement with Watt and Zoric (2010), who found that the slenderness of radiata pine had a significant positive effect on the stiffness of mature wood. However, unlike the current study, stem slenderness was also found to influence wood stiffness within the juvenile wood zone. For loblolly pine, Antony et al. (2012) noted that increased slenderness had a positive effect on the rate of increase of wood stiffness. However, wood stiffness in the mature wood zone achieved a similar level, regardless of tree slenderness.

From a silvicultural stand-point, the finding that stem slenderness has a significant effect on the stiffness of mature wood in spruce is encouraging. Various silvicultural practices have been shown to influence stem slenderness, including manipulation of planting density (Opio et al. 2000) and thinning (Bergqvist 1999). Among these practices, increasing the planting density appears to be the most practical for white spruce. Determining an appropriate target planting

density to achieve a desired wood stiffness could be accomplished by linking the model presented here to a growth simulator. Tree growth under different planting densities could then be simulated, with the output generated used as input into the model of wood stiffness.

In addition to stem slenderness, wood stiffness in the mature wood of spruce was also affected by the mean growth rate of the tree. The negative relationship that was observed between wood stiffness and mean growth rate has been reported for other coniferous species (Kliger et al. 1998; Leban and Haines 1999; Steffenrem et al. 2009). In general, the relationship between radial growth rate and wood stiffness is said to be moderate to strong (Leban and Haines 1999). The connection between radial growth and wood stiffness is said to be primarily through changes in the microfibril angle, which decrease as radial growth rate decreases (Auty et al. 2013). However, the specific gravity of wood has also been described as an underlying factor. Cown et al. (1999), for example, noted that microfibril angle and specific gravity both influenced wood stiffness within the juvenile zone in radiata pine. However, only specific gravity was found to have a significant effect on stiffness within the mature wood. For white spruce, Park et al. (2012) found that while growth rates within the first 19 rings affected microfibril angle, this did not translate into changes in wood stiffness. This would appear to be in agreement with the current set of results, given that radial growth rate was only found to have a significant effect on wood density in the mature wood zone. Silvicultural practices aimed at increasing the radial growth rate of older spruce (e.g., partial removal of aspen with understory protection of spruce) should, therefore, be carefully considered. For situations such as this, added gains in spruce volume may be offset by a reduction of wood stiffness.

Finally, the finding that growth rate did not affect the pith to bark wood stiffness in aspen is in line with reports from hybrid poplars (Matyas and Peszlen 1997; De Boever et al. 2007; and Yu et al. 2008). Consequently, silvicultural efforts to increase growth rates in aspen should not adversely affect wood stiffness.

2.5 Conclusions

The decision to model pith to bark wood stiffness in white spruce and aspen as a function of cambial age or distance from pith was evaluated. Based on evidence from an analysis that was derived from Kojima et al. (2009), it appears that pith to bark wood stiffness in spruce and aspen develops in closer association with cambial age than distance from pith. The final models for pith to bark wood stiffness indicated that wood stiffness tended to increase with increasing position within the stem for both spruce and aspen. For white spruce, increased slenderness and a decrease in radial growth rate result in an increase in wood stiffness. For aspen, no other covariates were found to affect wood stiffness.

References

- Alberta Sustainable Resource Development (ASRD). 2005. Permanent sample plot field procedures manual. Public Lands and Forest Division, Forest Management Branch, Edmonton, Alberta, 30p.
- Alteyrac, J., Cloutier, A., and Zhang, S. 2006. Characterization of juvenile wood to mature wood transition age in black spruce (*Picea mariana* [Mill.] BSP) at different stand densities and sampling heights. *Wood Sci. Technol.* **40**: 124-138.
- Alvarez-Clare S. 2005. Biomechanical properties of tropical tree seedlings as a functional correlate of shade tolerance. MSc thesis, University of Florida, Gainesville, FL, USA.
- ASTM. 1994. ASTM D-143 standard test methods for small clear specimens of timber. ASTM International, West Conshohocken, Pa.
- Antony, F., Schimleck, L.R., Jordan, L., Daniels, R.F., and Clark, Alex., III. 2012. Modeling the effect of initial planting density on within tree variation of stiffness in loblolly pine. *Ann. For. Sci.* **69**: 641-650.
- Auty, D., and Achim, A. 2008. The relationship between standing tree acoustic assessment and timber quality in Scots pine and the practical implications for assessing timber quality from naturally regenerated stands. *Forestry* **81**: 475-487.
- Auty, D., Gardiner, B.A., Achim, A., Moore, J.R., and Cameron, A.D. 2013. Models for predicting microfibril angle variation in Scots pine. *Ann. For. Sci.* **70**: 209-218.

- Beckingham, J.D., and Archibald, J.H. 1996. Field guide to ecosites of northern Alberta. Northern Forestry Centre, Forestry Canada, Northwest Region. Spec. Rep. 5.
- Bergqvist, G. 1999. Stand and wood properties of boreal Norway spruce growing under birch shelter. Acta Universitatis Agriculturae Sueciae – Silvestria, Issue: 108, 85 pp.
- Briggs, G.E. 1925. Plant yield and the intensity of external factors – Mitscherlich's 'Wirkungsgesetz'. Annals of Botany, Vol 39: 475-502
- Bruechert, F., and Gardiner, B. 2006. The effect of wind exposure on the tree aerial architecture and biomechanics of sitka spruce (*Picea sitchensis*, Pinaceae). Am. J. Bot. **93**: 1512-1521.
- Carmean, W. 1972. Site Index Curves for Upland Oaks in Central States. For. Sci. **18**: 109-120.
- Castéra, P., Faye, C., and El Ouadrani, A. 1996. Previsions of the bending strength of timber with a multivariate statistical approach. Annals of Forest Science 53: 885-896.
- Cowdrey, D.R. and Preston, R.D. 1966. Elasticity and microfibrillar angle in the wood of Sitka spruce. Proceedings from the Royal Society of London. Series B, Biological Sciences. 66: 245-272
- Cown, D.J., Hebert J., Ball R. 1999. Modelling *Pinus radiata* lumber characteristics. Part 1: mechanical properties of small clears. NZ J For Sci 29:203–213.
- De Boever, L., Vansteenkiste, D., Van Acker, J., and Stevens, M. 2007. End-use related physical and mechanical properties of selected fast-growing poplar hybrids (*Populus trichocarpa* x *P-deltoides*). Ann. For. Sci. **64**: 621-630.

- Dyer, M., and Bailey, R. 1987. A Test of 6 Methods for Estimating True Heights from Stem Analysis Data. *For. Sci.* **33**: 3-13.
- Evans, R., and Ilic, J. 2001. Rapid prediction of wood stiffness from microfibril angle and density. *Forest Products Journal*, 51: 53-57.
- Gartner, B.L. 1995. Patterns of xylem variation within a tree and their hydraulic and mechanical consequences. In B. L. Gartner, ed. *Plant Stems: Physiology and Functional Morphology*, pp. 125-149. Academic Press, San Diego, CA.
- Gartner, B.L., Lei, H., and Milota, M.R. 1997. Variation in the anatomy and specific gravity of wood within and between trees of red alder (*Alnus rubra* Bong). *Wood Fiber Sci.* **29**: 10-20.
- Groot, A. and Schneider, R. 2011. Predicting maximum branch diameter from crown dimensions, stand characteristics and tree species. *The Forestry Chronicle* 7: 542-551.
- Jordan, L., Re, R., Hall, D.B., Clark, Alexander, III, and Daniels, R.F. 2006. Variation in loblolly pine cross-sectional microfibril angle with tree height and physiographic region. *Wood Fiber Sci.* **38**: 390-398.
- Kliger, I.R., Perstorper, M., and Johansson, G. 1998. Bending properties of Norway spruce timber. Comparison between fast- and slow-grown stands and influence of radial position of sawn timber. *Ann. Sci. For.* **55**: 349-358.
- Kojima, M., Yamamoto, H., Yoshida, M., Ojio, Y., and Okumura, K. 2009. Maturation property of fast-growing hardwood plantation species: A view of fiber length. *For. Ecol. Manage.* **257**: 15-22.

- Koubaa, A., Hernandez, R.E., Beaudoin, M., and Poliquin, J. 1998. Interclonal, intraclonal, and within-tree variation in fiber length of poplar hybrid clones. *Wood Fiber Sci.* **30**: 40-47.
- Kubo, T., and Koyama, M. 1993. Maturation Rate of Tracheid Lengthening in Slow-Grown Young Sugi (*Cryptomeria-Japonica*) Trees. *Iawa Journal* **14**: 267-272.
- Lachenbruch, B., Moore, J.R., and Evans, R. 2011. Radial Variation in Wood Structure and Function in Woody Plants, and Hypotheses for Its Occurrence.
- Leban, J.M., and Haines, D.W. 1999. The modulus of elasticity of hybrid larch predicted by density, rings per centimeter, and age. *Wood Fiber Sci.* **31**: 394-402.
- Lenz, P., Cloutier, A., MacKay, J., and Beaulieu, J. 2010. Genetic control of wood properties in *Picea glauca* - an analysis of trends with cambial age. *Can. J. For. Res.* **40**: 703-715.
- Lundgren, C. 2004. Microfibril angle and density patterns of fertilized and irrigated Norway spruce. *Silva Fenn.* **38**: 107-117.
- Machado, S.d.A., Rodrigues da Silva, L.C., Figura, M.A., Teo, S.J., and Mendes Nascimento, R.G. 2010. Comparison of methods for estimating heights from complete stem analysis data for *Pinus taeda*. *Ciencia Florestal* **20**: 45-55.
- Matyas, C., and Peszlen, I. 1997. Effect of age on selected wood quality traits of poplar clones. *Silvae Genet.* **46**: 64-72.
- Middleton, G. R. and Munro, B. D. 2002. Wood density of Alberta white spruce - Implications for silvicultural practices. Forintek Canada Corp. Vancouver, BC. 66p.

- Opio, C., Jacob, N., and Coopersmith, D. 2000. Height to diameter ratio as a competition index for young conifer plantations in northern British Columbia, Canada. *For. Ecol. Manage.* **137**: 245-252
- Park, Y., Weng, Y., and Mansfield, S.D. 2012. Genetic effects on wood quality traits of plantation-grown white spruce (*Picea glauca*) and their relationships with growth. *Tree Genetics & Genomes* **8**: 303-311.
- Pinheiro, J.C., and Bates, D.M. 2000. Mixed-effects models in S and S-PLUS. Statistics and Computing Series, Springer-Verlag, New York.
- Pinheiro, J.C., Bates, D.M., DebRoy, S., Sarkar, D., and the R Development Core Team 2013. nlme: Linear and Nonlinear Mixed Effects Models. R package version 3.1-109. Available from www.R-project.org [accessed May 27, 2013].
- R Core Team. 2012. R: a language and environment for statistical computing. R Foundation for Statistical Computing, Vienna, Austria. ISBN 3-900051-07-0. Available from www.R-project.org [accessed May 27, 2013].
- Ricardo, P., Hein, G., and Lima, J.T. 2012. Relationship between microfibril angle, modulus of elasticity and compressive strength in *Eucalyptus* wood. *Ciencia y tecnologia*, **14**: 267-274.
- Samson, M., and Blanchet, L. 1992. Effect of Knots on the Flatwise Bending Stiffness of Lumber Members. *Holz Als Roh-Und Werkstoff* **50**: 148-152.
- Schneider, R., Zhang, S.Y., Swift, D.E., Begin, J., and Lussier, J. 2008. Predicting selected wood properties of jack pine following commercial thinning. *Can. J. For. Res.* **38**: 2030-2043.

- Steffenrem, A., Kvaalen, H., Hoibo, O.A., Edvardsen, O.M., and Skroppa, T. 2009. Genetic variation of wood quality traits and relationships with growth in *Picea abies*. *Scand. J. For. Res.* **24**: 15-27.
- Van Gelder, H. A., Poorter, L., and Sterck, F.J. 2006. Wood mechanics, allometry, and life-history variation in a tropical rain forest tree community. *New Phytologist* 171: 367-378.
- Waghorn, M.J., Watt, M.S., and Mason, E.G. 2007. Influence of tree morphology, genetics, and initial stand density on outerwood modulus of elasticity of 17-year-old *Pinus radiata* RID C-3813-2009. *For. Ecol. Manage.* **244**: 86-92.
- Wang, E.I.C., and Micko, M.M. 1984. Wood quality of white spruce from north central Alberta. *Can. J. For. Res.* **14**: 181-185.
- Watt, M.S., and Zoric, B. 2010. Development of a model describing modulus of elasticity across environmental and stand density gradients in plantation-grown *Pinus radiata* within New Zealand. *Can. J. For. Res.* **40**: 1558-1566.
- Watt, M.S., Zoric, B., Kimberley, M.O., and Harrington, J. 2011. Influence of stocking on radial and longitudinal variation in modulus of elasticity, microfibril angle, and density in a 24-year-old *Pinus radiata* thinning trial. *Can. J. For. Res.* **41**: 1422-1431.
- Yu, Q., Zhang, S.Y., Pliura, A., MacKay, J., Bousquet, J., and Perinet, P. 2008. Variation in mechanical properties of selected young poplar hybrid crosses. *For. Sci.* **54**: 255-259.

Chapter 3: Branch models for white spruce (*Picea glauca* (Moench) Voss) in naturally regenerated stands

3.1 Introduction

The link between branching characteristics and wood quality has been recognized for several tree species including black spruce (*Picea mariana* (Mill.) B.S.P.) (Benjamin et al. 2009), Norway spruce (*Picea abies*) (Colin and Houllier, 1991), Sitka spruce [*Picea sitchensis* (Bong.) Carr.] (Achim et al., 2006), Scots pine (*Pinus sylvestris* L.) (Mäkinen and Colin, 1999) and Douglas-fir [*Pseudotsuga menziesii* (Mirb.) Franco] (Maguire et al. 1994). This has motivated the development of a range of predictive models for different branch characteristics for several commercially important species. Many of these models use simple stand and tree-level measures to make predictions of branching characteristics and can, therefore, be incorporated into tree growth simulators which use the same set of measurements. The refinement of existing branch models, such the work by Hein et al. (2007) on Norway spruce and Auty et al. (2012) on Sitka spruce, is an indication of the importance of these models. White spruce (*Picea glauca* [Moench] Voss), which is located throughout much of the Canadian boreal forest region, is a commercially important species whose wood quality is known to be affected by branching characteristics. For example, through the use of computed tomography images, Tong et al. (2013) found that 7% of knots located on young plantation grown white spruce had the potential to downgrade from Select Structural to lower lumber grades.

Despite its economic importance, there are very few models that can be used by silviculturalists to predict branch characteristics for white spruce. The recent works by Groot and Schneider (2011) and Nemec et al. (2012) have helped to fill this gap. Nevertheless, there remains a need to develop models of branch characteristics for white spruce from stand-level and external tree characteristics, and in turn, integrate these models into growth simulators.

Groot and Schneider (2011) examined maximum branch diameter for white spruce, and developed regression-based equations using independent variables measured using remotely sensed data (e.g., LiDAR). The response variable was the average of the largest three branches within the crown (MBD). For white spruce, they found that when only tree-level variables were used, MBD increased with increasing tree height at a rate lower than other species examined, although similar to that of black spruce. Furthermore, MBD in white spruce displayed the highest positive response to increasing crown length indicating a strong age-related effect given that crown length is positively correlated with total tree age. MBD in white spruce also displayed a strong sensitivity to competition relative to the other species tested.

Rather than predict a single-tree average for maximum branch diameter, Nemec et al. (2012) describe a method which provides estimates of average branch diameter for branches within clusters, nested within shoots of different age classes which are in turn nested within trees. Using this hierarchical structure, Nemec et al. (2012) also present models for the number of clusters and the number of branches per cluster. For white spruce, branch diameters were found to increase with increasing distance from the tree apex and with increasing relative distance along an annual shoot. Additionally, two distance-dependent measures related to the proximity of neighbouring trees were significant, indicating the sensitivity of branch diameters to the effects

of local competition. Their model showed that there was a positive correlation between shoot age and branch shedding.

While the studies by Groot and Schneider (2011) and Nemeč et al. (2012) provide useful information with regards to white spruce branch characteristics, their wider use is somewhat limited. This is because they address a specific need and provide estimates on different scales. The former makes use of remotely sensed data and provides a single estimate of MBD per tree. The latter provides estimates of branch traits at the level of annual shoots, and requires a considerable amount of detailed information, including the age of shoots and the distance to the point of crown contact with neighbouring trees. The models presented by Nemeč et al. (2012) also employed a compound distribution under the assumption that branches grow in distinct clusters along shoots. However, the clustering of first order branches in mature white spruce grown in unmanaged stands is erratic, while nodal and internal branches are not easily distinguished. This leads to a further important distinction. Most of the data utilized by Groot and Schneider (2011) were from single species density management experiments. The white spruce data used by Nemeč et al. (2012) appear to be from single species stands, though it is unclear whether samples were from plantations, naturally regenerated stands, or both.

In contrast, the commercial harvest of white spruce within the Canadian boreal forest is mainly from naturally regenerated stands to which no silvicultural treatments have been applied. Furthermore, a large proportion of the harvested white spruce is obtained from mixed-species stands. Light environments within mixed-species stands differs from those of single species stands, which in turn has implications on crown dynamics. Garber and Maguire (2005), for example, reported shifts in the foliage distribution among three conifers when single species

stands were compared to mixed species stands. Differences in the amount of light received by the trees was cited as the underlying cause. The branch models presented by Garber and Maguire (2005) were able to account for the effects of species composition through the use of stand-level species composition index. However, for stands of white spruce and aspen, there is no strong consensus regarding which index of species composition to use. This may be because the light-changing effects on the crown are detectable only at the neighbourhood level. Thorpe et al. (2010), for example, noted that for interior spruce (*Picea glauca* × *engelmannii*), crown size decreased at a faster rate with increasing local density when the nearest competitors were composed of both shade tolerate and shade intolerant species versus conspecific competitors. Like Nemeč et al. (2012), the study by Thorpe et al. (2010) used distance-dependent measures of local competition, reinforcing the hypothesis that crown dynamics in boreal forests operate at the neighbourhood level.

Unfortunately, growth simulators used by silviculturalists are predominantly of the distance independent variety [e.g., mixedwood growth model (MGM) (Bokalo et al. 2005)]. Therefore, it would be preferable if branch models were built using independent variables already contained within these simulators. With this in mind, the objectives of the current study were to develop predictive models for: 1) branch frequency, 2) maximum branch diameter, 3) the diameter of all other branches and 4) branch angle. Through the development of these models, a further objective was to evaluate the marginal contribution of independent variables derived from the height to live crown. Such variables have shown considerable promise in branch modeling, however, they are not always collected in forest inventories. Evidence in favour of crown-derived variables could be used to build an argument for their inclusion in inventory sampling.

Additionally, the branch models developed here were used to test which, if any, stand-level indices of competition are useful in predicting branching traits for white spruce.

The set of tree and stand-level factors which influence the size of branches that limit the recovery of Select Structural or No. 1 grade lumber may be different from the factors affecting all other branches (Duchateau et al. 2013; Tong et al. 2013). For white spruce, lumber grading rules dictate that a maximum knot size of 12.5mm for a 50 mm-wide be permitted for No. 1 grade cut (NLGA 2003; Tong et al., 2013). Therefore, a final specification during model development was to provide an explicit link between the branch models and wood quality assessment guidelines. Specifically, an additional set of models for branch frequency and branch insertion angle were developed for branches with diameters ≥ 12.5 mm at the point of stem insertion. Within the literature, few branch models appear to have been developed under this intent.

3.2 Material and methods

3.2.1 Site description and measurements

Branch characteristics were determined for 65 white spruce trees located adjacent to 15 permanent sample plots (PSP). The PSPs, which had been installed by Alberta Sustainable Resource Development (ASRD, 2005), were situated within unmanaged stands that had established through natural regeneration. Although the selected PSPs spanned approximately 500 kilometers from east to west, climatic conditions over this region are reported to be similar (Beckingham and Archibald, 1996). All the sites sampled were classified to the ‘*reference*’ ecosite-type (i.e., upland forests with moderately well-drained, orthic-gray luvisolic soils, which generally transition from an aspen to white spruce overstory) of the central mixedwood natural subregion of Alberta, Canada (Beckingham and Archibald 1996). Given the common ecosite-

type, site index values were assumed to be relatively similar. In terms of total basal area ha^{-1} (Baha^{-1}), the sampled PSPs ranged from 25 to $56\text{m}^2 \text{ha}^{-1}$ and included spruce dominated stands ($>70\%$ of stand Baha^{-1}), mixtures of spruce and aspen (between 30 and 70% Baha^{-1} of each species), and aspen dominated stands ($>70\%$ of stand Baha^{-1}) with a white spruce understory (see supplementary material). The mean BH age of overstory trees within the PSPs ranged from 52 to 153 years, although the ages among white spruce trees within a PSP often varied by 10 or more years.

Selected trees were no more than 100 m from the adjacent PSP boundary and located within the same forest ecosite-type as that found within the PSP. The process of tree selection first involved defining the quartiles of the DBH range for white spruce trees within each PSP. This was done using measurements of DBH collected during the most recent inventory of the PSPs. A minimum of two trees with a DBH between the 2nd and 3rd quartile were then selected. Additionally, at least one other tree was selected which was larger than the DBH limit defined by the 3rd quartile. All sampled trees were free of major stem defects (e.g., missing tops, excessive lean); however, minor stem defects (e.g., leader-whip damage) were unavoidable. Following the measurement of DBH, trees were felled and branch measurements collected within the live crown. The base of the live crown was defined by the lowest living branch which was separated from the next living branch by no more than one whorl containing only dead branches. Total tree height was also recorded on the felled trees (Table 6).

Measurements were collected for all live branches with a diameter $\geq 5\text{mm}$ at the base of the branch (Table 7). To maintain consistency, measurements of branch diameter were taken at a distance from the main tree stem equal to the diameter of the branch at the point of stem

insertion. Calipers were used to record branch diameters < 50 mm while a diameter tape was used on larger branches. All measurements were taken to the nearest millimeter. The angle of branch insertion, measured with a protractor and taken to the nearest degree (°), was defined as the angle between the main stem and the branch (0° representing a vertical branch pointing toward the tree apex).

Table 6 Summary statistics for diameter at breast height (DBH), crown length (Cl), height to live crown (Htlcrn), and slenderness (Slc). Values are averages for the plot. Minimum and maximum values are in braces { }.

Plot	n	DBH (cm)	Cl (m)	Htlcrn (m)	Slc
52	6	28.9 {23.3-38.6}	16.85 {8.01-23.34}	8.26 {3.05-18.24}	0.83 {0.65-1.08}
267	6	39.8 {32.4-43.1}	20.45 {16.15-25.03}	11.41 {7.87-14.91}	0.80 {0.76-0.88}
368	4	17.7 {25.5-13.8}	12.36 {10.25-15.22}	3.3 {2.8-3.79}	0.88 {0.74-1.05}
379	4	35.9 {30.3-41.2}	13.29 {9.62-16.66}	17.2 {15.04-22.65}	0.84 {0.77-0.98}
383	3	39.1 {31.1-44.1}	22.14 {19.9-25.45}	6.99 {4.90-12.20}	0.74 {0.69-0.8}
386	6	21.2 {18.0-29.0}	10.24 {7.9-11.46}	9.31 {5.71-14.14}	0.93 {0.78-1.04}
401	5	22.9 {20.7-25.2}	13.39 {11.18-15.48}	3.93 {2.15-5.58}	0.75 {0.66-0.85}
430	3	17.0 {13.7-21.4}	12.53 {8.28-15.23}	3.09 {1.98-4.64}	0.88 {0.8-1.04}
434	4	20.8 {15.8-23.2}	11.97 {7.35-14.54}	5.35 {2.06-8.35}	0.82 {0.75-0.99}
435	3	15.0 {14.5-16.1}	12.82 {11.63-14.01}	2.08 {1.67-2.67}	0.99 {0.92-1.05}
436	4	17.2 {14.8-21.6}	11.3 {9.2-13.09}	2.37 {1.80-2.93}	0.78 {0.72-0.86}
440	4	37.8 {30.5-43.8}	21.89 {19.87-25.46}	9.36 {6.47-14.87}	0.83 {0.79-0.95}
444	6	33.7 {22.1-45.2}	17.9 {11.98-24.32}	9.68 {5.97-14.00}	0.81 {0.68-1.08}
645	3	28.5 {25.7-31.9}	14.07 {11.07-15.95}	6.75 {6.25-7.25}	0.72 {0.70-0.76}
648	4	24.7 {21.7-28.1}	12.19 {10.64-13.42}	8.86 {8.13-9.61}	0.86 {0.77-1.02}

Table 7 Summary statistics for branch diameter, maximum branch diameter (mm), number of branches (≥ 5 mm) per 1m section and branch angle for branches ≥ 5 mm diameter. Values are averages for the plot. Values in braces {} represent the minimum and maximum.

Plot	Branch Diameter (mm)	Maximum Diameter (mm)	Branch	No. of Branches (≥ 5mm) / 1m Section	Branch Angle (≥ 5mm)
52	23.68 {5-39.8}	27.32 {9.6-41.9}		10.97 {1-35}	75.28 {8-140}
267	24.06 {5.0-43.6}	29.54 {8.2-44.5}		10.69 {1-53}	82.9 {10-160}
368	13.12 {5.3-28.3}	18.14 {8.1-25.5}		17.38 {2-39}	72.92 {17-130}
379	27.83 {6.2-56.1}	36.07 {10.6-56.1}		9.72 {1-36}	78.99 {10-162}
383	28.45 {5.5-48}	33.14 {11.8-51.1}		8.78 {1-31}	69.21 {10-129}
386	17.03 {5-32.2}	22.65 {11.0-34.7}		15.20 {2-37}	77.45 {10-140}
401	18.95 {5-38.9}	22.76 {10.3-43.4}		13.0 {2-40}	78.94 {10-158}
430	13.61 {5-28.4}	20.52 {10.9-33.8}		13.71 {3-28}	78.91 {12-165}
434	16.63 {5.6-29.1}	22.29 {6-33.2}		13.55 {6-23}	81.82 {10-141}
435	12.44 {5.4-24.8}	16.31 {7.5-30.3}		13.41 {5-20}	87.21 {20-136}
436	16.7 {5.2-31.6}	21.78 {9-37.6}		14.35 {5-22}	84.84 {5-151}
440	25.33 {5.3-47.4}	30.52 {9.4-51.5}		10.52 {1-47}	73.43 {14-159}
444	22.25 {5.1-42.1}	26.81 {10.9-45.6}		11.18 {1-34}	73.7 {10-159}
645	20.5 {5-52.3}	25.56 {6-40.8}		19.3 {1-46}	70.69 {8-126}
648	17.25 {5.1-34.1}	21.63 {9.4-30.9}		18.36 {1-51}	73.37 {12-151}

3.2.2 Model building

Due to the nature of the sampling methods used when measuring branch-level variables, a hierarchical approach is often employed when fitting models of branch characteristics (Hein et al., 2007). Typically, branches are nested within whorls, whorls nested within trees and trees nested within plots. While the data structure for the current study includes trees within plots, it was not possible to clearly distinguish branch whorls for the white spruce trees sampled. Furthermore, a consistently clear distinction could not be made between nodal and internodal branches. Therefore, for modelling purposes the live crown was divided into 1 m sections,

starting from crown base. Since full crown lengths did not necessarily divide exactly into 1m sections, stem sections at the crown apex which were less than 1m were discarded from the model datasets.

For predictions of the number of branches per section, two set of models were developed. The first model was constructed to provide estimates of the total number of living branches with a diameter ≥ 5 mm. The second model was constructed to provide estimates of the total number of living branches per section with a diameter ≥ 12.5 mm (maximum allowable knot size for No 1 grade lumber for 50mm wide white spruce structural lumber). Within each 1m section, all live branches ≥ 5 mm in diameter were ranked in terms of their diameter relative to the largest (i.e. second largest branch per section had rank= 1, 3rd largest had rank= 2, etc.). This ranking was then tested as an independent variable in the branch-level models (i.e., relative diameter of smaller branches and branch angle). As was done for the number of branches per section, two models were developed for branch angle; one using all branches ≥ 5 mm and a second for all branches ≥ 12.5 mm.

Guiding the development of the models was the intention that they would eventually be incorporated into growth and yield simulators such to the Mixedwood Growth Model (MGM) (Bokalo et al. 2010; Bokalo et al., 2013), which is currently used in Alberta for the types of stands that were sampled. The covariates considered for inclusion, therefore, were those that are typically collected during standard forest inventories and which are used as input variables to initiate a growth cycle within simulators such as MGM (Table 8) for variable symbols and descriptions). The variable selection process began by fitting the models using only tree-level variables and no random effects. The ‘drop1’ function in the glm package for R (R Core Team

2013), was used to evaluate the marginal contribution of a given covariate given the presence of the other covariates in the model. When a pair of covariates were significant (assessed at $\alpha = 0.05$) but also highly correlated ($r^2 > 0.8$), only the covariate which provided the greatest improvement to the model (assessed using Akaike's information criterion [AIC]; Akaike 1974) was retained. Stand-level variables were then progressively added, with the covariates in the models re-evaluated upon each addition.

Table 8 Description of tree and stand-level variables tested in the branch models. Natural log transformations of the variables were also tested and are denoted in the text with the prefix 'ln'.

Symbol	Description
DBH	Diameter at 1.3m
TotalHt	Total tree height (m)
Cl	Length of live crown (m)
Cr	Crown ratio
HtLcrn	Height to base of live crown (m)
Slc	Height (m) / DBH (cm) (i.e., slenderness)
ScHt	Height to top of each 1m section (m) from base of tree
Dist	Difference between tree apex and top of 1m section (TotalHt – ScHt) (m)
RDist	Relative position of section in live crown (Dist/Cl)
Rank	Rank of the diameter of a branch relative to the largest branch within a 1m section
Bal	Basal area of larger trees ($\text{m}^2 \text{ha}^{-1}$)
Baha ⁻¹	Basal area of the stand ($\text{m}^2 \text{ha}^{-1}$)
PctSwBaha ⁻¹ ; PctAwBaha ⁻¹	Percent of stand basal area that is white spruce (Sw) and trembling aspen (Aw)
hL	Lorey's height; tree height weighted by basal area (m)
SwTopHt; AwTopHt	Top height for white spruce (Sw) and trembling aspen (Aw); calculated as the average height of the largest 100 trees ha^{-1} by DBH

With the fixed effect covariates selected, the models were then refit with random intercepts included for the hierarchical levels appropriate for the given dependent variable. For example, the model for maximum branch diameter (i.e., with a single estimate per section) included plot (p) and tree (t) -level random effects, while the model for the relative diameter of smaller branches (i.e., with a single estimate for each branch (l)) included, plot, tree, and section (s) - level random effects.

For models fit to count or binomial data (i.e., branch frequency and relative branch diameter), the final set of fixed-effect covariates retained in the mixed-model were all significant at $\alpha = 0.05$ level. For the models fit to continuous data (i.e., maximum branch diameter and branch angle), significance tests of the individual covariates are considered to be unreliable (Bolker et al., 2009). Thus, the decision to retain a variable was assessed using the leave-one-variable-out approach. A given covariate was dropped when AIC values between the full model (all covariates, plus fixed and random effects) and the reduced model (single covariate removed, plus fixed and random effects) differed by ≥ 10 (Burnham and Anderson 2002). If the final model for a given branch characteristic contained covariates derived from the measured crown length, then the model was refit without these variables in order to evaluate the contribution to the respective model. Evaluation of the models fitted with and without crown-derived measurements was done through the comparison of error statistics. Since the models were fit using datasets that included a wide range of tree sizes and ages, the need to extrapolate beyond the range of data tested was not a significant concern.

Variability in the dependent variable partitioned to the random effects was assessed through the calculation of adjusted- R^2 and visually through the use of plots of the random effects (i.e., the

conditional means) and associated prediction intervals (referred to as caterpillar plots). An examination of the residuals resulting from preliminary mixed-effect models indicated that autocorrelation was not significant for the branch characteristics being tested. Therefore, covariance structures appropriate for correlated data were not specified. The lmer function in the lme4 package (Bates et al. 2014) for R which fits generalized linear mixed-effect models (GLMMs) was used for this stage of model fitting.

The error statistics used to evaluate the performance of the fixed effect component of the models were calculated on the scale of the original data and included:

$$[\text{Eq. 5}] \quad \text{RMSE} = \sqrt{\frac{\sum (y_i - \hat{y}_i)^2}{n}} \quad \text{Root mean square error}$$

$$[\text{Eq. 6}] \quad \bar{E} = \frac{\sum (y_i - \hat{y}_i)}{n} \quad \text{Mean error}$$

$$[\text{Eq. 7}] \quad |\bar{E}| = \frac{\sum |y_i - \hat{y}_i|}{n} \quad \text{Mean absolute error}$$

$$[\text{Eq. 8}] \quad \text{RE}(\%) = \frac{\sum \left(\frac{|y_i - \hat{y}_i|}{\hat{y}_i} \right)}{n} \times 100 \quad \text{Relative error}$$

where y_i is the observed value and \hat{y}_i is the predicted value on the original scale for the i th observation ($i = 1, 2, \dots, n$), and n is the total number of observations used when fitting a given model. The RMSE provides a measure of the average magnitude of error and is in the units of measure of the dependent variable, while \bar{E} is the mean prediction bias. $|\bar{E}|$ is an unweighted

measure of precision and when compared to RMSE is used to assess the variance of the errors, while RE% is scale-independent measure used to evaluate the relative precision of the predictions. In addition, plots of the residuals against predicted values and the individual covariates included in the models were used to examine for possible prediction bias.

3.3 Results

3.3.1 Number of branches per stem section

Frequency plots of the number of branches per section revealed clear differences in the distribution of the number of sections containing branches $\geq 5\text{mm}$ and branches $\geq 12.5\text{mm}$ (Figure 9). The models for all branches $\geq 5\text{mm}$ and those $\geq 12.5\text{mm}$ were both fit using a Poisson distribution with a log-link function. No adjustment for overdispersion was needed as an examination of the Pearson residuals resulting from the two models showed that the estimated dispersion parameter was close to the assumed value of 1 (1.39 for Equation 9 and 1.31 for Equation 10) (Venables and Ripley 2002).

The model to predict the number of branches with a diameter $\geq 5\text{mm}$ per section ($NBrTot$) was:

$$[\text{Eq. 9}] \quad \ln(NBrTot_{pts}) = a_0 + a_1 \text{Dist}_{pts} + a_2 \text{Bal}_{pt} + \alpha_p + \alpha_{pt}$$

where a_0 is the population-average intercept, a_1 and a_2 are fixed effect parameters, and α_p , α_{pt} , are the random effects at the plot and tree level, respectively. Distance from the tree apex showed a negative relationship with the total number of live branches and provided a large improvement in model performance when compared to relative distance (model AIC with Dist = 1460, with RDist = 1730). The number of branches was also negatively related to the basal area of larger trees. The estimated variation explained by the fixed-effect component of the model was 60%

and increased to 73% with the addition of plot and tree-level random effects. This additional variation was largely attributable to between tree differences (Figure 10). Although overall mean bias was small (Table 9), plots of observed values against model predictions revealed a tendency to underestimate when the number of branches was higher than 30 per 1m section (Figure 11). This occurred mainly within the top 5m of the crown.

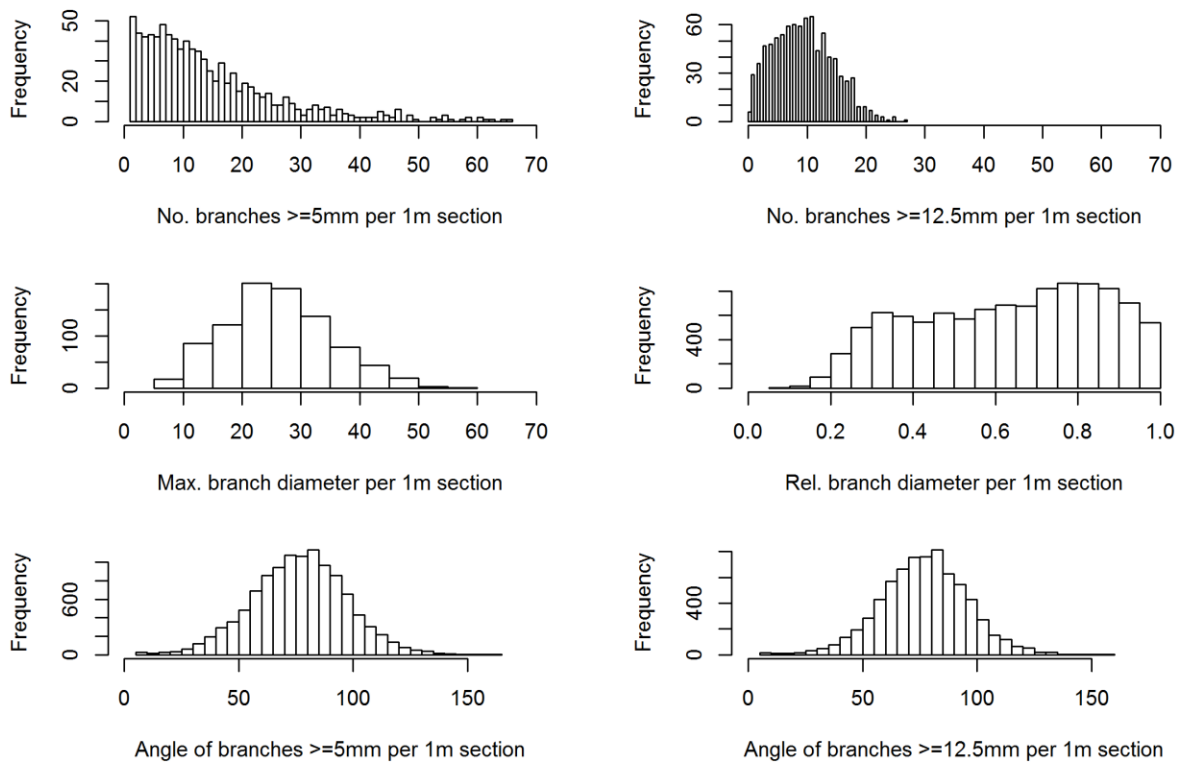


Figure 9 Frequency plots for branch characteristics. Graphs were generated from 15 plots, 64 trees and 874 1m sections.

Table 9 Estimated fixed effect parameters with standard errors and significance tests (p-value) for z-values for Equation 9 (No. branches $\geq 5\text{mm}$; $NBrTot$). Standard deviations of the random intercept for the plot and tree-level and estimated overdispersion parameter are listed with the error statistics from the fixed effects component (RMSE = root mean square error).

Parameters	Estimate	Standard error	p-value
a_0 – intercept	3.593	0.070	<0.000
a_1 – Dist	-0.118	0.002	<0.000
a_2 – Bal	-0.009	0.002	<0.000

Random effects	Standard deviation
Plot	0.127
Tree	0.167
Over-dispersion	1.391

Error Statistics	RMSE	Mean error	Absolute mean error	Relative error
$NBrTot$	5.453	-0.520	4.000	32.525

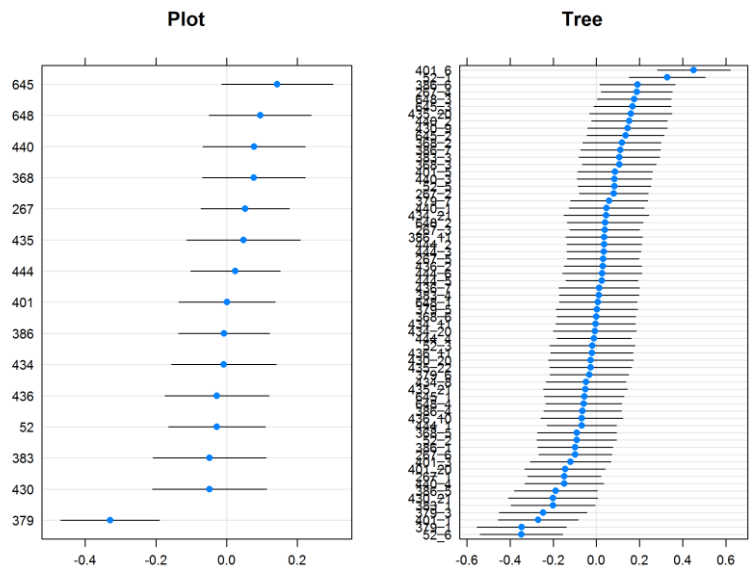


Figure 10 Caterpillar plots showing distribution of plot and tree level random effects for Equation 9 (No. branches $\geq 5\text{mm}$; $NBrTot$). Y-axis is the plot or tree number.

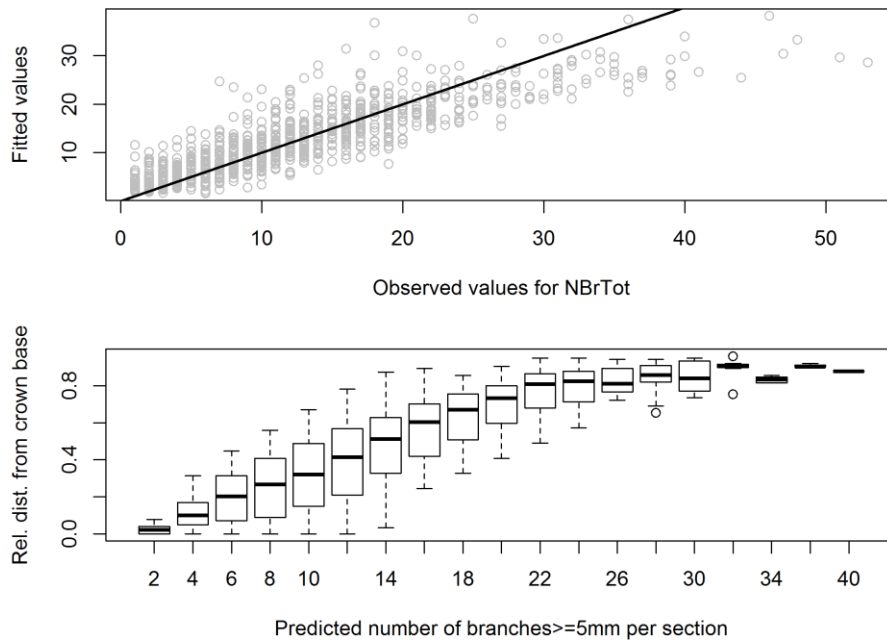


Figure 11 Fitted values from the fixed effect component of Equation 9 (No. branches ≥ 5 mm; $NBrTot$) versus observed values (top) and boxplot showing the range for the predicted number of branches ≥ 5 mm across relative distance into the crown.

For the prediction of the number of branches ≥ 12.5 mm per section ($NBrNo1Grd$), the model selected was:

[Eq. 10]

$$\ln(NBrNo1Grd_{pts}) = b_0 + b_1 Dist_{pts} + b_2 \ln RDist_{pts} + b_3 Cl_{pt} + b_4 Slc_{pt} + \beta_p + \beta_{pt}$$

where b_0 to b_4 are the parameters to be estimated for the given covariates, while β_p and β_{pt} are the random effects. Based on predictions from the final model, the number of branches ≥ 12.5 mm per 1m section first increased and then decreased with increasing distance from crown apex, peaking at a relative distance of approximately 20% from the tree top. There was a decrease in the number of branches ≥ 12.5 mm per section with increasing slenderness, while longer crowns

produced 1m sections with more branches $\geq 2.5\text{mm}$ diameter. From the Pseudo- R^2 calculations, the fixed part of the model explained 47% of the variation, increasing to 55% with the inclusion of the random effects. This was mainly due random variation between trees (Figure 12).

Predictions showed that stem sections with 10 to 12 branches $\geq 12.5\text{mm}$ could be found anywhere from the crown base to near the crown apex (Figure 13). There were no obvious trends in the residuals resulting from the fixed effects when examined against the covariates, while the mean error statistics indicated that overall, there was very little bias in the predictions (Table 10). The model, however, underestimated the number of branches $\geq 12.5\text{mm}$ when $\sim > 12$ branches were observed in a stem section (Figure 13). Without crown length, the error statistics from the fixed effect part indicated a nearly 11% decrease in the precision of the model and a decrease in the accuracy and increase in bias (Table 10).

Table 10 Estimated fixed effect parameters with standard errors and significance tests (p-value) for z-values for Equation 10 (No. branches $\geq 12.5\text{mm}$; *NoBrNoIGrd*). Standard deviations of the random intercept for the plot and tree-level and estimated overdispersion parameter are listed with the error statistics from the fixed effects component (RMSE = root mean square error).

Parameters	Estimate	Standard error	p-value	
	4.154	0.190	<0.000	
b_1 - Dist	-0.192	0.007	<0.000	
b_2 - lnRDist	0.836	0.047	<0.000	
b_3 - Cl	0.062	0.005	<0.000	
b_4 - Slc	-0.829	0.182	<0.000	
Random effects	Standard deviation			
Plot	0.026			
Tree	0.120			
Over-dispersion	1.31			
Error Statistics	RMSE	Mean error	Absolute mean error	Relative error
<i>NoBrNoIGrd</i> (with crown length)	3.745	0.061	2.916	34.441
<i>NoBrNoIGrd</i> (without crown length)	4.435	0.239	3.373	43.652

Simulated predictions from Equation 9 demonstrate how at the same distance from the crown base, a tree with a given DBH but in a higher social position will have more branches $\geq 5\text{mm}$ per section (Figure 14). Furthermore, the difference in the number of branches per section between a subordinate and dominant tree becomes greater with increasing distance from the crown base. Predictions from Equation 10 simulated for three levels of tree slenderness show that trees with greater taper will have more branches $\geq 12.5\text{mm}$ per section (Figure 14). Also, trees with short crowns will have more branches $\geq 12.5\text{mm}$ near crown base and will peak in the number of branches near mid-crown compared to a similar size tree with a longer crown, where the peak in the number of branches occurs at a distance equal to 75% from crown base.

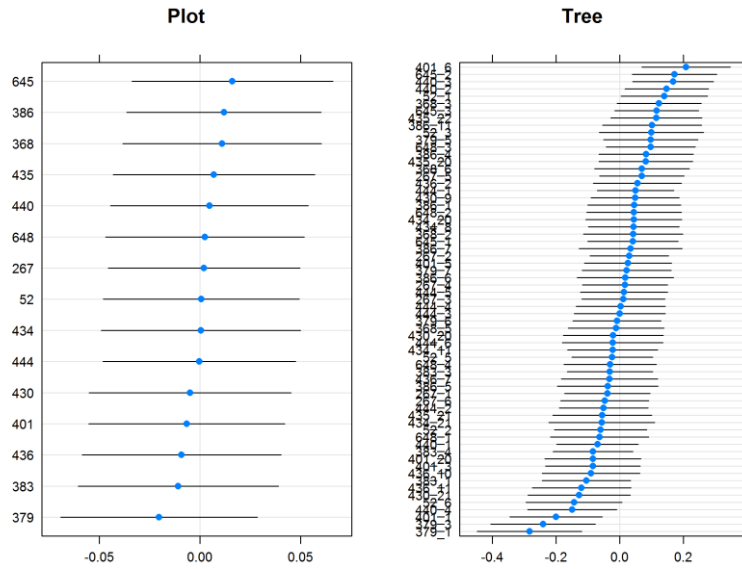


Figure 12 Caterpillar plots showing distribution of plot and tree level random effects for Equation 10 (No. branches $\geq 12.5\text{mm}$; *NBrNo1Grd*). Y-axis is the plot or tree number.

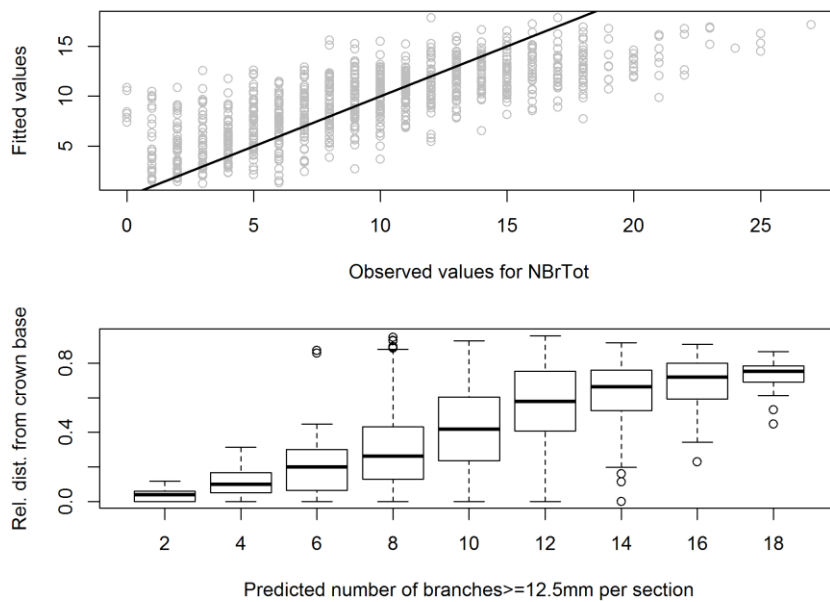


Figure 13 Fitted values from the fixed effect component of Equation 10 (No. branches $\geq 12.5\text{mm}$; *NBrNo1Grd*) versus observed values (top) and boxplot showing the range for the predicted number of branches $\geq 12.5\text{mm}$ across relative distance into the crown.

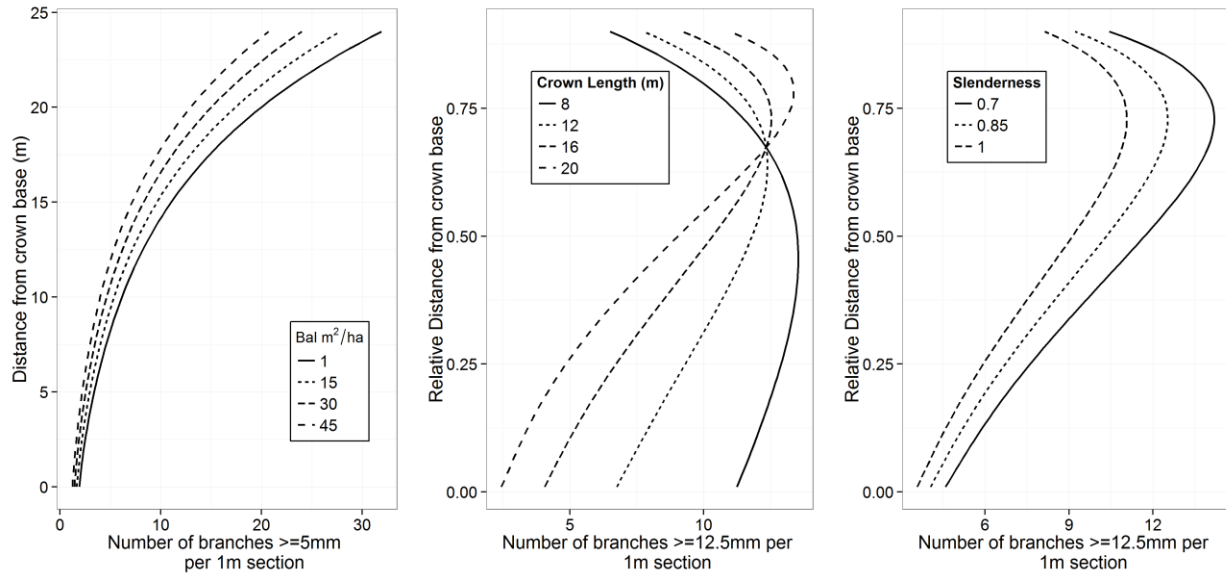


Figure 14 Simulated predictions for the number of branches $\geq 5\text{mm}$ and (left panel) and the number of branches $\geq 12.5\text{mm}$ at different levels of the covariates included in the respective models.

3.3.2 Diameter of the largest branch per stem section

The final model for the maximum branch diameter (mm) per 1m section ($MaxBrD$) was:

[Eq.11]

$$\ln(MaxBrD_{pts}) = c_0 + c_1 RDist_{pts} + c_2 \ln RDist_{pts} + c_3 Cl_{pt} + c_4 Slc_{pt} + c_5 Htlnrn_{pt} + \chi_p + \chi_{pt} + \varepsilon_{pts}$$

which was fit using a Gaussian distribution with a log-link function and where c_0 to c_5 were the parameters to be estimated, χ_p and χ_{pt} were the plot and tree random effects and ε_{pts} the residual error. Maximum branch diameter was positively related to crown length and height to live crown (Table 11). Tree slenderness, on the other hand, showed a negative relationship to the diameter

of the largest branch. The fixed-effect part of the model explained 61% of the variability, while the addition of random effects only explained an additional 4% of the variability. Nearly all of the random variability was due to variation between plots (Figure 15).

There was good agreement between fitted and observed values across the full range of measurements. Boxplots of the predictions indicated that maximum branch diameters from 20mm to 34mm are most often estimated to occur within 20% to 70% of the crown base, while maximum branch diameters ≥ 36 mm are restricted to the lower 40% of the crown (Figure 16).

When the model was refit without the variables for crown length and height to live crown, there was a large drop in the precision and accuracy of the estimates from the fixed effect component (Table 11). Furthermore, without the crown size related variables, the model showed greater bias and tended to under-estimate maximum branch diameter.

Table 11 Estimated fixed effect parameters with standard errors for Equation 11 (*MaxBrD*), standard deviations of the random effects (Plot, Tree and Residuals) and error statistics from the fixed effects component (RMSE = root mean square error).

Parameters	Estimate	Standard error
c_0 – intercept	4.020	0.118
c_1 – Rdist	-0.730	0.084
c_2 - lnRDist	0.557	0.039
c_3 – Cl	0.027	0.002
c_4 – Slc	-0.742	0.082
c_5 - Htlern	0.028	0.002

Random effects	Standard deviation
Plot	0.347
Tree	0.000
Residuals	5.131

Error Statistics	RMSE	Mean error	Absolute mean error	Relative error
<i>MaxBrD</i> (with crown variables)	5.129	-0.021	3.949	15.353
<i>MaxBrD</i> (without crown variables)	7.521	1.904	5.915	24.925

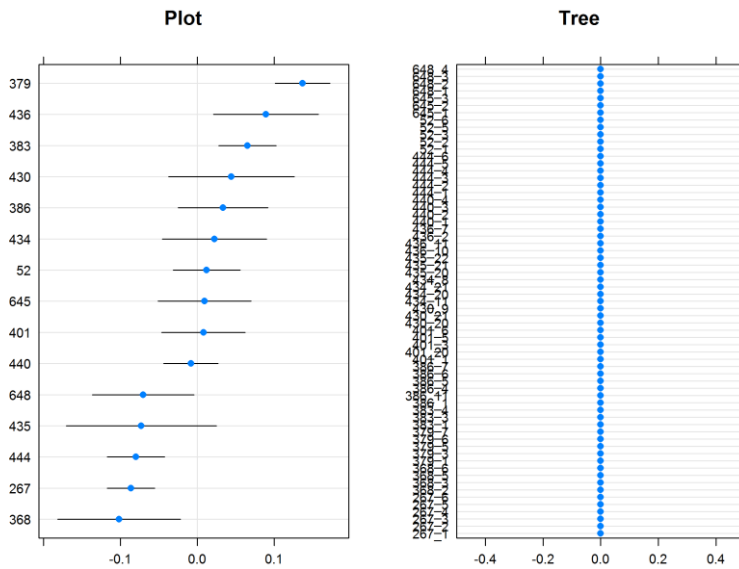


Figure 15 Distribution of plot and tree level random effects for Equation 11 (*MaxBrD*). Y-axis is the plot or tree number.

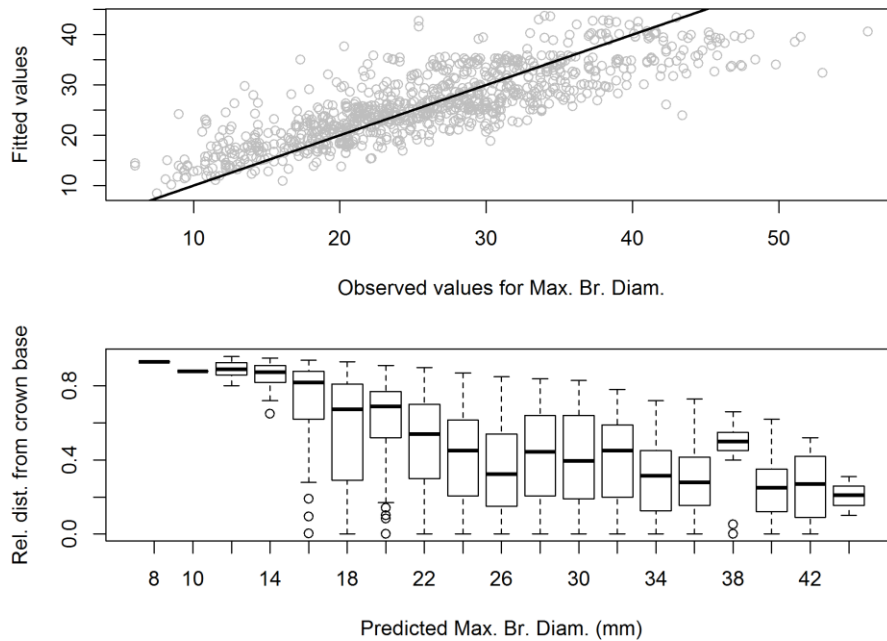


Figure 16 Fitted values from Equation 11 (*MaxBrD*) versus observed values for maximum branch diameter (top) and boxplot showing the range for the predicted maximum branch diameter across relative distance into the crown.

Model predictions (Figure 17) indicate that for crown length, height to live crown, and tree slenderness, maximum diameters increase rapidly descending from the tree apex until roughly 60% from crown base, after which point they increase at a slower rate until they peak at about 25% from the crown base. For all simulated scenarios, the greatest differences in maximum branch diameter are observed over the lower half of the crown.

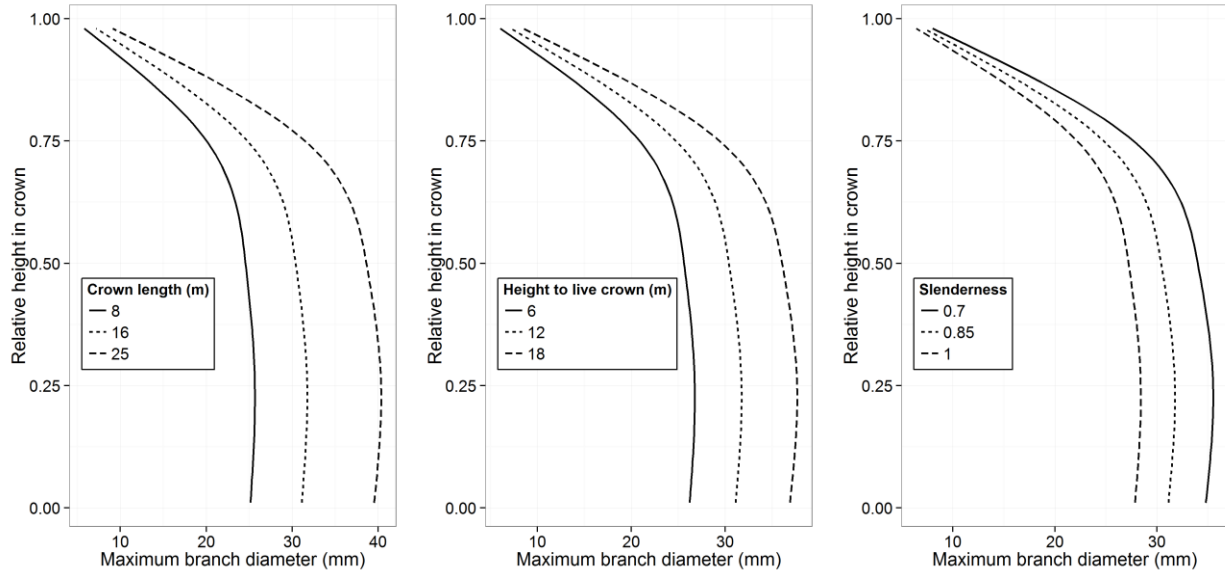


Figure 17 Simulated predictions for maximum branch diameter for different levels of the covariates used in the model.

3.3.3 Diameter of branches smaller than the largest

For relative branch diameter (*RelBrD*), a binomial distribution with a logit link function was used, with the final model expressed as:

[Eq.12]

$$\ln \left[\frac{BrD_{ptsl} / MaxBrD_{pts}}{1 - (BrD_{ptsl} / MaxBrD_{pts})} \right] = d_0 + d_1 RDist_{pts} + d_2 Rank_{ptsb} + d_3 Slc_{pts} + \delta_p + \delta_{pt} + \delta_{pts}$$

The fixed effect parameters to be estimated were d_0 to d_3 , while the random effects for the plot, tree and section level were δ_p , δ_{pt} , and δ_{pts} , respectively. The rank of the branch appeared to be the most important in terms of explaining the relative diameter. Relative branch diameters increased as the rank of the branch increased (e.g., from rank 8 to rank 1). Also, the relative

diameter of branches per section increased with increasing relative distance from the tree apex while more slender trees had smaller relative branch diameters per 1m section. Caterpillar plots showed that most of the variability in the random effects was between sections within trees, followed by tree-to-tree and plot-to-plot variability (Figure 18). Using only the fixed effects part of the model, the pseudo- R^2 was 79%, while adding plot, tree and section random effects increased this value to 91%. Although overall mean error was quite small (Table 12), residuals from the fitted fixed effect part of the model showed that the model tended to overestimate at small relative branch diameters and underestimate at relative branch diameters $>70\%$. The greatest difference between fitted and observed values occurred for branches that were $\sim <40\%$ of the maximum branch diameter within a 1m section (Figure 19). Boxplots of the predictions revealed the large variability in branch sizes at all relative distances within the crown (Figure 19).

Table 12 Estimated fixed effect parameters with standard errors and significance tests (p-value) for z-values for Equation 12 (*RelBrD*). Standard deviations of the random intercept for the plot, tree, and section-level are listed with the error statistics from the fixed effects component (RMSE = root mean square error).

Parameters	Estimate	Standard error	p-value	
d_0 – intercept	2.581	0.252	<0.000	
d_1 – RDist	-0.213	0.066	<0.000	
d_2 – Rank	-0.142	0.001	<0.000	
d_3 – Slc	-0.759	0.295	<0.010	
Random effects	Standard deviation			
Plot	0.120			
Tree	0.191			
Section	0.486			
Error Statistics	RMSE	Mean error	Absolute mean error	Relative error
<i>RelBrD</i> (on proportion scale)	0.140	0.009	0.110	43.891
<i>RelBrD</i> (diameter scale (mm))	3.935	-0.410	2.814	42.686

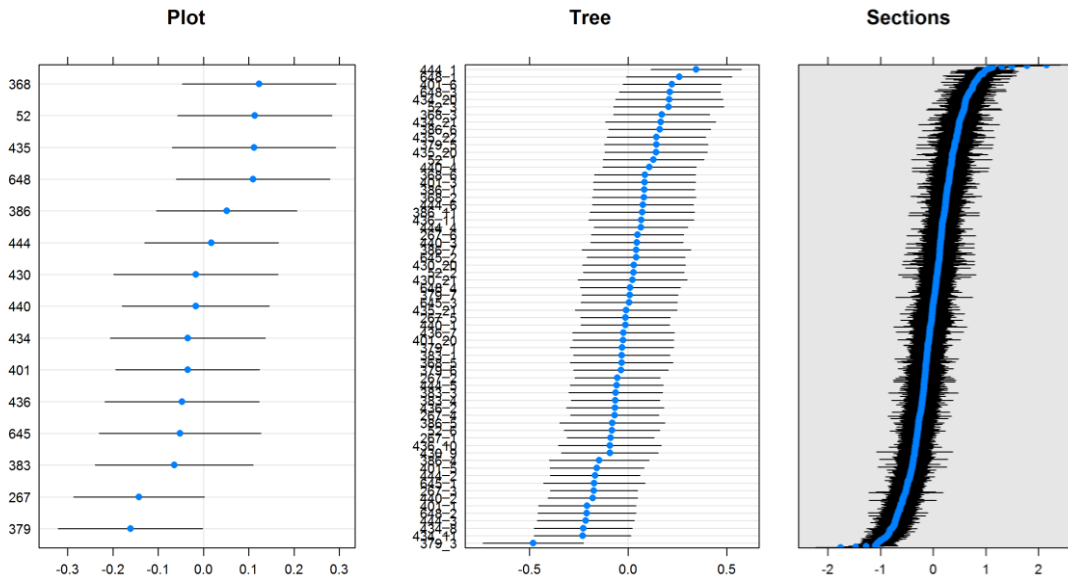


Figure 18 Distribution of plot, tree and section (i.e., 1m sections of the stem) random effects for Equation 12 (*RelBrD*). Y-axis is the plot or tree. Section numbers have been omitted (i.e., a list of Plot+tree+section) is omitted.

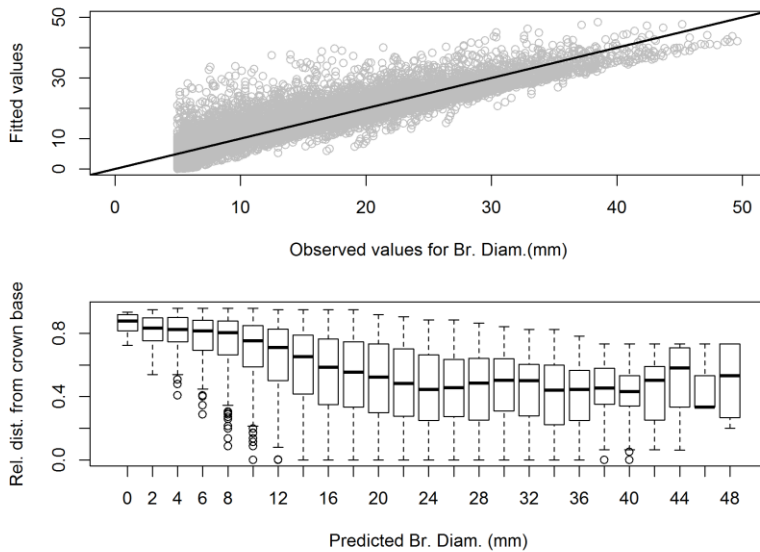


Figure 19 Fitted values from the fixed effect component of Equation 12 versus observed values for branch diameters (top), and boxplot showing the range for the predicted branch diameter across relative distance into the crown.

Predictions from Equation 12 simulated for four branch ranks and three levels of tree slenderness (Figure 20) show that there is a rapid decrease in branch diameter from about 60% relative crown depth to crown apex. Also, given a similar DBH, a more slender tree will have slightly smaller branch diameters than one which is less slender.

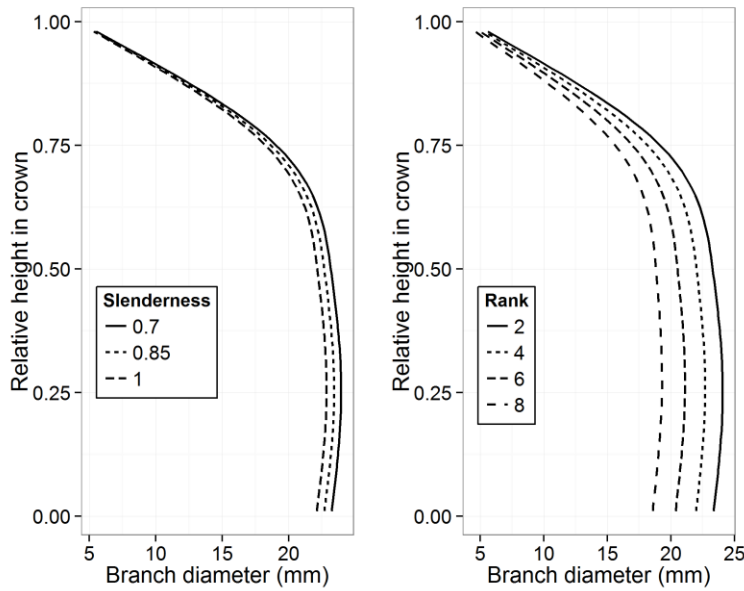


Figure 20 Simulated predictions from Equation 12 (*RelBrD*) for different levels of the covariates used in the model.

3.3.4 Branch angle

The model selected to provide estimates of branch angle for all live branches ≥ 5 mm diameter (*BrAngTot*) was:

$$[Eq. 13] \quad BrAngTot_{ptsl} = e_0 + e_1 RDist_{pts} + e_2 Rank_{ptsb} + \varphi_p + \varphi_{pt} + \varphi_{pts} + \varepsilon_{ptsl}$$

where e_0 to e_2 were the fixed effect parameters to be estimated and ϕ_p , ϕ_{pt} , ϕ_{pts} , and ε_{ptsl} were the random effects. The same model structure was used for estimates of insertion angle for branches $\geq 12.5\text{mm}$ (*BrAngNo1Grd*):

$$[\text{Eq. 14}] \quad \text{BrAngNo1Grd}_{ptsl} = f_0 + f_1 \text{RDist}_{pts} + f_2 \text{Rank}_{ptsb} + \phi_p + \phi_{pt} + \phi_{pts} + \varepsilon_{ptsl}$$

where f_0 to f_2 were the fixed effect parameters and ϕ_p , ϕ_{pt} , ϕ_{pts} , and ε_{ptsl} were the random effects (Table 14). Branch rank was the most important coefficient for estimates of branch angle, regardless of branch size and indicated that branch angle decreased as the branch rank increased. With increasing distance from tree apex branch angles decreased at a similar rate for both branches $\geq 5\text{mm}$ and those $\geq 12.5\text{mm}$.

The fixed effect part of the model for all branches $\geq 5\text{mm}$ explained 29% of the variability in branch angle, while the model for branches $\geq 12.5\text{mm}$ explained 32% of the variability. The addition of the random effects to each of the models increased the variance explained by an additional 28% and 32%, respectively. Partitioning of the random variability was nearly identical for the two equations and was relatively evenly distributed among plot, tree and section (Figure 21; due to the similarity, results are only shown for branches $\geq 5\text{mm}$).

The mean error from the fitted model for branches with a diameter $\geq 5\text{ mm}$ showed that there was an overall tendency to overestimate branch angles (Table 13). Conversely, the mean error from the model for branches with a diameter $\geq 12.5\text{mm}$ indicated that there was an overall tendency to underestimate branch angles (Table 14). However, for both models, there was a clear bias when branches were near vertical or when branches had insertion angles greater than 90° (Figure 22).

Table 13 Estimated fixed effect parameters with standard errors for Equation 13 (*BrAngTot*). Standard deviations of the random components (Plot, Tree, Section and Residuals) are listed with the error statistics for the fixed effects component (RMSE = root mean square error)

Parameters	Estimate	Standard error		
e_0 – intercept	45.710	1.565		
e_1 – RDist	50.342	1.076		
e_2 – Rank	1.105	0.021		
Random effects		Standard deviation		
Plot	4.195			
Tree	7.115			
Section	6.946			
Residuals	13.960			
Error Statistics	RMSE	Mean error	Absolute mean error	Relative error
<i>BrAngTot</i> >=5mm	17.486	-0.723	13.332	17.622

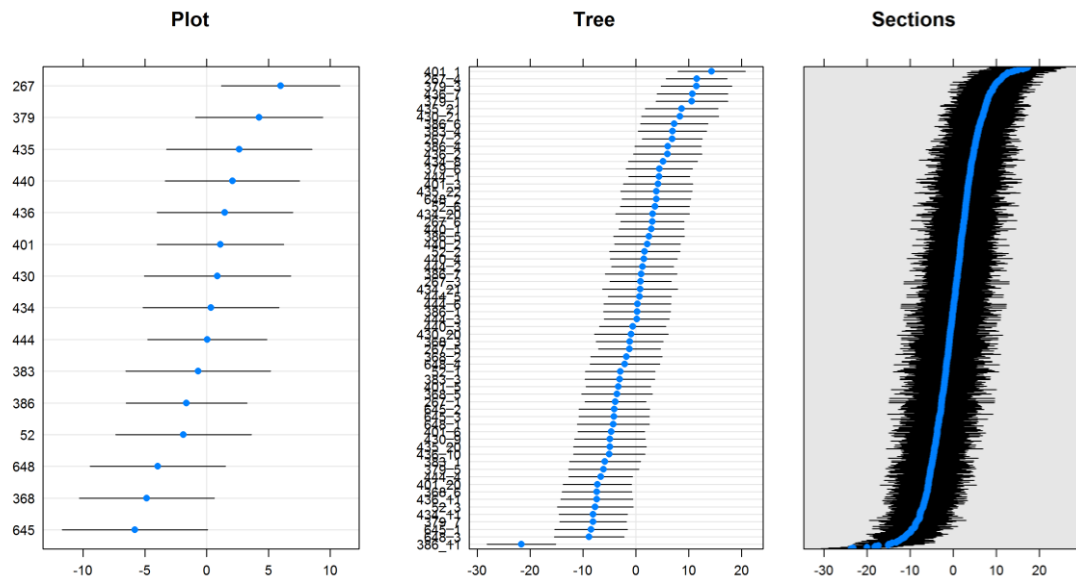


Figure 21 Distribution of plot, tree and section (i.e., 1m sections of the stem) random effects from Equation 13 (*BrAngTot*). Distributions for Equation 14 (*BrAngNo1Grd*) are not shown, but are similar to those seen here.

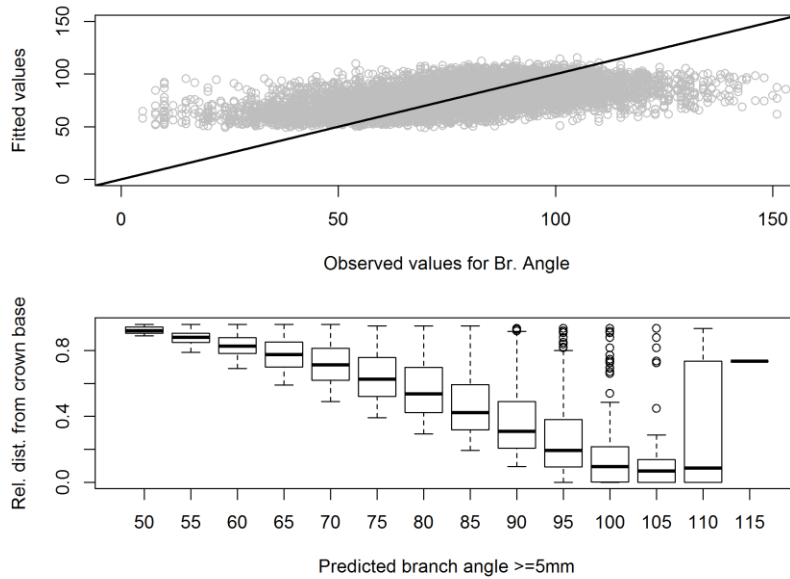


Figure 22 Fitted values from the fixed effect component of Equation 13 versus observed values for branch angle (branch diameters ≥ 5 mm) (top), and boxplot showing the range for the predicted branch angle across relative distance into the crown.

Table 14 Estimated fixed effect parameters with standard errors for Equation 14 (*BrAngNo1Grd*). Standard deviations of the random components (Plot, Tree, Section and Residuals) are listed with the error statistics for the fixed effects component (RMSE = root mean square error).

Parameters	Estimate	Standard error		
f_0 – intercept	46.160	1.653		
f_1 – RDist	49.471	1.035		
f_2 – Rank	0.929	0.040		
Random effects		Standard deviation		
Plot	4.417			
Tree	7.676			
Section	6.148			
Residuals	11.957			
Error Statistics	RMSE	Mean error	Absolute mean error	Relative error
<i>BrAngNo1Grd</i> ≥ 12.5 mm	15.820	0.592	11.913	16.038

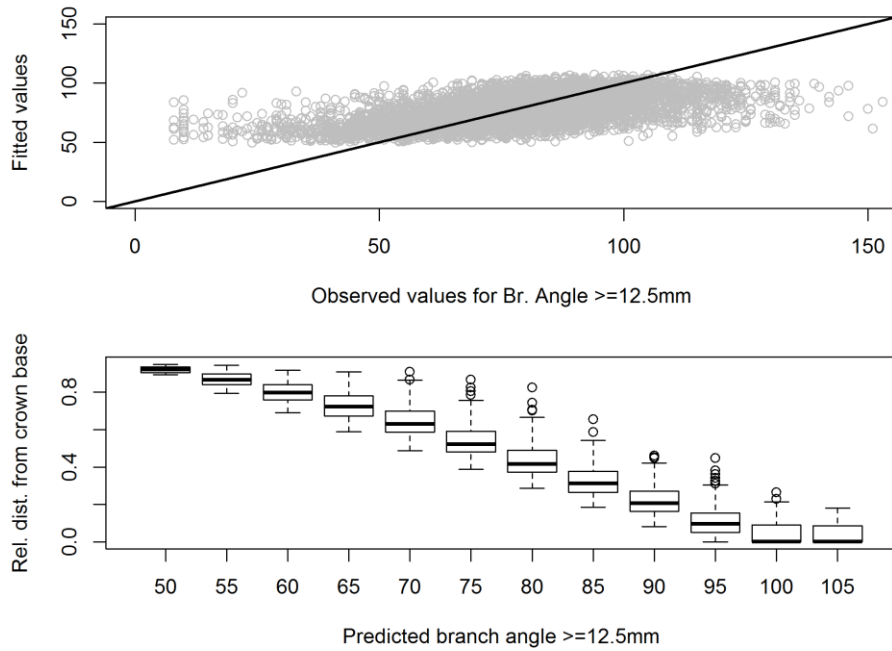


Figure 23 Fitted values from the fixed effect component of Equation 14 versus observed values for branch angle (branch diameters ≥ 12.5 mm), and boxplot showing the range for the predicted branch angles (diameters ≥ 12.5 mm) across relative distance into the crown.

Simulations showed that the predicted rate of increase in branch angle with increasing relative distance from the tree top was nearly the same for branches ≥ 5 mm and those ≥ 12.5 mm (Figure 24).

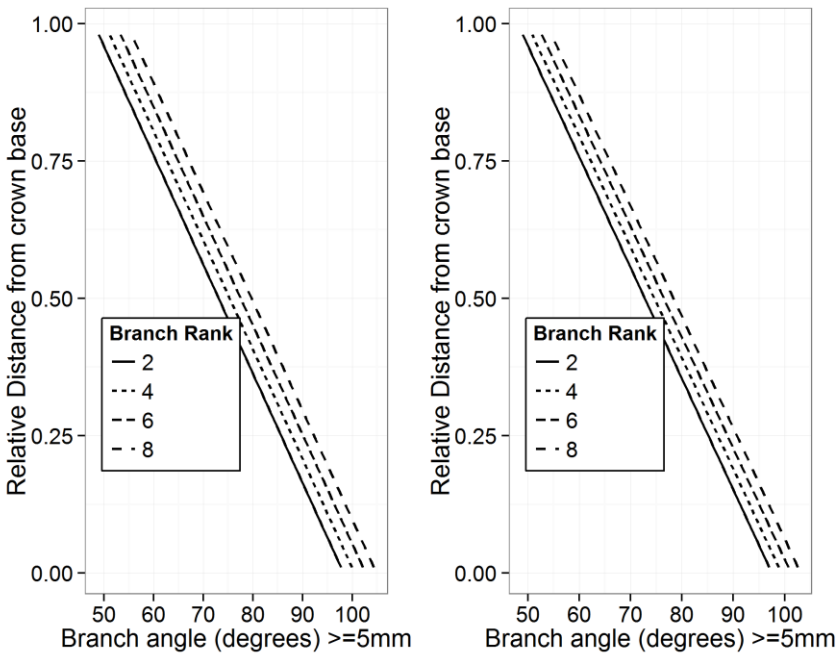


Figure 24 Simulated predictions from Equations 13 and 14 showing branch angles for different levels of branch rank.

3.4 Discussion

3.4.1 Number of branches per section

Using stand and tree-level variables to predict branch frequency for species where this characteristic is under strong genetic control will generally yield poor results. Hein et al. (2007), for example, cited moderate genetic control in Norway spruce as a possible reason why only <6% of the total variability for the number of branches in a whorl could be explained using a mixed effect model. In contrast, the fixed components of the model presented here explained 60% of the total variance using only distance from tree apex and tree social status. This suggests a weaker genetic control over branch frequency within white spruce, implying that positional and stand-level effects have a greater impact on branch initiation and self-pruning. This would be

consistent with Merrill and Mohn (1985), who found low heritability for the number of branches per whorl within an open-pollinated 20 year old plantation of white spruce.

Within the model dataset, the longest crowns were measured on large, old (>125 years) overstory trees. Thus, the oldest branches within the dataset are found at large absolute distances from the crown apex of these trees. Age-related effects such as reduced photosynthesis and diminished stomatal conductance (Bond 2002) are likely to have a strong impact on branch loss at these distances. Conversely, for the same dataset, large relative distances from the crown apex will not only include very old branches from large trees with long crowns, but also younger branches on smaller, understory trees. However, for the younger trees, age-related effects on branch loss will be less prominent (Ishii and McDowell, 2002). Therefore, absolute distance into the crown seems to be a better proxy to describe the gamut of effects (e.g., branch age, shading, damage from contact with neighbouring trees) causing branch loss. In comparison, the model used by Nemeček et al. (2012) to explain the frequency of branch clusters along older annual shoots (>5 years) in white spruce included both a relative and absolute measure of shoot height, with no distinction made between the effects attributable to these two variables. Their model for branch number per cluster, however, included no positional effects. Rather, shoot age was cited as a minor factor.

Among the models presented in this study, that for branch frequency (for diameters ≥ 5 mm) was the only one to include an explicit measure of competition, namely the basal area of larger trees. This seems to confirm our earlier conclusion that the growing environment, and not heritability, plays an important role in determining the frequency of branches in white spruce. The results indicate that trees in a dominant position have a greater number of branches per stem section than suppressed trees. This can be attributed to increased levels of light received by dominant

trees, which in turn increases the development of new branches (Maguire et al. 1994; Weiskittel et al. 2010). These differences appear to be the greatest at the tops of trees and become negligible near the base of the crown. Nemeč et al. (2012) did not test the inclusion of stand-level derived measures of competition in their models for cluster and branch frequency, presumably because they assumed that the effects of competition would be captured by the tree and shoot-level predictor variables they tested. The basal area of larger trees has been recommended as an appropriate competition index, particularly for complex stands (Wykoff et al. 1982; Wykoff 1986; Temesgen et al., 2005). The fact that tree social status, and not a species-specific competition index, was found to significantly affect branch frequency suggests that this characteristic is not strongly influenced by the type (e.g., deciduous or coniferous) of species in the stand.

The initial increase in the frequency for branches $\geq 12.5\text{mm}$ moving down from the crown apex is mainly a reflection of the time required for branches to attain at least 12.5mm. The subsequent decrease in frequency from roughly 20% of crown length to crown base reflects the increasing effects of branch age and shading (either self-shading or from competitors) on branch loss. The frequency of branches $\geq 12.5\text{mm}$ was also positively correlated to crown length and negatively related to tree slenderness. Thus, it appears that crown length was the variable that captured best the effects of shade and age on branch frequency. The differences in branch frequency between slender trees and trees with large taper was most notable at around 20% from the crown apex. For Norway spruce, Hein et al. (2007) also found tree slenderness to be a significant predictor for the frequency of branches $\geq 5\text{mm}$, while Weiskittel et al. (2007a) reported a similar increase in the branch frequency (also for branches $\geq 5\text{mm}$) with increasing crown length.

3.4.2 Diameter of the largest branch per section

There were strong positional effects acting on maximum branch diameter given that relative distance into the crown was the most important variable for this model. Although Nemeč et al. (2012) did not specifically model maximum branch diameters in white spruce, positional effects were also important when predicting the diameter of live branches. Two of the five within-crown positional variables they included were based on distance dependent measures of neighbouring competitors, indicating that both shelf-shading and shading from competitors had an effect on light availability, which in turn limited branch diameter growth. Tree-level variables, however, were not important in their models, indicating that the positional effects were the same regardless of tree size. In contrast, the results here indicate that crown length, height to live crown and tree slenderness were all related to maximum branch diameter even after within-crown positional effects were taken into account. The difference in findings may at least partially be attributable to the two distance-dependent measures of competition used by Nemeč et al. (2012). In the absence of distance-dependent branch-level measures of inter-tree competition, tree-level variables that are sensitive to stand density appear to be able to account for some of the competition-related variability in maximum branch diameters. Large values for crown length and height to live crown were associated with some of the oldest trees in the model dataset. Thus, these two variables may also reflect the effects of branch age on maximum branch diameters.

The greatest difference in maximum branch diameters for slender trees versus trees with greater taper was over the lower half of the crown. This is important information for forest managers since this indicates that silvicultural practices that affect crown length and tree taper can have a large impact on knot size, particularly within the merchantable portion of the crown. Wang et al.

(2000) found that tree slenderness for white spruce within boreal mixedwood forests was positively correlated with stand density and site index. This suggests that silviculturalists could control maximum branch diameters by planting spruce at higher densities within areas with high site index.

3.4.3 Branch diameter other than the largest branch

The relative distance into the crown and the branch rank had the strongest influence on relative branch diameter. The fact that within-crown and within-section variables accounted for most of the variability in relative branch diameters is in agreement with the findings from Nemec et al. (2012). There was a general pattern of increasing branch diameter with increasing distance from the tree top, which followed closely to the patterns displayed by maximum branch diameter. The finding that the diameter of branches per section (other than the largest) peaks near the base of the crown indicates that nearly all branches, regardless of size, continue to grow despite diminishing levels of light due to shelf-shading and shading from competitors. Previous studies on other shade-tolerant species have also reported peaks in branch diameter at low crown positions (Hein et al. 2007; Benjamin et al. 2009). The inclusion of tree slenderness indicates that stand density has a minor effect on smaller branches, but not as strong as with maximum branch size.

3.4.4 Branch angle

The angle of branches $\geq 5\text{mm}$ and those $\geq 12.5\text{mm}$ appeared to be under the influence of the same factors given that the models included the same variables and only showed minor differences in the estimated coefficients. Similar to relative branch diameter, within-crown and within section positioning effects had the greatest influence on branch angles, regardless of

branch size. Since no variables that would indicate the presence of tree-age related effects were included in the model (e.g., DBH, CI), the trends observed for branch angle appear to be the same for both young and old trees. Nemec et al. (2012) did not model branch angles for white spruce, and no other studies for branch angle on naturally regenerated white spruce could be found. However, for Sitka spruce, Achim et al. (2006) also found that tree-size related effects did not influence branch insertion angle.

For white spruce, the larger branches within a section (i.e., smaller rank) displayed the smallest angles (i.e., they pointed more towards tree apex) and is consistent with the findings from Sitka spruce reported by Auty et al. (2012). This has significant implications in terms of appearance grading of structural lumber, since small angles on branches with large diameters will produce a large knot surface area. No stand-level variables or tree-level variables that are sensitive to changes in stand density were included in the model, suggesting that prescribed thinning or changes in planting densities will have little effect over the control of branch angles. The positive relationship between relative distance into the crown and branch angle observed here was also observed on Norway spruce (Colin and Houllier 1992). The trend may be related to the increase in branch mass with age. Yamamoto et al. (2002) concluded that higher amounts of biomass carried by larger branches pulled the branches downward. Thus, as successive growth rings are added to the main stem of the tree, branch insertion angle on the main stem will increase while the relative distance of the branch from the tree apex also increases.

3.4.5 Model applications and conclusions

The models here represent an important addition to the tools required to manage stands with wood quality objectives in mind. Existing branch models for white spruce were designed for use

with LiDAR data or distance dependent growth models. The current suite of models differ from these existing models since they were explicitly developed to be used within distance-independent growth simulators. Furthermore, branch models designed for use in naturally regenerated, unmanaged stands were lacking. Their development using data from both mixed and pure species stands means that they should be suitable for use in the mixedwood growth model (MGM) simulator. The models are applicable to the '*reference*' (i.e., modal) ecosite of the central mixedwood subregion of Alberta (Natural Regions Committee, 2006). Since plot-level random effects were important in several of the models, calibration of the parameters to specific areas (e.g., other natural subregions within the Boreal forest) is likely required. Validation of the models will also be necessary before they can be used operationally.

The results of the models appear to largely confirm our limited knowledge of crown architecture for white spruce and are, for the most part, in line with results from other coniferous species. Many of the explanatory variables used in the models presented here have been previously used to predict branch characteristics for other conifers. However, most of the pre-existing knowledge of branch characteristics has been derived using data from spacing trials or from single species stands. The data collected for the current study presented an opportunity to test these assumptions in naturally regenerated, mixed species stands. Our finding that only tree-level variables were required for most of the models is, therefore, interesting since it suggests that species composition effects on the branching characteristics of individual white spruce cannot be easily detected at the stand-level. Thorpe et al. (2010) found that crown size for interior spruce was highly sensitive to local, inter-tree competition; crown radius decreased more rapidly with an increasing number of local competitors when competitors were composed of both shade-

tolerant and shade intolerant species versus only conspecifics. Although the tree-level variables included in the current models do not capture species-specific effects, they are good proxies for the effects of local competition. Thus, their presence in the models here are in agreement with the more general findings by Thorpe et al. (2010) that crown architecture is affected by local “neighbourhood” conditions.

References

- Achim A, Gardiner BA, Leban J-M, Daquitane R., 2006. Predicting the branching properties of Sitka spruce grown in Great Britain. *NZ J For Sci* 36:246–264
- Akaike H., 1974. A new look at the statistical model identification. *IEEE Trans Autom Control* 19:716–723
- Alberta Sustainable Resource Development (ASRD). 2005. Permanent sample plot field procedures manual. Public Lands and Forest Division, Forest Management Branch, Edmonton, Alberta, 30p.
- Auty, D., Weiskittel, A.R., Achim, A., Moore, J.R., Gardiner, B.A., 2012. Influence of early re-spacing on Sitka spruce branch structure. *Ann. For. Sci.* 69, 93-104.
- Bates D, Maechler M, Bolker B and Walker S. 2014. *lme4: Linear mixed-effects models using Eigen and S4*. R package version 1.1-7, <http://CRAN.R-project.org/package=lme4>.
- Beckingham, J.D., and Archibald, J.H., 1996. Field guide to ecosites of northern Alberta. Northern Forestry Centre, Forestry Canada, Northwest Region. Spec. Rep. 5.
- Benjamin, J.G., Kershaw, J.A., Jr., Weiskittel, A.R., Chui, Y.H., Zhang, S.Y., 2009. External knot size and frequency in black spruce trees from an initial spacing trial in Thunder Bay, Ontario. *For. Chron.* 85, 618-624.

- Bokalo, M., Stadt, K.J., Comeau, P.G., Titus, S.J., 2010. Mixedwood Growth Model (MGM) (version MGM2010.xls). University of Alberta, Edmonton, Alberta, Canada. 2010. Available online: <http://www.rr.ualberta.ca/Research/MixedwoodGrowthModel.aspx>. (accessed on 7 July 2011).
- Bokalo, M., Stadt, K.J., Comeau, P.G., Titus, S.J., 2013. The Validation of the Mixedwood Growth Model (MGM) for Use in Forest Management Decision Making. *Forests* 4, 1-27.
- Bolker, B.M., Brooks, M.E., Clark, C.J., Geange, S.W., Poulsen, J.R., Stevens, M.H.H., White, J.S., 2009. Generalized linear mixed models: a practical guide for ecology and evolution. *Trends in Ecology & Evolution* 24, 127-135.
- Bond, B.J., 2000. Age-related changes in photosynthesis of woody plants. *Trends in plant science. Reviews*. Vol 5, No. 8: 349-353.
- Burnham KP, Anderson DR., 2002. Model selection and multimodel inference: a practical information-theoretic approach. Springer, New York
- Colin, F., Houllier, F., 1992. Branchiness of Norway Spruce in Northeastern France - predicting the main crown characteristics from usual tree measurements. *Ann. Sci. For.* 49, 511-538.
- Duchateau, E., Longuetaud, F., Mothe, F., Ung, C., Auty, D., Achim, A., 2013. Modelling knot morphology as a function of external tree and branch attributes. *Can. J. For. Res.* 43: 266-277.

- Garber, S., Maguire, D., 2005. Vertical trends in maximum branch diameter in two mixed-species spacing trials in the central Oregon Cascades. *Can. J. For. Res.* 35: 295-307.
- Goudie, J.W., and Parish R., 2008. Modelling the impact of silviculture treatments on the wood quality of interior spruce. http://www.for.gov.bc.ca/hfd/library/FIA/2008/FSP_Y081078a.pdf (5 May 2008) [accessed Aug 26, 2013].
- Groot, A., Schneider, R., 2011. Predicting maximum branch diameter from crown dimensions, stand characteristics and tree species. *For. Chron.* 87, 542-551.
- Hein, S., Mäkinen, H., Yue, C., Kohnle, U., 2007. Modelling branch characteristics of Norway spruce from wide spacings in Germany. *For. Ecol. Manage.* 242, 155-164.
- Ishii, H., McDowell, N., 2002. Age-related development of crown structure in coastal Douglas-fir trees. *For. Ecol. Manage.* 169, 257-270.
- Maguire, D., Moeur, M., Bennett, W., 1994. Models for Describing Basal Diameter and Vertical-Distribution of Primary Branches in Young Douglas-Fir. *For. Ecol. Manage.* 63, 23-55.
- Mäkinen, H., Colin, F., 1999. Predicting the number, death, and self-pruning of branches in Socts pine. *Can. J. For. Res.* 29: 1225-1236.
- Merrill, R., Mohn, C., 1985. Heritability and Genetic Correlations for Stem Diameter and Branch Characteristics in White Spruce. *Can. J. For. Res.* 15, 494-497.

- Natural Regions Committee, 2006. Natural Regions and Subregions of Alberta. Compiled by D.J. Downing and W.W. Pettapiece. Government of Alberta. Pub. No. T/852.
- Nemec, A.F.L., Parish, R., Goudie, J.W., 2012. Modelling number, vertical distribution, and size of live branches on coniferous tree species in British Columbia. *Can. J. For. Res* 42, 1072-1090.
- NLGA, 2003. Standard grading rules for Canadian lumber. National Lumber Grades Authority, New Westminster, British Columbia, Canada
- R Core Team, 2013. R: A language and environment for statistical computing. R Foundation for Statistical Computing, Vienna, Austria. URL <http://www.R-project.org/> [accessed May 27, 2013].
- Sustainable Resource Development (SRD), 2009. Sustainable Forest Management: Current Facts and Statistics. ISBN No. 978-0-7785-8722-4 No. I/398. August 2009.
- Temesgen, H., LeMay, V., Mitchell, S., 2005. Tree crown ratio models for multi-species and multi-layered stands of southeastern British Columbia. *For. Chron.*81, 133-141.
- Thorpe, H.C., Astrup, R., Trownbridge, A. and Coates, K.D., 2010. Competition and tree crowns: A neighborhood analysis of three boreal tree species. *For. Ecol. and Manage.* 259: 1586-1596.
- Tong, Q., Duchesne, I., Belley, D., Beaudoin, M., Swift, E., 2013. Characterization of Knots in Plantation White Spruce. *Wood Fiber Sci.*45, 84-97.

- Venables, W.N. and Ripley, B.D., 2002. *Modern Applied Statistics with S, Fourth Edition*. New York: Springer.
- Wang, Y., Titus, S.J., and LeMay, V.M. 2000. Relationships between tree slenderness coefficients and tree or stand characteristics for major species in boreal mixedwood forests. *Can. J. For. Res.* 28: 1171-1183.
- Weiskittel, A.R., Maguire, D.A., Monserud, R.A., 2007a. Response of branch growth and mortality to silvicultural treatments in coastal Douglas-fir plantations: Implications for predicting tree growth. *For. Ecol. Manage.* 251, 182-194.
- Weiskittel, A.R., Maguire, D.A., Monserud, R.A., 2007b. Modeling crown structural responses to competing vegetation control, thinning, fertilization, and Swiss needle cast in coastal Douglas-fir of the Pacific Northwest, USA. *For. Ecol. Manage.* 245, 96-109.
- Weiskittel, A.R., Seymour, R.S., Hofmeyer, P.V. and Kershaw, J.A. Jr., 2010. Modelling primary branch frequency and size for five conifer species in Maine, USA. *For. Ecol. and Manage.* 259: 1912-1921.
- Wykoff, W.R., Crookston, N.L., and Stage, A.R., 1982. User's guide to the stand prognosis model. USDA For. Serv. Gen. Tech. Rep. INT-133.
- Wykoff, W.R., 1986. Supplement to the User's Guide for the Stand Prognosis Model – Version 5.0. Gen. Tech. Rep. INT-208. USDA For. Serv., Ogden, UT. 36 p.

Yamamoto H, Yoshida M, Okuyama T., 2002. Growth stress controls negative gravitropism in woody plant stems. *Planta* 216: 280–292.

Chapter 4: Crown allometry and application of the *Pipe Model Theory* to white spruce (*Picea glauca* (Moench) Voss) and aspen (*Populus tremuloides* Michx.)

4.1 Introduction

Crobas (Mäkelä 1997) is a process-based model which is based on the principle of carbon balance, but also incorporates principles related to the functional balance (Davidson 1969; Valentine and Mäkelä 2005). Among the structural regularities of trees that are assumed within the Crobas model, the two which have received considerable attention are: 1) that a constant allometric relationship exists between foliage mass (W_f) and crown length (Cl), and 2) that the ratio of foliage mass to sapwood area at crown base ($A_{s_{cb}}$) is invariant across tree size, social class and stand density.

Within Crobas, the relationship between foliage mass and crown length is used to obtain tree-level estimates of foliage mass, which in turn, are used to infer $A_{s_{cb}}$. By inferring foliage mass from crown length, the Crobas model ties the growth of the crown to the allocation of carbon within the tree (Mäkelä 1997). The assumption of a constant allometric relationship between foliage mass and crown length is supported by empirical observations from several tree species including Silver birch (*Betula pendula* L.) (Ilomäki et al. 2003), Norway spruce (*Picea abies* (L.) Karst.) (Kantola and Mäkelä 2006) and Scots pine (*Pinus sylvestris* L.) (Berninger and Nikinmaa 1994). Notably, Mäkelä and Sievänen (1992) postulated that the physiological basis for such a relationship is that it represents the optimal balance between added photosynthetic ability from

increased foliage mass and the additional maintenance and respiration costs associated with a longer crown. However, it is acknowledged that the assumption of a constant allometric relationship between foliage mass and crown length is a generalization and findings from (Mäkelä and Vanninen 1998) and Schneider et al. (2008), among others, have demonstrated that competition, tree age, and climate may influence this relationship.

Notwithstanding the effects of age, size and competition, it is postulated that the exponent parameter of the relationship between foliage mass and crown length should lie between 2 and 3 (Zeide and Pfeifer 1991). This range is an adjustment from the theoretical scaling exponent of 3, which is obtained if we assume that the crown is a fractal-like object formed by a volume filling branching network and is of constant shape (Mäkelä and Valentine 2006). The adjustment is supported by empirical observations of scaling between foliage mass and crown volume (Mäkelä and Vanninen 1998; Duursma et al. 2010).

There is sufficient evidence to suggest that the relationships described above cannot always be extended to describe scaling within the crown (Baldwin et al. 1997; Kantola and Mäkelä 2004). It is suggested that variation in the amount of foliage mass per unit crown length is under strong environmental control, which could be related to the progressive increase in self-shading with increased distance from tree apex or increased competition from neighbouring trees; in practice, it is difficult to separate these two effects. Within Crobas, these alterations need to be taken into account if within-crown estimates of foliage mass from crown-length are desired.

The assumption that there is a constant and linear relationship between foliage mass and $A_{s_{cb}}$ is derived from the pipe model theory of plant form (Shinozaki et al. 1964). Following an initial estimate of foliage mass from crown length, the pipe model relationship is used within Crobas to

estimate $A_{s,cb}$. Several empirical studies support the assumption of a constant relationship between foliage mass and $A_{s,cb}$, (Kaipiainen and Hari 1985; Eckmullner and Sterba 2000), while others have found the relationship to vary according to tree size, site productivity or geographic location (Gilmore et al. 1996; Berninger et al. 2005). Nevertheless, among the tree's structural relationships with foliage mass, the pipe model appears to be the most constant. Furthermore, the relationship between foliage mass and sapwood area is supposedly constant within the crown (Waring et al. 1982). Thus, estimates of cumulative foliage mass above a given point in the crown can be predicted from the sapwood area from a specified point within the crown.

Similar to the foliage mass – crown length relationship, a constant within crown relationship between cumulative foliage mass and sapwood area does not automatically follow from a constant foliage mass – $A_{s,cb}$ relationship at the whole-crown level (Schneider et al. 2011). This inconsistency may be due to the re-activation of disused pipes or a lag in time between the disuse of pipes and changes in foliage mass within the crown. Alternatively, the model of hydraulic architecture described by Whitehead and Jarvis (1981) and Whitehead et al. (1984a) has been used to explain within-tree variation in the relationship between foliage area and sapwood area (Medhurst and Beadle 2002). The hydraulic model predicts that the ratio of leaf area to sapwood area should decrease as evapotranspirative demands increase. The model also predicts that the leaf area to sapwood area ratio should decrease with increasing distance from stump. This is a result of increasing hydraulic path length with increasing tree height. Given the tight correlation between leaf area and foliage mass, the same trend should be seen for the ratio of within-crown foliage mass to the sapwood area. Indeed, modifications to the pipe model relationship have been

tested within Crobas to account for the within-crown variation in the relationship between foliage mass and sapwood area (Mäkelä and Vanninen 2001; Mäkelä 2002).

For the current study, we examine two main structural regularities assumed by the Crobas model. As a first main objective, we test for constant allometric scaling between foliage mass and crown length in white spruce [*Picea glauca* (Moench)] and aspen (*Populus tremuloides* Michx.). We then examine within-crown patterns of foliage mass with respect to crown length to determine if they are consistent with the relationships observed at the whole crown. As a second main objective, we test the assumption of a constant linear relationship between foliage mass and A_{scb} , which is derived from pipe model theory. We then test the null hypothesis that predictions of foliage mass from A_{scb} under the assumption of the pipe model are dissimilar to observed values. Finally, we look at the within-crown relationship between cumulative foliage mass and sapwood area. We examine this relationship within the framework of the pipe model theory and contrast it with the relationship viewed within the framework of the hydraulic model. The results of this study will contribute to the evaluation of the Crobas model for use on white spruce and aspen within the western Canadian boreal forest.

4.2 Material and methods

4.2.1 Site description

The sampling of trees used in this study was performed adjacent to Permanent Sample Plots (PSPs) which had previously been installed by Alberta Sustainable Resource Development (ASRD 2005). All PSPs were situated within unmanaged stands that had been established through natural regeneration. Although the selected PSPs span approximately 500 kilometers along an east-west latitude, climatic conditions over this region are reported to be similar

(Beckingham and Archibald 1996). All stands in which the sampled PSPs are located were classified to the ‘*reference*’ ecosite-type (i.e., upland forests with moderately well-drained, orthic-gray luvisolic soils) of the central mixedwood natural subregion of Alberta, Canada (Beckingham and Archibald 1996). Given the common ecosite-type, site index values were assumed to be relatively similar.

4.2.2 Field and laboratory measurements

In total, 65 white spruce trees from 15 PSPs and 46 aspen trees from 12 PSPs were felled (Table 15). The process of selecting trees to be felled for biomass sampling is described in Sattler et al. (2014). Briefly, however, trees were selected in order to provide a range in sizes (DBH) and tree ages (cambial age at BH) for the given plot. Once felled, all live branches greater than 0.3 cm in diameter at the point of insertion with the main stem (9332 branches) were measured for branch diameter, branch angle, and location along the main stem. A subsample of 6 branches on each felled tree was then randomly selected after first dividing the live crown in two equal halves (3 in the upper half and 3 in the lower half). Subsampled branches were first measured for total branch length (Hb (cm)). Foliage was then separated from woody components, oven dried (minimum 72hours @ 70C) and then weighed. Sapwood in the tree bole was measured on discs cut at crown base, mid-crown, half-way between crown base and mid-crown and finally half-way between mid-crown and the apex of the crown. Sapwood widths were measured at four orthogonal points after holding the discs up to a light source and tracing around the darkened heartwood centre.

Table 15 Means (with standard deviation in parentheses) by diameter class (Diam class) of tree-level variables for the sampled spruce and aspen trees.

Diameter class	DBH (cm)	Height (m)	Cl (m)	Wf (Kg)	As _{cb} (m ²)	n
Spruce						
Diam class1 (<16cm)	15.07 (0.86)	13.97 (1.87)	10.72 (1.94)	9.92 (3.49)	0.009 (0.002)	11
Diam class2 (16.0-22.5cm)	20.56 (1.72)	18.01 (2.45)	11.73 (2.04)	16.12 (6.35)	0.014 (0.007)	14
Diam class3 (22.5-30.0cm)	25.72 (2.21)	20.92 (3.94)	13.22 (3.11)	20.09 (5.93)	0.014 (0.005)	15
Diam class4 (30.0-36.5cm)	32.12 (2.16)	26.64 (2.75)	16.09 (4.04)	29.69 (12.39)	0.019 (0.008)	10
Diam class5 (+36.5cm)	41.28 (2.23)	31.64 (1.67)	19.71 (4.56)	39.64 (12.46)	0.024 (0.009)	15
Aspen						
Diam class1 (<16cm)	14.54 (1.09)	18.89 (2.31)	6.81 (1.46)	1.26 (0.43)	0.004 (0.001)	15
Diam class2 (16.0-22.0cm)	18.83 (1.54)	20.52 (1.87)	7.62 (1.58)	2.01 (0.43)	0.006 (0.002)	11
Diam class3 (22.0-28.0cm)	25.37 (1.82)	24.72 (2.42)	9.68 (1.31)	3.34 (1.10)	0.013 (0.004)	14
Diam class4 (+28cm)	31.38 (1.89)	26.06 (2.64)	8.00 (2.27)	3.87 (1.19)	0.013 (0.005)	6

Note: Variable symbols are DBH (diameter at breast height; 1.3m); Height (total tree height); Cl (live crown length); Wf (foliage mass); As_{cb} (sapwood area at crown base); n (sample size).

4.2.3 Scaling up from branch to tree

To scale-up measurements of foliage mass (see Table 16 for variable descriptions) from branch to tree, we developed a nonlinear mixed effect model which included both plot and tree-level random effects. For white spruce and aspen, the nonlinear mixed effects model used to obtain estimates of foliage mass (Wf) at the branch level was:

$$[15] \quad Wf_{jkl} = \beta_1 \times A_{b,jkl}^{(\beta_2 + b_{2j} + b_{2jk})} \times Rdinc_{jkl}^{(\beta_3 + b_{3j} + b_{3jk})} + \varepsilon_{1jkl}$$

where A_b is branch basal area (cm²) and $Rdinc$ is the relative distance into the crown from tree apex and Wf_{jkl} is foliage mass (in Kg) for branch l in tree k , nested within plot j . The $\beta_1, \beta_2, \beta_3$ are fixed effect parameters, while $b_{2,j}, b_{2,jk}, b_{3,j}$ and $b_{3,jk}$ are the random effects for tree k ,

nested within plot j . Independent variables tested in the models were limited to those that were measured on all live branches. A power variance weight structure that was a function of branch basal area was used to account for heteroskedasticity, while autocorrelation was addressed through a continuous autoregressive structure. For spruce, the fixed + random effects explained 68% of the variability in branch-level Wf (RMSE = 0.08 Kg; $\beta_1=50.41, \beta_2=1.07, \beta_3=-0.63$). For aspen, fixed + random effects accounted for 86% of the variability in branch-level Wf (RMSE=0.03 Kg; $\beta_1=21.53, \beta_2=1.07, \beta_3=-1.67$).

For white spruce and aspen, the models were comparable to those reported by (Kantola and Mäkelä 2004) and (Ceulemans et al. 1990). For each species, the fitted model was used to calculate foliage mass for all live branches ≥ 5 mm. Tree-level totals for foliage mass were obtained by summing across all branches within a tree.

Table 16 Symbols and associated description of variables used for the analyses.

Variable Symbol	Description
Wf	Foliage mass (Kg)
AS _{cb}	Sapwood area at crown base (cm ²)
Ra _k	Ratio of cumulative Wf to CPA at the base of crown quarter section k
Rp _k	Ratio of cumulative Wf to As at the base of crown quarter section k
Cl	Length of live crown (m)
Rdinc	Relative crown depth from tree apex
H _k	Distance along main stem from stump (m)
Diam class	Diameter class (1 to 5 for spruce; 1 to 4 for aspen) ¹
Bal	Basal area of larger trees (m ² ha ⁻¹)

¹ See Table 15 for diameter class ranges used for each species.

4.2.4 Whole crown allometry

Tests for a constant or variable allometric relationship (CAR or VAR, respectively) between Wf and Cl were performed using the following two equations:

$$[16] \quad Wf = \delta_{0,Cl} Cl^{\delta_{1,Cl}}$$

$$[17] \quad Wf = \delta_{0,Cl} Cl^{\delta_{1,Cl}} \exp^{Cl\delta_{2,Cl}}$$

where Wf and Cl are as previously defined and δ_0 , δ_1 and δ_2 are parameters to be estimated from the data. For both Equation 16 and Equation 17, δ_0 is the rate parameter, while δ_1 is the scale parameter. Equation 16 assumes constant allometry, while Equation 17 is formulated following Ruark's variable allometric equation (VAR) (Ruark et al. 1987). If the relationship is constant, then there should be no improvement in model performance between Equation 16 and Equation 17. Furthermore, estimates resulting from Equation 16 should be unbiased across Cl. Since the competitive status of the tree may influence scaling between Wf and Cl, residuals were also examined across the basal area of larger trees (Bal). Equations 16 and 17 were fitted using a power variance weighting structure that was a function of Cl. Comparisons between equations were performed using likelihood ratio tests and adjusted- R^2 values.

4.2.5 Within-crown allometry

Within-crown scaling between Wf and Cl was assessed by first dividing total Cl into four equal sections ($k=1, 2, 3, 4$); where 1 is the top section and 4 is the section at the base of the live crown. The within-crown scaling between the foliage mass and length of the k th quarter section was then examined using the following equation:

$$[18] \quad Wf_k = \varphi_{0,k} Cl_k^{\varphi_{1,k}}$$

where $\varphi_{0,k}$ and $\varphi_{1,k}$ are parameters to be estimated, while Wf_k and Cl_k are the foliage mass and crown length of the k th crown quarter section, respectively. A power variance weight function was used while residual plots were used to identify bias and model performance assessed via root mean square error (RMSE) and adjusted- R^2 .

4.2.6 Whole-crown foliage mass from pipe model theory

Using pipe model theory, the following equation was fitted to the spruce and aspen data:

$$[19] \quad Wf = \alpha_0 As_{cb}$$

where Wf is as previously defined, As_{cb} (cm^2) is sapwood area at the base of the live crown and α_0 is the pipe model ratio. Our evaluation of the pipe model for use on spruce and aspen was conducted using equivalence testing as described by Robinson et al. (2005). Specifically, equivalence tests were used to determine if, for each species, predicted foliage mass for the crown (from Equation 19) was equivalent to measured values. The equivalence tests were performed for the whole dataset as well as by individual diameter classes. Two-one sided bootstrapped confidence intervals for the intercept and slope of the regression were calculated and the null hypothesis of dissimilarity between the measured and predicted values was evaluated. Tests of the null hypothesis on the intercept were used to test for lack of bias, while tests of the null hypothesis on the slope was used to test for appropriate association between measured and predicted values. As a region of equivalence, we began with $\pm 10\%$ for the intercept and $\pm 10\%$ for the slope, and increased the region in increments of 5% until we could reject the null hypothesis of dissimilarity. As a point of comparison for the pipe-based models,

we calculated Wf using DBH and height-based equations from the parameters provided by Manning (1984; for white spruce) and Alemdag (1984; for aspen). The same equivalence tests were then performed on the resulting predictions.

4.2.7 Within-crown foliage mass from pipe model theory

To examine within-crown scaling between cumulative Wf and As, the ratio of these two variables at the base of the k th crown section was calculated as:

$$[20] \quad R_{p_k} = \frac{\sum_1^k Wf_k}{As_k}$$

where R_{p_k} is the ratio between cumulative Wf_k and As_k at the base of the k th crown quarter section. R_{p_k} was then modeled using the following equation:

$$[21] \quad R_{p_k} = \lambda_0 * X_k^{\lambda_1}$$

$$X = H_k, Rdinc$$

where H_k is height (m) to the base of the k th crown quarter section. To investigate the possibility of tree size effects on R_{p_k} , we included a parameter to account for the effect of diameter class. Specifically, we used the diameter class 1 as our reference and tested for differences with the other size classes. With this method, the null hypothesis is that there is no difference between the parameters estimated for diameter class 1 and those estimated for all other size classes. Using the parameter λ_1 as an example, we incorporated this test into Equation 21 using the following notation:

$$\lambda_1 = \lambda_{1,dclass=1} + \lambda_{1,dclass}$$

where $\lambda_{1,dclass=1}$ is the reference value for diameter class 1 and $\lambda_{1,dclass}$ is the difference between the reference value and that for any other size class. Tests for significant differences in the scale parameter between diameter classes were used to test the null hypothesis that Rp_k remains constant over increasing hydraulic path length, represented here as H_k . Under the null hypothesis, the scale parameter should be similar across all diameter classes. As a complimentary tests, Equation 21 was fitted after replacing H_k with relative depth into the crown ($Rdinc$). If hydraulic path length does indeed affect Rp (i.e., rejection of null hypothesis), then we should expect to find non-significant differences across diameter classes in the scale parameter when the model is fitted using $Rdinc$. Heteroskedasticity and correlation between observations were addressed as was done in previous equations. Parameters for all equations were estimated using the `gnls` function (generalized nonlinear least squares) in the `nlme` package (Pinheiro et al. 2015) for R (R Core Team 2013).

4.3 Results

4.3.1 Foliage mass and crown length: whole crown allometry

The estimated parameters and fit statistics for the CAR (Equation 16) and VAR (Equation 17) models for spruce and aspen are presented in Table 17. Likelihood ratio tests and values for the RMSE indicated that for both spruce and aspen, the VAR model was not superior to the CAR. Thus, for both spruce and aspen, scaling between foliage mass and crown length appeared to be constant. For spruce, the CAR model indicated that foliage mass scaled with crown length with an exponent of 1.45 (Figure 25a), while for aspen the exponent was 1.29 (Figure 25b). For both species, the residuals resulting from the CAR model showed no trends across crown length. However, for spruce, there was noticeable bias when the residuals were plotted against Bal .

Specifically, the CAR model under-estimated foliage mass on trees in a dominant position and over-estimated foliage mass for trees in a suppressed position. For aspen, there were no trends in the residuals when plotted across Bal.

Table 17 Estimated parameters (standard error, SE, in parentheses) and fit statistics from the constant and variable allometric models (CAR and VAR; Equation 16 and 17 in text) fitted to spruce and aspen data. For each species, the CAR and VAR models were fitted as a function of crown length (Cl; m).

	δ_0	δ_1	δ_2	Adj.- R^2	Likelihood ratio test ¹	p-value	RMSE
Spruce							
CAR	0.47 (0.18)	1.45 (0.14)	-	61%	-	-	8.41
VAR	0.09 (0.15)	2.41 (0.95)	-0.06 (0.06)	61%	1.101	0.2939	8.36
Aspen							
CAR	0.15 (0.09)	1.29 (0.28)	-	31%	-	-	1.02
VAR	0.19 (0.48)	1.07 (2.21)	0.02 (0.27)	30%	0.01	0.917	1.03

¹ Likelihood ratio tests and associated p-value were the result of comparing the CAR to the VAR model.

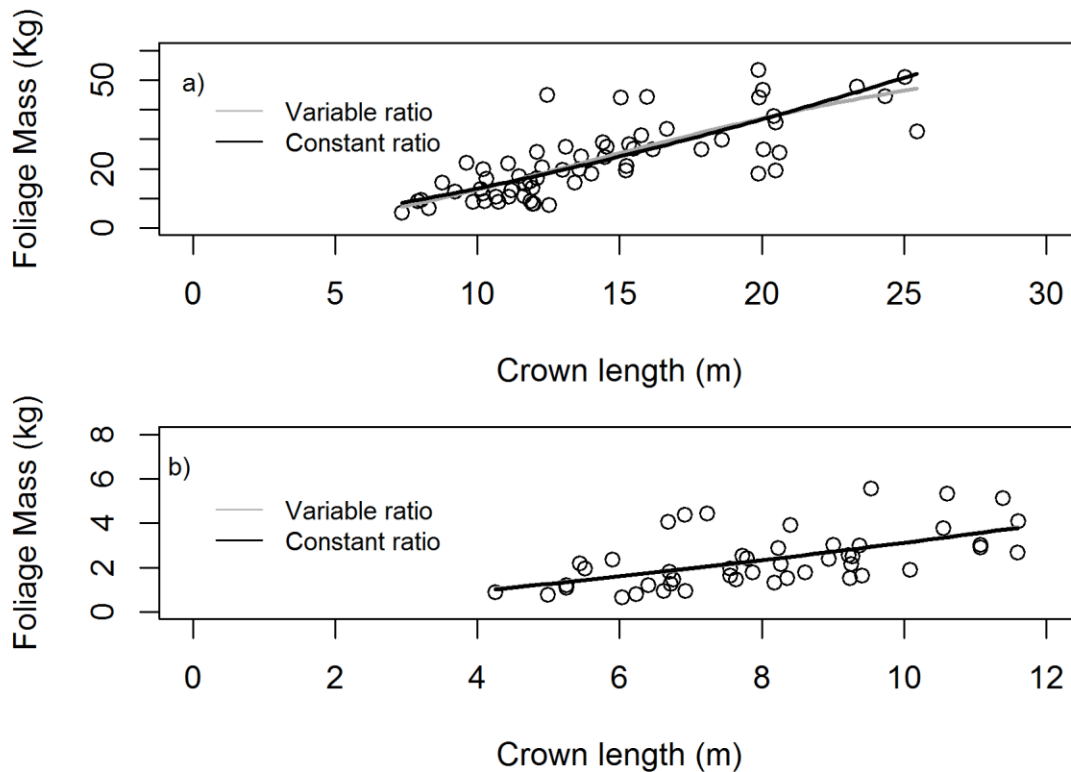


Figure 25 Whole-crown allometry between foliage mass (Kg) and crown length (m) for white spruce (a) and aspen (b). Lines are predictions from the fitted constant (black lines) and variable (grey lines) allometric equations (Equation 16 and 17, respectively).

4.3.2 Foliage mass and crown length: within-crown allometry

For spruce, results from Equation 18 indicated that foliage mass and crown length in the top quarter section (i.e., $Wf_{k=1}$ and $Cl_{k=1}$, respectively) scaled at a value near to that postulated for open grown trees (cf. Mäkelä and Sievänen 1992). For each subsequent crown quarter section, the exponent parameter was lower than that for the above quarter section (Figure 26). Crown section $k=2$ had the most foliage mass per given crown length, followed by $k=1$ (i.e., the top section), $k=3$ and finally, $k=4$ (i.e., the bottom quarter section). Goodness of fit statistics revealed that the crown length of the quarter section explained progressively less of the variation in the

foliage mass moving from the top section to the bottom section (Table 18). Analysis of the residuals from each quarter section revealed that there was no bias across quarter section crown length. For the top quarter section, there was also minimal bias across Bal. Bias in relation to Bal, however, was evident within all three lower crown quarter sections, with trends in the residuals mirroring those from the CAR model fitted to the whole-crown (Figure 27).

Table 18 Parameter estimates (standard error, SE, in parentheses) for Equation 18, describing the relationship between within-crown Wf_k and Cl_k (k =crown quarter section 1, 2, 3, 4) for spruce and aspen.

Model: $Wf_k=f(Cl_k)$	$\varphi_{0,k}$	$\varphi_{1,k}$	p-value	RMSE	Adj.-R^2
Spruce					
Top - 25% ($k=1$)	0.26 (0.07)	2.23 (0.19)	<0.05	2.54	71%
25 - 50% ($k=2$)	0.85 (0.19)	1.71 (0.17)	<0.05	3.70	54%
50 - 75% ($k=3$)	1.4 (0.30)	1.14 (0.17)	<0.05	2.76	26%
75% - Crown base ($k=4$)	1.79 (0.46)	0.62 (0.20)	<0.05	1.99	9%
	$\varphi_{0,k}$	$\varphi_{1,k}$	p-value	RMSE	Adj.-R^2
Aspen					
Top - 25% ($k=1$)	0.1 (0.01)	1.2 (0.3)	<0.05	0.14	14%
25 - 50% ($k=2$)	0.18 (0.04)	1.79 (0.28)	<0.05	0.26	53%
50 - 75% ($k=3$)	0.32 (0.09)	1.43 (0.41)	<0.05	0.56	22%
75% - Crown base ($k=4$)	0.35 (0.1)	0.92 (0.43)	<0.05	0.46	5%

The pattern of scaling between within-crown estimates of foliage mass from crown length in aspen was quite different from that of spruce (Figure 26). For aspen, the largest value for the allometric exponent was found in crown section $k=2$. Crown section $k=4$ had the smallest allometric exponent, which was also the case for white spruce. However, there was no decreasing trend from crown top to crown base in the value of the exponent parameter. The largest amount of foliage mass supported by a given crown length section in aspen trees was in crown section $k=3$. The top section supported the smallest amount of foliage mass for a given

crown length. The best indices of fit (adjusted- R^2 , RMSE) were for crown section $k=2$, followed by $k=3$, $k=4$ and finally, $k=1$. As was the case with the CAR model fitted at the whole crown level, the within-crown relationship between foliage mass and crown length section showed no bias with respect to crown length or Bal (Figure 28).

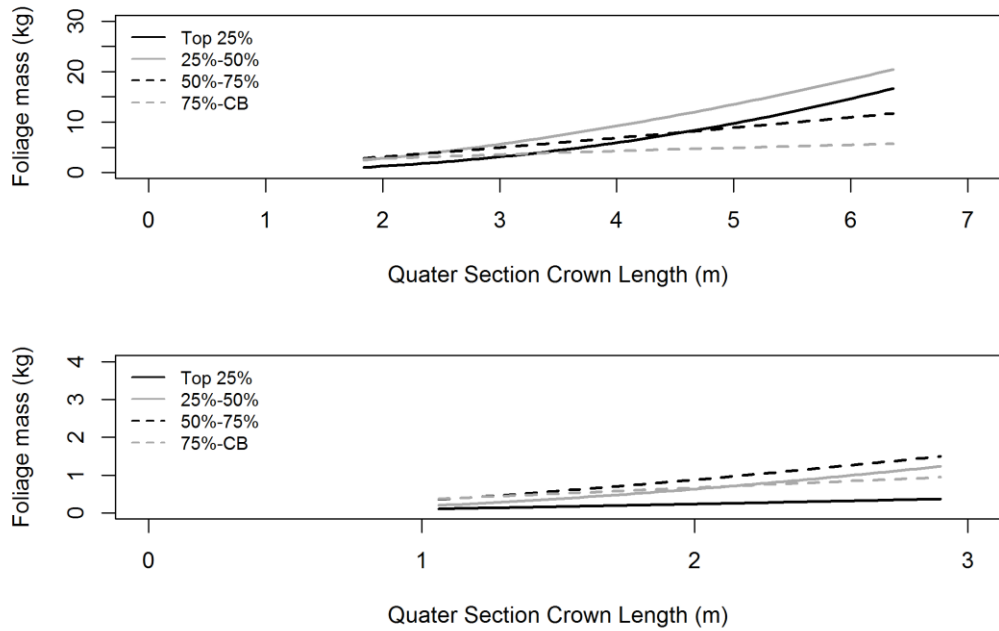


Figure 26 Within-crown scaling between foliage mass (Kg) and crown length (m) for quarter sections of the crown (Equation 18). Top panel is for spruce, bottom panel is for aspen.

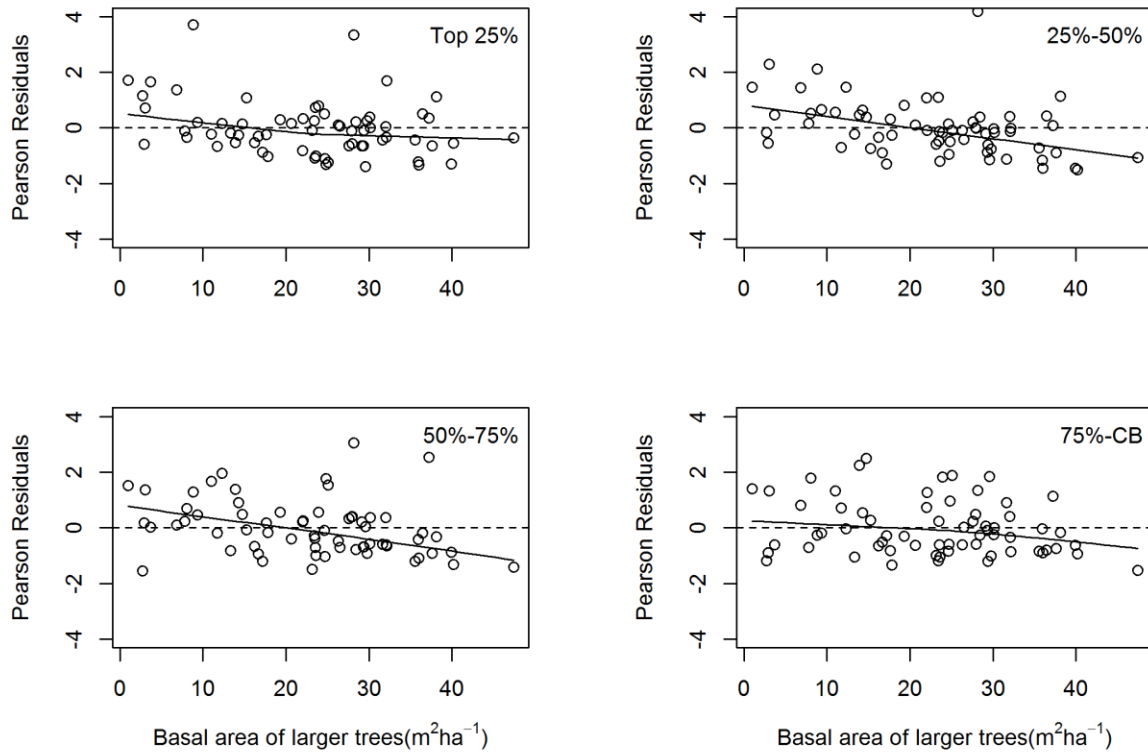


Figure 27 Pearson residuals from the relationship between foliage mass and crown length in white spruce by crown quarter section (Equation 18) plotted against basal area of larger trees (m^2ha^{-1} ; Bal).

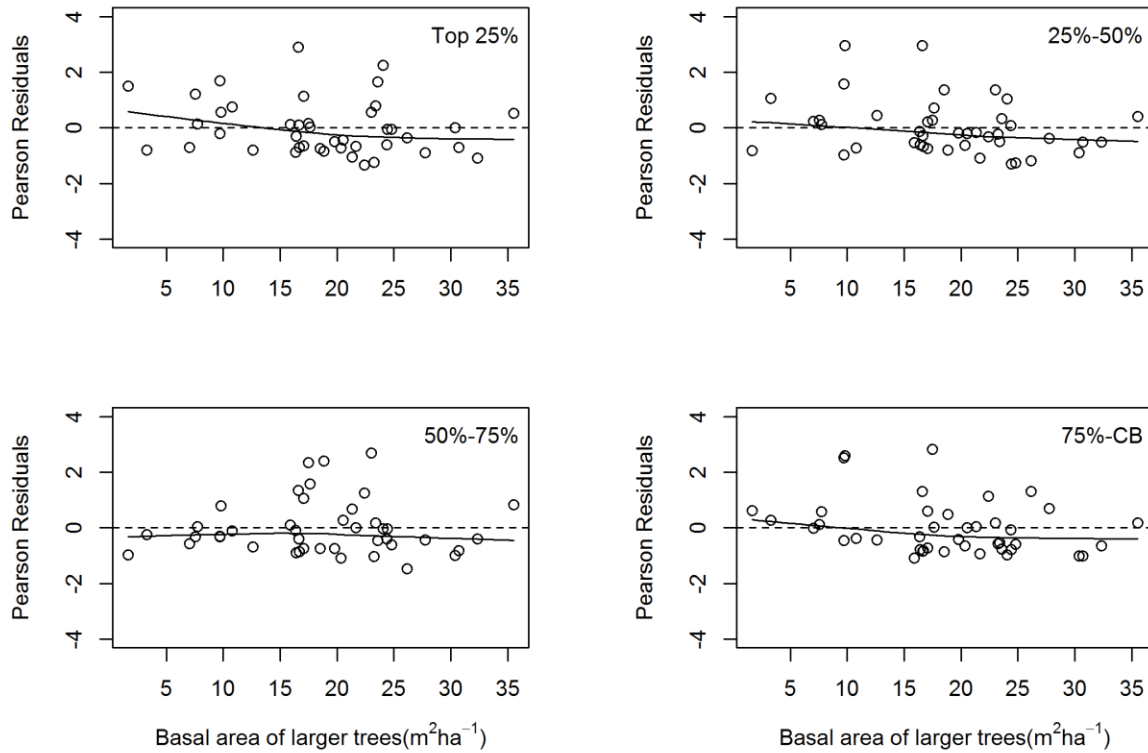


Figure 28 Pearson residuals from the relationship between foliage mass and crown length in aspen by crown quarter section (Equation 18) plotted against basal area of larger trees (m²ha⁻¹; Bal).

4.3.3 Pipe model ratio: whole-crown allometry

The estimated pipe model ratio in Equation 19 (α_0) was 0.14 (SE=0.005) for spruce and 0.03 (SE=0.001) for aspen. The pipe model explained a far greater proportion of the variability in foliage mass for spruce (Adj.- R^2 =69%; RMSE=7.48 Kg; bias=-0.11) than for aspen (Adj.- R^2 =25%; RMSE=1.09 Kg; bias=-0.19). When fitted to the dataset containing all diameter classes, equivalence tests on the intercept (test of bias) and the slope (test of accuracy) had a smaller minimum region to reject the null hypothesis of dissimilarity for spruce than for aspen (Table 19). For individual diameter classes, equivalence tests on the intercept for spruce showed

comparable results to that found for aspen, with minimum regions of rejection between 15 and 40%. However, tests on the slope indicated that the pipe model tended to provide greater accuracy in estimates of foliage mass for spruce than for aspen. For any one diameter class, we judged the regions of equivalence required to reject the null hypothesis for the slope to be quite large for both spruce and aspen. Nevertheless, there was stronger evidence in favour of the pipe model than the regionally calibrated DBH and height-based equations provided by Manning et al. (1984) and Alemdag (1984) (Table 19).

Table 19 Results of equivalence tests on prediction of Wf from the fitted pipe model (Equation 19) and from published DBH and Height-based equations [Spruce = Manning (1984); Aspen = Alemdag (1984)]. Equivalence tests of predictions from the fitted pipe model are for the full dataset (all DBH classes) and by individual DBH classes (diam class 1 to 5 for spruce and diam class 1 to 4 for aspen).

Spruce						
Data Grouping	CI (Intercept)	Region of Similarity	Min. Region of Equivalence for Intercept	CI (Slope)	Region of Similarity	Min. Region of Equivalence for Slope
Full dataset	21.77-25.46	21.30-26.03	10%	0.76-1.14	0.75-1.25	25%
diam class 1	35.33-44.46	22.07-45.85	35%	0.24-1.07	0.2-1.8	80%
diam class 2	25.94-34.12	17.36-36.05	35%	0.59-1.36	0.55-1.45	45%
diam class 3	18.50-22.97	18.25-24.69	15%	0.06-0.75	0.04-1.9	90%
diam class 4	14.77-17.14	14.28-26.53	30%	0.44-0.72	0.45-1.55	55%
diam class 5	8.82-10.89	8.40-19.61	40%	0.36-1.01	0.35-1.65	65%
Manning	21.40-25.78	19.08-89.96	65%	0.16-0.27	0.15-1.85	85%
Aspen						
Data Grouping	CI (Intercept)	Region of Similarity	Min. Region of Equivalence for Intercept	CI (Slope)	Region of Similarity	Min. Region of Equivalence for Slope
Full dataset	2.15-2.68	2.06-3.10	20%	0.38-0.92	0.35-1.65	65%
diam class 1	1.16-1.38	1.06-1.43	15%	0.78-1.27	0.7-1.3	30%
diam class 2	1.68-2.18	1.41-2.63	30%	-0.33-0.56	-0.35-2.35	135%
diam class 3	2.84-4.31	2.68-4.99	30%	-0.21-1.60	-0.35-2.35	120%
diam class 4	3.05-4.00	2.91-4.86	25%	-0.13-0.76	-0.2-2.2	120%
Alemdag	2.17-2.60	1.41-55.34	90%	0.04-0.06	0.03-1.95	100%

Note: Confidence intervals (CI) for the intercept (test of bias) and slope (test of accuracy) were obtained using a non-parametric bootstrap based on 5000 replicates. Regions of similarity, which fall within the CIs, were obtained after determining the minimum region of equivalence at which the null hypothesis of dissimilarity could be rejected. All tests were evaluated at $\alpha=0.05$.

4.3.4 Pipe model ratio: within-crown allometry

For spruce, the estimated exponent parameter in Equation 21 fitted using distance from stump (H_k) as the independent variable was not significant for diameter class 1 (Table 20). That is,

within the crown, the pipe model ratio (R_{pk}) was unchanged over increasing distance from stump in the smallest trees. For all other diameter classes, there was a significant increase in the pipe model ratio with increasing distance from stump (Table 20). Furthermore, the rate of increase in the pipe model ratio with respect to distance from stump increased with increasing diameter class. Overall, the model explained 43% of the variability in R_{pk} , while Pearson residuals indicated that the model was unbiased with respect to both distance from stump and relative depth into the crown (Figure 29). With the Equation 21 fitted using relative depth into crown (R_{dinc}) in place of distance from stump, the variance explained was 38%. For all but diameter class 5, the exponent parameter was not significant indicating that the pipe model ratio was unchanged over increasing relative depth in the crown. For diameter class 5, there was a slight decrease in the pipe model ratio with increasing relative distance from crown apex. Predictions were unbiased with respect to relative depth into the crown. However, there was noticeable bias when residuals were plotted against distance from stump (Figure 30).

Table 20 Estimated parameters (with standard errors, SE, in parentheses) for the relationship of the within-crown pipe model ratio (R_{pk} = foliage mass/sapwood area at crown quarter section k) as a function of distance from stump (H_k) and as a function of relative depth from crown apex (R_{dinc}) (see Equation 21).

Spruce	Model: $R_{pk}=f(H_k)$ Adj.-$R^2=42\%$		Model: $R_{pk}=f(R_{dinc})$ Adj.-$R^2=38\%$	
	Parameters (SE)		Parameters (SE)	
	λ_0^1	λ_1^1	λ_0^1	λ_1^1
diam class 1	986.17 [†] (42.62)	0.01 (0.04)	1013.59 [†] (103.9)	0.015 (0.10)
diam class 2	-93.03 (105.47)	0.10* (0.05)	175.43 (140.14)	-0.13 (0.12)
diam class 3	38.29 (110.69)	0.16* (0.04)	468.32* (137.65)	-0.04 (0.12)
diam class 4	-137.31 (161.06)	0.21* (0.04)	805.82* (153.44)	-0.11 (0.13)
diam class 5	-72.03 (142.22)	0.22* (0.04)	739.79* (138.89)	-0.17 (0.14)

Aspen	Model: $R_{pk}=f(H_k)$ Adj.-$R^2=8\%$		Model: $R_{pk}=f(R_{dinc})$ Adj.-$R^2=6\%$	
	Parameters (SE)		Parameters (SE)	
	λ_0^1	λ_1^1	λ_0^1	λ_1^1
diam class 1	107.13 [†] (57.12)	0.44 [†] (0.20)	314.51 [†] (23.42)	-0.15 (0.08)
diam class 2	-38.59 (73.58)	0.16 (0.32)	8.52 (35.95)	-0.03 (0.12)
diam class 3	-57.25 (71.17)	0.18 (0.35)	-18.63 (33.61)	0.04 (0.12)
diam class 4	-87.06 (64.38)	0.47 (0.53)	6.43 (44.96)	0.09 (0.17)

¹ For diam class 1 (i.e., base value), values for λ_0 and λ_1 are the estimated parameters for Equation 21. For all other diam classes, values for λ_0 and λ_1 are $\lambda_0 + \lambda_{0,dclass}$ and $\lambda_1 + \lambda_{1,dclass}$, respectively.

[†] Denotes a base value parameter that is significantly different from zero at alpha=0.05.

* Denotes parameters that are significantly different from the base value.

With Equation 21 fitted to the aspen data using distance from stump as the independent variable, a significant increase in pipe model ratio was detected for all diameter classes. Furthermore, the rate of increase was similar for all diameter classes. However, we found that at any given distance from stump, trees in diameter classes 3 and 4 had significantly less foliage mass per unit sapwood area than trees in diameter class 1 and 2 (Table 20). Using distance from stump in Equation 21, the model was able to explain only 5% of the within-crown variability in the pipe model ratio. When using relative distance into the crown as the independent variable in Equation

21, no significant within-crown trends in the pipe model ratio were detected in any of the diameter classes. Estimates of the within-crown pipe model ratio derived from relative depth into the crown were unbiased with respect to both relative distance into the crown and distance from stump (Figure 30), which was in contrast to the results for spruce.

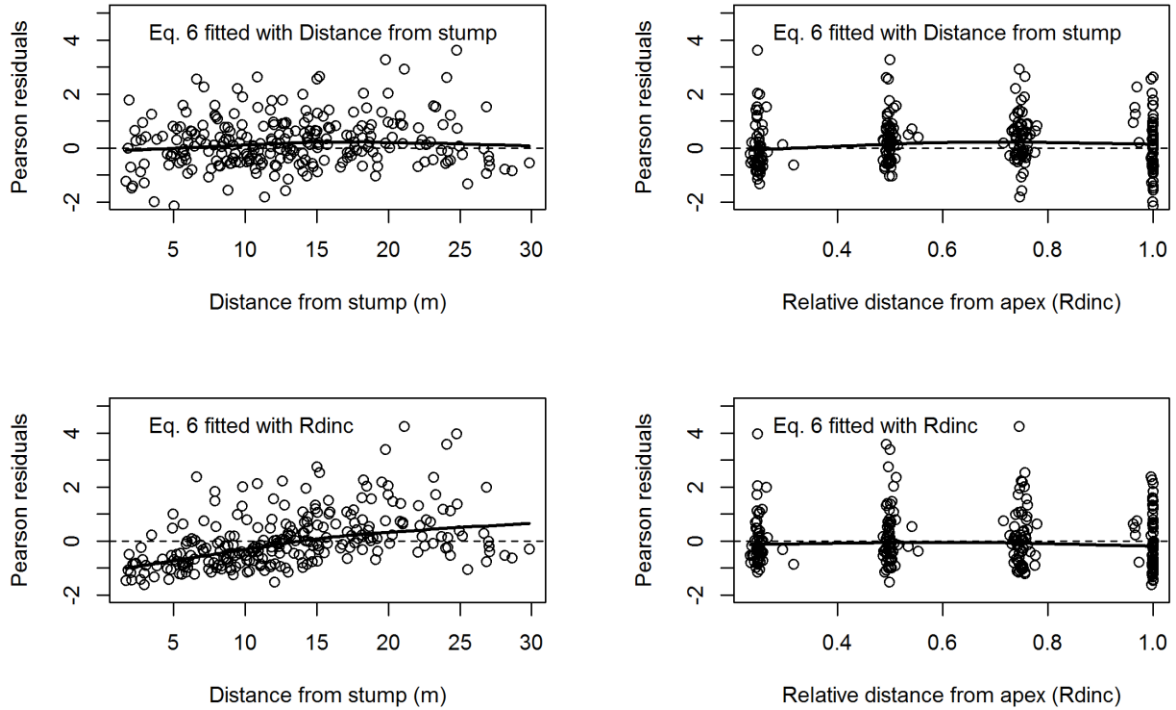


Figure 29 Pearson residuals from Equation 21 fitted to the white spruce data. Top panels show residuals from Equation 21 fitted using distance from stump (H_k ; m) while bottom panels show residuals from Equation 21 fitted using relative distance from tree apex (R_{dinc}).

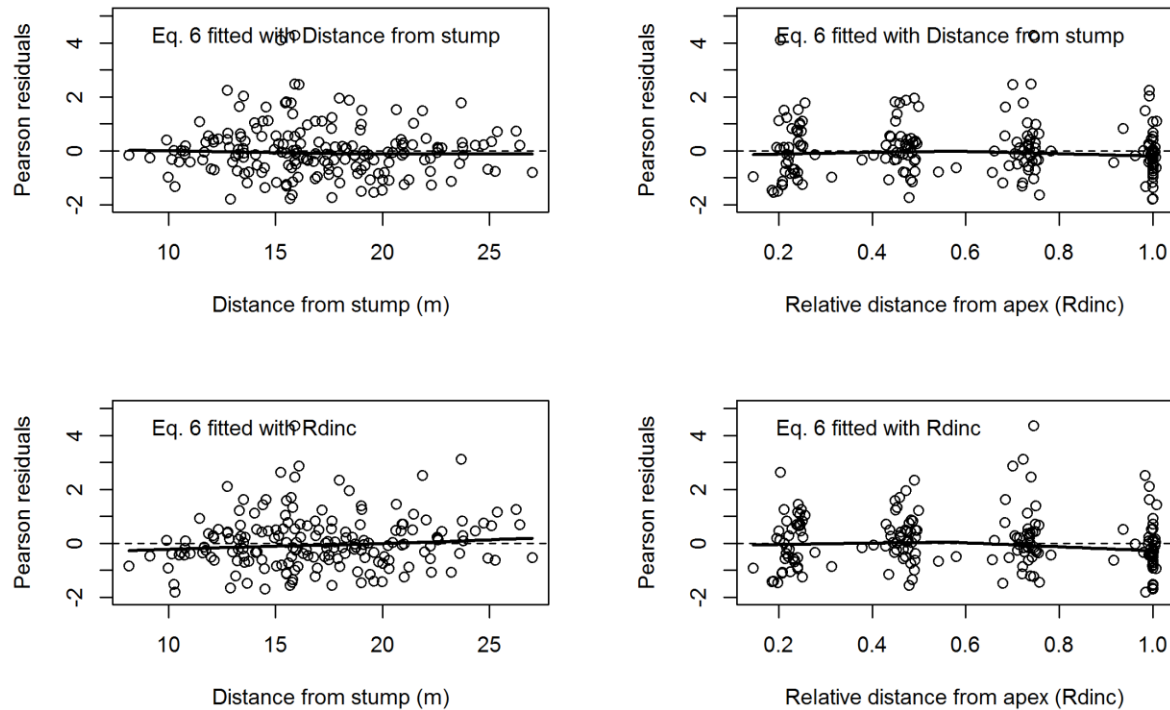


Figure 30 Pearson residuals from Equation 21 fitted to the aspen data. Top panels show residuals from Equation 21 fitted using distance from stump (H_k ; m) while bottom panels show residuals from Equation 21 fitted using relative distance from tree apex (R_{dinc}).

4.4 Discussion

4.4.1 Foliage mass – crown length allometry

That whole-crown foliage mass in spruce showed constant allometric scaling with crown length was unexpected. Given the low self-pruning of branches, high needle retention and a reduction in height growth with age, our prior expectation was that the largest and most mature spruce trees within the sample dataset would accumulate more foliage mass for a given increase in crown length, leading to variable allometric scaling. For aspen, we also expected whole crown foliage

mass to show variable scaling with crown length. This was based on the general understanding that age-related decline in foliage mass usually appears soon after the peak in mean annual increment for shade intolerant species (Satoo 1962), and was previously used to explain a reduction in foliage area in aspen (Lieffers and Stadt 1994).

For spruce, the finding contrary to our expectations suggests that this species employs a strategy of carbon allocation which accounts for the retention of old needles and adjusts the rate of production of new foliage in order to maintain a constant relationship with the vertical growth of the crown. Moreover, this strategy of carbon allocation appears to be maintained beyond the peak mean annual growth of spruce given that the oldest trees we sampled were approximately 150 years old. The allometric exponent for the relationship between foliage mass to crown length indicate that for spruce, there is an increase in foliage density with respect to crown length over increasing tree size. Although the findings are contrary to our expectations, similar trends were found in Norway spruce, a species which displays a shade-tolerance similar to that of white spruce (Kantola and Mäkelä 2004). However, it should be noted that Kantola and Mäkelä (2004) did not explicitly test the possibility that a VAR model would have better suited their data.

As was the case for spruce, aspen showed a constant allometric relationship between foliage mass and crown length. For aspen, it appears that despite age-related effects such as increased incidence of disease and reduced stomatal conductance (Smith et al. 2011), carbon continues to be allocated in a manner which maintains the same amount of foliage production for a given increase in crown length. Similarly, Ilomäki et al (2003) reported a constant allometric relationship between foliage mass and crown length for silver birch. However, as was previous

noted, there was no indication that Ilomäki et al. (2003) explicitly tested for a variable allometric relationship.

Supposing that the full crown of both spruce and aspen are exposed to sunlight, then the relative rates of growth for foliage mass and crown length should, in theory, be in response to the need to regulate self-shading (Okerblom and Kellomaki 1982). In such a case, a constant allometric relationship between foliage mass and crown length will be one that provides the optimal compromise between the benefits of increased foliage mass (i.e., increased photosynthesis) and the increased respiration costs that come with maintaining the structures to support a larger crown (Mäkelä and Sievänen 1992). For the aspen in the current study, one can argue in support of this supposition given that its growth strategy is to maintain the near entirety of the crown above that of competing vegetation. It is less defensible for white spruce, however, where a large proportion of the crown lies within the shade cast by competitors and is therefore, less photosynthetically active (Schoonmaker et al. 2014). Consequently, competition from neighbouring trees is also likely to be an important factor driving size-related changes in foliage growth. Indeed, bias across B_{all} in the residuals resulting from the CAR model in spruce indicated that competition from neighbouring trees had an effect on the relationship between whole crown foliage mass and crown size beyond that posed by self-shading.

In comparison to other boreal tree species, the estimated exponent parameter for Equation 16 was low for both spruce and aspen. For the shade tolerant Norway spruce, Kantola and Mäkelä (2006) reported a value of 1.78. A value of in the range of 2-3 was reported by Mäkelä and Sievänen (1992) for open grown Scots pine and red pine, both shade-intolerant species. For Silver birch, also a shade intolerant species, Ilomäki et al. (2003) reported an exponent parameter

of 2.62. It is likely that differences in site fertility and local climate are at least partially responsible for the observed discrepancies and thus, direct comparison is not possible. Nevertheless, it was interesting to note that the aforementioned studies used trees from either open grown or evenly spaced, single-species, managed stands. Within the unmanaged mixed-species stands sample for the current study, greater heterogeneity of within canopy light levels and increased competition for light may possibly explain why the allometric exponents we found were low relative to those reported in other studies.

4.4.2 Within-crown scaling between foliage mass and crown length

Scaling between foliage mass and crown length within the top crown quarter section in spruce was within the range postulated for open grown trees by (Mäkelä and Sievänen 1992), while residual plots indicated that the relationship was unrelated to the competitive status of the tree (Bal). We can, therefore, imply that shade cast by neighbouring competitors on the tops of the spruce trees has little effect on how foliage density within the top 25% of the crown is regulated with respect to crown length. This is in line with the results of Kantola and Mäkelä (2004), where the allometric relationship between foliage mass and crown length in the top 5m of Norway spruce crowns was unaffected by tree age or competition. Our finding that there was progressively less foliage mass for a given crown length with increasing depth into the crown is likely a reflection of the diminishing light levels with increased crown depth. The question then is one of determining to what extent does shading from neighbouring trees influence within-crown scaling between foliage mass and crown length above which is controlled by self-shading? Based on the trends in the residuals across Bal observed in crown sections 2-4, the additional effects of shading from competitors appear to be strongest in middle section of the

crown. Overall, results of within-crown scaling suggest that in order to maintain constant allometric scaling between foliage mass and crown length at the whole-crown level, spruce trees allocate a greater proportion of foliage to points higher in the crown, which is similar to what was reported for Norway spruce (Mäkelä and Vanninen 1998).

For aspen, within-crown scaling between foliage mass and crown length differed from spruce in that the top crown section did not display an allometric exponent parameter close to the theoretical values proposed for open grown trees. Furthermore, there was no decreasing pattern in the allometric exponent parameter from the top to the bottom crown section. From this latter point it appears that, regardless of position within the crown, competition from neighboring trees has little influence on foliage production with respect to crown length. This seems to confirm our earlier suggestion that scaling of foliage mass with crown length in aspen is largely driven by the need to control self-shading. It remains unclear, however, why the allometric scaling exponents for all crown sections were much lower than the expected value for open grown trees. Greater investment into branch wood production and a decreased foliage production during drought years may be at least partially responsible for this discrepancy.

4.4.3 Whole crown foliage mass from pipe model theory

Mäkelä (1997) notes that the assumption of a constant relationship between whole crown foliage mass and As_{cb} will hold on average, but is expected to show some deviation. Viewed within this context, the results of the equivalence testing on white spruce are in line with expectations. That is, for the full dataset, the regions of equivalence to reject the hypothesis that model predictions are both biased and dissimilar, were within the 25% limit suggested by Wellek (2003). However, for any one diameter class, we can expect considerable dissimilarity between observed and

predicted values. While this latter point raises questions regarding the robustness of the pipe model, it must be weighed against the superior performance of the pipe model relative to the regionally calibrated DBH and height based equations. This finding is in accordance with Lehtonen (2005) where it was reported that the basal area of the stem at crown base was a better predictor of foliage mass than DBH or DBH and height-based equations for Norway spruce and Scots pine. Therefore, we conclude that further efforts to validate the pipe model theory for use on white spruce appears to be warranted.

For aspen, the large regions of equivalence required to reject the null hypothesis of dissimilarity for the full dataset as well as for any given diameter class suggest that the pipe model, as was tested here, is not appropriate for this species. That being said, using a pipe-based model to predict foliage mass in aspen should still be considered given its performance relative to that of the regionally calibrated DBH and height-based equations. Mäkelä (2002) proposed a modification of the pipe model which accounts for the gradual transition of heartwood to sapwood, and should be considered at a 'next step' in the evaluation of the pipe model for use on aspen. Alternatively, issues related to the measurement of sapwood in aspen may have influenced our results. For example, swelling of the main stem near the crown base of aspen we sampled may be a source of bias. Additionally, the visual delineation of sapwood area in aspen was hampered by the frequent occurrence of isolated pockets of sapwood within the heartwood, which were absent in spruce. Similar considerations were also discussed by Mäkelä and Vanninen (2001), who suggest that an examination of the hydraulic capabilities would help explain such discrepancies.

4.4.4 Within-crown foliage mass from pipe model theory

Our examination of the within-crown pipe model ratio with respect to distance from stump (H_k) and relative crown depth (R_{dinc}) provided conflicting results. On one hand, the constant pipe model ratio with respect to relative crown depth across all diameter classes lent support to the pipe model theory. However, we also found that the within-crown pipe model ratio increased with increasing distance from stump (H_k) for both spruce and aspen. The sole exception being that for diameter class 1 in spruce. This finding was not consistent with pipe model theory, which assumes this ratio to be independent from tree size and position within the crown.

These findings are also not consistent with the hydraulic model of tree architecture. In contrast to the pipe model theory, the hydraulic model of tree architecture predicts that the ratio of whole crown foliage mass to sapwood area at breast height should decrease with increasing tree height (Whitehead and Jarvis 1981; McDowell et al. 2002). It is postulated that in order to maintain leaf-specific hydraulic sufficiency, taller trees require greater sapwood area per foliage mass given the longer hydraulic path length and associated gravitational constraints. Whitehead et al. (1984b), Coyea and Margolis (1992), McDowell et al. (2002) and Mencuccini (2002) all reported decreasing R_p ratios with increasing tree size. Furthermore, the hydraulic model predicts that there should be progressively less foliage mass per unit sapwood area with increasing distance from the stump. Mäkelä and Vanninen (2001), for example, found the pipe model ratio to decrease from crown base to tree apex for Scots pine. Similarly, Medhurst and Beadle (2002) found the leaf area to sapwood area ratio to decrease with increasing distance from crown base in Eucalyptus (*Eucalyptus nitens*). In contrast, for the current study we found the pipe model ratio to increase with increasing distance from stump for both spruce and aspen.

An increasing pipe model ratio with increasing height within the tree is not without precedence. At the whole-crown level, Mokany et al. (2003) and Schneider et al. (2008) both reported an increase in the pipe model ratio with increasing tree size for alpine ash (*Eucalyptus delegatensis* R.T. Baker) and jack pine, respectively. Furthermore, McDowell et al. (2002) noted an increasing pipe model ratio with increasing tree height in Norway spruce and Balsam fir [*Abies balsamea* (L.) Mill.]. Within the crown, Schneider et al. (2011) found that the pipe model ratio decreased with increasing distance from tree apex in Jack pine sampled at three different sites in eastern Canada. They rationalized that differences in the turnover rates of sapwood and foliage could explain the trends they observed. Specifically, they argued that the presence of heartwood in older branches and the re-activation of disused sapwood near crown base leads to greater hydraulic inefficiency lower in the crown, which in turn causes the pipe model ratio to be lower near crown base. However, under this hypothesis we would have expected trends for the within-crown pipe model ratio to show a significant nonlinear relationship with relative depth into the crown for trees in the larger diameter classes. Increased sapwood permeability and soil-to-leaf water potential difference have been cited as possible mechanisms that could explain an increase in pipe model ratio with tree size, although the current set of arguments in favour of these mechanisms is not convincing (McDowell et al. 2002). Leaf specific conductivity, which measures the ability to supply water to unit of foliage, is assumed to be constant according to the hydraulic path length theory. However, Mokany et al. (2003) found that leaf specific conductivity increased with tree size and, therefore, could explain increases in the pipe model ratio with increasing tree height. Despite the findings that lend support to our current set of

results, an examination of leaf specific conductivity in spruce and aspen would be needed to explore the potential link to the within-crown trends for the pipe model ratio we observed.

We found the relationship between the pipe model ratio and distance from stump varied by diameter class for spruce but not for aspen. This suggests that for spruce, there is greater size dependency in the relative rates of increase between foliage mass and sapwood area within the crown. A second point separating the two species was the relationship between the pipe model ratio and the relative depth into the crown (Figure 29 and 30). For spruce, it appears that the relative position within the crown does not account for the effect of increasing hydraulic path length on the pipe model ratio given that there was bias in the residuals when plotted against distance from pith. Conversely, for aspen, using relative position in the crown produced unbiased estimates with respect to both relative position in the crown and distance from stump (Figure 30). This finding could be related to differences in hydraulic conductance between coniferous and diffuse-porous trees. McCulloh et al. (2010) noted that scaling between stem hydraulic conductivity and stem size, which they defined as network conductance, was more dependent on stem size for conifers compared to diffuse-porous trees. Regardless of the mechanism responsible for these differences, the finding is consistent with our results from the examination of within-crown scaling of the pipe model ratio, which also showed size dependence in spruce but not aspen. Consequently, the modifications to the pipe model theory would be needed to account for these size-related changes if within-crown estimation of foliage mass from sapwood area (or vice versa) is desired.

4.5 Conclusions

The results presented here show that the assumption of constant allometric scaling between whole crown foliage mass and crown length generally holds for both spruce and aspen. The assumption of a constant relationship between whole crown foliage mass and As_{cb} also appears to hold on average for spruce. However, there are concerns over the precision in the estimates of foliage mass given the model's poor performance for any single diameter class. For aspen, tests of the pipe model were not convincing. Thus, we conclude that if the Crobas model is to be used within larger areas represented by our study sites, consideration must first be given to how sapwood is measured and how adjustments could improve predictions across all tree sizes. With respect to the latter, this may include the use of additional tree- or stand-level covariates as suggested by Schneider et al. (2008) or a modification to accommodate the gradual transition of sapwood to heartwood as proposed by Mäkelä (2002). Finally, for the relationships that we examined, inconsistencies between the trends seen at the whole-crown level and those seen at the within-crown level were noted. Specifically, those at the whole-crown level appeared far more regular than those at the within-crown level. This feature has been also noted by Mäkelä and Vanninen (2001) and Schneider et al. (2008; 2011). Testing the adjustments that have been suggested to reconcile these differences would be the next logical step.

References

- Alberta Sustainable Resource Development. 2005. Permanent sample plot field procedures manual. Public Lands and Forest Division, Forest Management Branch, Edmonton, Alberta, 30p.
- Alemdag, I.S. 1984. Total tree and merchantable stem biomass equations for Ontario hardwoods. Can. For. Ser. Pi-X-46, 54 p.
- Baldwin, V.C., Peterson, K.D., Burkhart, H.E., Amateis, R.L., and Dougherty, P.M. 1997. Equations for estimating loblolly pine branch and foliage weight and surface area distributions. Can. J. of For. Res. **27**: 918-927.
- Beckingham, J.D., and Archibald, J.H. 1996. Field guide to ecosites of northern Alberta.
- Berninger, F., and Nikinmaa, E. 1994. Foliage area – sapwood area relationships of Scots pine (*Pinus sylvestris*) trees in different climates. Can. J. For. Res. 24: 2263-2268.
- Berninger, F., Coll, L., Vanninen, P., Mäkelä, A., Palmroth, S., and Nikinmaa, E. 2005. Effects of tree size and position on pipe model ratios in Scots pine. Can. J. of For. Res. **35**: 1294-1304.
- Ceulemans, R., Stettler, R., Hinckley, T., Iserbrands, J., and Heilman, P. 1990. Crown Architecture of Populus Clones as Determined by Branch Orientation and Branch Characteristics. Tree Physiol. **7**: 157-167.
- Coyea, M.R., and Margolis, H.A. 1992. Factors Affecting the Relationship between Sapwood Area and Leaf-Area of Balsam Fir. Can. J. of For. Res. **22**: 1684-1693.

- Davidson, R.L. 1969. Effect of root/leaf temperature differentials on root/shoot ratios in some pasture grasses and clover. *Annals of Botany* **33**: 561-569.
- Duursma, R.A., Mäkelä, A., Reid, D.E.B., Jokela, E.J., Porte, A.J., and Roberts, S.D. 2010. Self-shading affects allometric scaling in trees. *Funct. Ecol.* **24**: 723-730.
- Eckmullner, O., and Sterba, H. 2000. Crown condition, needle mass, and sapwood area relationships of Norway spruce (*Picea abies*). *Can. J. of For. Res.* **30**: 1646-1654.
- Geron, C.D., and Ruark, G.A. 1988. Comparison of Constant and Variable Allometric Ratios for Predicting Foliar Biomass of various Tree Genera. *Can. J. of For. Res.* **18**: 1298-1304.
- Gilmore, D.W., Seymour, R.S., and Maguire, D.A. 1996. Foliage-sapwood area relationships for *Abies balsamea* in central Maine, USA. *Can. J. of For. Res.* **26**: 2071-2079.
- Ilomäki, S., Nikinmaa, E., and Mäkelä, A. 2003. Crown rise due to competition drives biomass allocation in silver birch. *Can. J. of For. Res.* **33**: 2395-2404.
- Kaipainen, L.; Hari, P., 1985: Consistencies in the structure of Scots pine. Crop physiology of forest trees. Proceedings of an international conference on managing forest trees as cultivated plants, held in Finland, 23-28 July 1984: 31-37
- Kantola, A., and Mäkelä, A. 2004. Crown development in Norway spruce [*Picea abies* (L.) Karst.]. *Trees-Structure and Function* **18**: 408-421.
- Kantola, A., and Mäkelä, A. 2006. Development of biomass proportions in Norway spruce (*Picea abies* [L.] Karst.). *Trees-Structure and Function* **20**: 111-121.

- Kantola, A., Mäkinen, H., and Mäkelä, A. 2007. Stem form and branchiness of Norway spruce as a sawn timber - Predicted by a process based model. *For. Ecol. Manage.* **241**: 209-222.
- Lehtonen, A. 2005. Estimating foliage biomass in Scots pine (*Pinus sylvestris*) and Norway spruce (*Picea abies*) plots. *Tree Physiol.* **25**: 803-811.
- Lieffers, V.J., and Stadt, K.J. 1994. Growth of Understory *Picea-Glauca*, *Calamagrostis-Canadensis*, and *Epilobium-Angustifolium* in Relation to Overstory Light Transmission. *Can. J. of For. Res.* **24**: 1193-1198.
- Mäkelä, A., and Sievänen, R. 1992. Height Growth Strategies in Open-Grown Trees. *J. Theor. Biol.* **159**: 443-467.
- Mäkelä, A. 1997. A carbon balance model of growth and self-pruning in trees based on structural relationships. *For. Sci.* **43**: 7-24.
- Mäkelä, A., and Vanninen, P. 1998. Impacts of size and competition on tree form and distribution of aboveground biomass in Scots pine. *Can. J. of For. Res.* **28**: 216-227.
- Mäkelä, A., and Vanninen, P. 2001. Vertical structure of Scots pine crowns in different age and size classes. *Trees-Structure and Function* **15**: 385-392.
- Mäkelä, A. 2002. Derivation of stem taper from the pipe theory in a carbon balance framework. *Tree Physiol.* **22**: 891-905.
- Mäkelä, A., and Valentine, H.T. 2006. Crown ratio influences allometric scaling in trees. *Ecology* **87**: 2967-2972.

- Manning, G.H., M.R.C. Massie and J. Rudd. 1984. Metric single-tree weight tables for the Yukon Territory. Inf. Rep. BC-X-250. Environment Canada, Canadian Forestry Service, Pacific Forest Research Centre, Victoria, BC, 60 p.
- McCulloh, K., Sperry, J.S., Lachenbruch, B., Meinzer, F.C., Reich, P.B., and Voelker, S. 2010. Moving water well: comparing hydraulic efficiency in twigs and trunks of coniferous, ring-porous, and diffuse-porous saplings from temperate and tropical forests. *New Phytol.* **186**: 439-450.
- McDowell, N., Barnard, H., Bond, B., Hinckley, T., Hubbard, R., Ishii, H., Kostner, B., Magnani, F., Marshall, J., Meinzer, F., Phillips, N., Ryan, M., and Whitehead, D. 2002. The relationship between tree height and leaf area: sapwood area ratio. *Oecologia* **132**: 12-20.
- Mencuccini, M. 2002. Hydraulic constraints in the functional scaling of trees. *Tree Physiol.* **22**: 553-565.
- Okerblom, P., and Kellomaki, S. 1982. Effect of Angular-Distribution of Foliage on Light-Absorption and Photosynthesis in the Plant Canopy - Theoretical Computations. *Agricultural Meteorology* **26**: 105-116.
- Pinheiro, J., Bates, D., DebRoy, S., Sarkar, D., and R Core Team 2015 nlme: Linear and Nonlinear Mixed Effects Models. R package version 3.1-120.
- R Core Team 2013. R: A Language and Environment for Statistical Computing. R Foundation for Statistical Computing, Vienna, Austria. URL: <http://R-project.org>.

- Robinson, A.P., Duursma, R.A., and Marshall, J.D. 2005. A regression-based equivalence test for model validation: shifting the burden of proof. *Tree Physiol.* **25**: 903-913.
- Ruark, G.A., Martin, G.L., and Bockheim, J.G. 1987. Comparison of Constant and Variable Allometric Ratios for Estimating *Populus Tremuloides* Biomass. *For. Sci.* **33**: 294-300.
- Satoo, T. 1962. Notes on Kittredge's method of estimation of amount of leaves of forest stand. *Jour Japanese Forest Soc* **44**: 267-272.
- Schneider, R., Zhang, S.Y., Swift, D.E., Begin, J., and Lussier, J. 2008. Predicting selected wood properties of jack pine following commercial thinning. *Can. J. of For. Res.* **38**: 2030-2043.
- Schneider, R., Berninger, F., Ung, C., Mäkelä, A., Swift, D.E., and Zhang, S.Y. 2011. Within crown variation in the relationship between foliage biomass and sapwood area in jack pine. *Tree Physiol.* **31**: 22-29.
- Schoonmaker, A.L., Lieffers, V.J., and Landhaeusser, S.M. 2014. Uniform versus Asymmetric Shading Mediates Crown Recession in Conifers. *PLoS One* **9**: e104187.
- Shinozaki, K.K., Yoda, K., Hozumi, K., and Kira, T. 1964. A quantitative analysis of plant form — the pipe model theory. 1. Basic analyses. *Jpn. J. Ecol.* **14**: 97–105.
- Smith, E.A., Collette, S.B., Boynton, T.A., Lillrose, T., Stevens, M.R., Bekker, M.F., Eggett, D., and St Clair, S.B. 2011. Developmental contributions to phenotypic variation in functional leaf traits within quaking aspen clones. *Tree Physiol.* **31**: 68-77.
- Valentine, H.T., Baldwin, V.C., Gregoire, T.G., and Burkhart, H.E. 1994. Surrogates for Foliar Dry-Matter in Loblolly-Pine. *For. Sci.* **40**: 576-585.

- Valentine, H.T., and Mäkelä, A. 2005. Bridging process-based and empirical approaches to modeling tree growth. *In* Tree Physiology, JUL, *Edited by* Anonymous pp. 769-779.
- Waring, R.H., Schroeder, P.E., and Oren, R. 1982. Application of the Pipe Model-Theory to Predict Canopy Leaf-Area. *Can. J. of For. Res.* **12**: 556-560.
- Wellek, S. 2003. Testing statistical hypotheses of equivalence. Chapman and Hall/CRC. 284 pp.
- Whitehead, D. and P.G. Jarvis. 1981. Coniferous forests and plantations. *In* Water Deficits and Plant Growth. Vol. VI. Ed. T.T. Kozlowski. Academic Press, New York, pp 49–152.
- Whitehead, D., Jarvis, P.G., and Waring, R.H. 1984a. Stomatal Conductance, Transpiration, and Resistance to Water-Uptake in a Pinus-Sylvestris Spacing Experiment. *Can. J. of For. Res.* **14**: 692-700.
- Whitehead, D., Edwards, W.R.N., and Jarvis, P.G. 1984b. Conducting Sapwood Area, Foliage Area, and Permeability in Mature Trees of Picea-Sitchensis and Pinus-Contorta. *Can. J. of For. Res.* **14**: 940-947.
- Whitehead, D., and Gower, S.T. 2001. Photosynthesis and light-use efficiency by plants in a Canadian boreal forest ecosystem. *Tree Physiol.* **21**: 925-929.
- Zeide, B., and Pfeifer, P. 1991. A Method for Estimation of Fractal Dimension of Tree Crowns. *For. Sci.* **37**: 1253-1265.

Chapter 5: Conclusion and recommendations

The impetus for this study came from the realization that if the Canadian forest industry were to remain competitive in the global market, changes to the wood fibre chain were needed. This study has begun to address this need by focusing on the forest management end of the fibre chain. Specifically, a model for the prediction of within-tree wood stiffness was presented as were models for the prediction of branch characteristics. Furthermore, functional-structural relationships pertaining to foliage mass, crown length and sapwood area were examined. While the subject material addressed in this thesis is quite diverse, the individual studies are connected in the sense that each is important to the development of decision support tools which have the goal of helping silviculturalists achieve wood quality-based objectives.

The models presented for wood stiffness and branch traits demonstrate that for white spruce and aspen, these characteristics can be effectively predicted using easily measured tree and stand-level variables. Although previous studies, including those by Wang and Micko (1983), Merrill and Mohn (1985), Middleton and Munro (2002) and Tong et al. (2013) had quantified some of these characteristics for white spruce, similar studies on aspen were sparse. Even fewer studies had successfully transferred this knowledge into practical applications through the development of models for the purpose of prediction (e.g., Groot and Schneider 2011). Thus, the models for wood stiffness and branching characteristics presented in this thesis represent an important step forward in terms of managing forests for wood quality based objectives. During the initial stages of planning for this study, the goal was for these models to work in association with the Crobas model in a framework similar to that used by the PipeQual simulator (Mäkinen and Mäkelä

2002). However, the wood stiffness and branch models are constructed in a manner which would allow them to be easily added to existing growth and yield simulators, such as the mixedwood growth model (Bokalo et al. 2013). Doing so would allow the models to be evaluated under a variety of different tree growth scenarios.

With regards to wood stiffness, the results from this study suggest that cambial age and not distance from pith is the main physiological driver behind the development of pith-to-bark trends for both white spruce and aspen. Drawing from arguments presented by Lachenbruch et al. (1995, etc.), this implies that investment into wood stiffness is driven to a greater degree by hydraulic constraints than by mechanical constraints. This is in contrast to the findings by Rosner et al. (2007), where it was reported that hydraulic function was unrelated to the mechanical properties of wood. While the results presented in this thesis do shed light on this debate, it is important to recognize the limitations of the study and the implications which can be drawn. For example, changes in specific hydraulic conductivity, a factor not considered in the current study, may offset increased hydraulic stress that comes with increased tree growth. In such a situation, there would be little or no need to trade-off hydraulic function in favour of mechanical function. Furthermore, one would need to examine the frequency and severity of cavitation under different levels of mechanical stress in order to quantify the consequences of not investing in wood stiffness. Therefore, it is recommended that such measures be collected in future studies so as to further advance our understanding of structural-functional relationships related to wood mechanics in white spruce and aspen.

A more direct result of the findings from Chapter 2 is the recommendation that subsequent models for radial wood stiffness in white spruce and aspen use rings-from-pith as the base

variable. The importance of establishing a base variable (i.e., rings from pith or cambial age) when modeling radial trends for any wood property should not be understated. The failure to do so by several authors in previous studies on specific gravity (cf. Wang and Stewart 2013 with Auty et al. 2014) and wood stiffness (cf. Antony et al. 2012 with Vincent and Duchesne 2014) among others, has likely been a source of seemingly conflicting results. A further recommendation resulting from Chapter 2 is that silvicultural activities that alter slenderness and radial growth rate in white spruce are likely to have the greatest impact on wood stiffness. Conversely, there appears to be little opportunity for silvicultural activities to influence wood stiffness in aspen.

The results from Chapter 3 indicated that individual tree-level variables were the most useful in explaining variation in the branch characteristics which were examined. Furthermore, the findings highlighted that a distinction must be made when using absolute distance from tree apex and relative distance. Within the branch models, use of the former variable confers a greater importance to the effects of branch age relative to branch position. In contrast, the latter variable suggests that both positional and age-related effects are more important.

Many of the tree-level variables used in the branch models suggested that local competition effects had a significant effect on branch characteristics. In general, the trend was for branches to become larger and occur with greater frequency as local competition decreased. Variables which measured competition at the stand level, on the other hand, were not useful. This has importance in terms of how the models should be applied. Specifically, it is recommended that the models be used within individual tree growth simulators which directly measure local competition (e.g., in distance dependent models) or use a proxy for local competition.

The overall performance of the branch models was encouraging. Aside from the frequency of small branches, the variance of the tree-level random effects in the models suggest that heritability is likely an important factor influencing branching in white spruce. Thus, branch models developed for planted white spruce may wish to consider including information pertaining to the genetic stock. Finally, it is recommended that a similar suite of branch models be developed for aspen. The decision to examine only white spruce for the current study was based largely on the high lumber value for this species. Furthermore, linking the branch models to wood quality was far more evident for white spruce given the current grading system which is applied to spruce saw-logs. The use of aspen lumber, however, has begun to gain acceptance in the construction market. For this trend to continue, delivery of a consistent, high quality product is needed. Branch models for aspen will help achieve this goal as they will provide silviculturalists with a tool to identify stands that are likely to provide the quality of wood they require.

Chapter 4 of this thesis examined two of the key structural-functional relationships used in Crobas. Specifically, it was found that a constant allometric relationship could be used to define scaling between foliage mass and crown length for both white spruce and aspen. Furthermore, it was determined that the assumption of a constant relationship between foliage mass and sapwood area at the base of the live crown held reasonably well for spruce. However, a similar assertion for aspen was not possible. Additionally, it was found that scaling at the whole crown level for white spruce was not mirrored by scaling within the crown for the two structural-functional relationships examined. With regards to the foliage mass – sapwood area relationship, adjustments to account for within-crown differences in the ratio have already been proposed.

Specifically, the foliage mass – sapwood area ratio is allowed to vary as a function of whorl age. Therefore, the next logical step for white spruce would be to examine the incremental change in sapwood area and foliage mass between whorls. For aspen, further work will need to be done in order to identify the main sources of variation in sapwood area – foliage mass relationship.

The tests of the structural-functional relationships used by Crobas provided important insight into the allocation of carbon for white spruce and aspen. The tests also served as a first step in the evaluation of the Crobas model for use in mixedwood stands in Northern Alberta. On a practical level, the results were not overly encouraging. Specifically, the confidence intervals on the predictions of foliage mass for any given diameter class were quite large. The results, however, must be placed within context. As a practical tool, Crobas and other process-based models, are most informative when used in conjunction with empirical models. As pointed out by Mäkelä et al. (2000), process-based models may be used to generate projections from a wide area and over a long timeframe. This will provide model users with an idea on how a given characteristic (e.g., foliage mass) will behave on average. Conversely, predictions from empirical models may be used for projections over a smaller area and over a shorter time frame. Valentine and Mäkelä (2005) go on to suggest that projections from empirical models be used to define the limits of acceptable error on projections from process-based models. Viewed in this light, the results presented in Chapter 3 are slightly more encouraging given that for spruce, the structural assumptions of the Crobas model seemed to hold on average.

Presently, there are no process-based models of tree growth which have been calibrated for use in the boreal forest natural region of Alberta. Within Canada, most existing process-based models are only in their infancy. This is an important gap which needs to be filled given the

growing importance of establishing long-term forest planning guidelines (e.g., carbon budgets). For this reason, the evaluation of key structural assumptions in Crobas is an important step forward. As a next step, it is recommended that a more complete evaluation of Crobas be undertaken for white spruce as was done for Jack pine in Eastern Canada (Shcherbinina 2012; Ewen 2013). Given that the sampling for the current study was performed adjacent to permanent sample plots, it would make sense to use the long-term data from these plots when performing such an evaluation.

Bibliography

Achim A, Gardiner BA, Leban J-M, Daquitane R., 2006. Predicting the branching properties of Sitka spruce grown in Great Britain. *NZ J For Sci* 36:246–264

Acuna, M.A., and Murphy, G.E. 2007. Estimating relative log prices of Douglas-fir through a financial analysis of the effects of wood density on lumber recovery and pulp yield. *For. Prod. J.* 57: 60-65.

Akaike H., 1974. A new look at the statistical model identification. *IEEE Trans Autom Control* 19:716–723

Alberta Sustainable Resource Development. 2005. Permanent sample plot field procedures manual. Public Lands and Forest Division, Forest Management Branch, Edmonton, Alberta, 30p.

Alberta Environment and Sustainable Resource Development (ASRD). 2014. Sustainable forest management facts and statistics: Annual allowable cut. ISBN 978-1-4601-1944-0 ISSN 2368-4844. Fall 2014, Environment and sustainable Resourced Development. <http://esrd.alberta.ca/lands-forests/forest-management/forest-management-facts-statistics/default.aspx> Accessed May 2015.

Alemdag, I.S. 1984. Total tree and merchantable stem biomass equations for Ontario hardwoods. *Can. For. Ser. Pi-X-46*, 54 p.

- Alteyrac, J., Cloutier, A., and Zhang, S. 2006. Characterization of juvenile wood to mature wood transition age in black spruce (*Picea mariana* [Mill.] BSP) at different stand densities and sampling heights. *Wood Sci. Technol.* 40: 124-138.
- Alvarez-Clare S. 2005. Biomechanical properties of tropical tree seedlings as a functional correlate of shade tolerance. MSc thesis, University of Florida, Gainesville, FL, USA.
- Amishev, D., and Murphy, G.E. 2009. Estimating breakeven prices for Douglas-fir veneer quality logs from stiffness graded stands using acoustic tools. *For. Prod. J.* 59: 45-52.
- Antony, F., Schimleck, L.R., Jordan, L., Daniels, R.F., and Clark, A., III. 2012. Modeling the effect of initial planting density on within tree variation of stiffness in loblolly pine. *Ann. For. Sci.* 69: 641-650.
- Archer, R.R. 1987. On the origin of growth stresses in trees. Micro mechanics of the developing cambial cell-wall. *Wood Sci. Technol.* 21: 139-154.
- ASTM. 1994. ASTM D-143 standard test methods for small clear specimens of timber. ASTM International, West Conshohocken, Pa.
- Auty, D., and Achim, A. 2008. The relationship between standing tree acoustic assessment and timber quality in Scots pine and the practical implications for assessing timber quality from naturally regenerated stands. *Forestry* 81: 475-487.
- Auty, D., Weiskittel, A.R., Achim, A., Moore, J.R., Gardiner, B.A., 2012. Influence of early re-spacing on Sitka spruce branch structure. *Ann. For. Sci.* 69, 93-104.
- Auty, D., Gardiner, B.A., Achim, A., Moore, J.R., and Cameron, A.D. 2013. Models for predicting microfibril angle variation in Scots pine. *Ann. For. Sci.* 70: 209-218.

- Bates D, Maechler M, Bolker B and Walker S. 2014. *lme4: Linear mixed-effects models using Eigen and S4*. R package version 1.1-7, <http://CRAN.R-project.org/package=lme4>.
- Baldwin, V.C., Peterson, K.D., Burkhart, H.E., Amateis, R.L., and Dougherty, P.M. 1997. Equations for estimating loblolly pine branch and foliage weight and surface area distributions. *Can. J. of For. Res.* 27: 918-927.
- Beckingham, J.D., and Archibald, J.H. 1996. Field guide to ecosites of northern Alberta. Northern Forestry Centre, Forestry Canada, Northwest Region. Spec. Rep. 5.
- Benjamin, J.G., Kershaw, J.A., Jr., Weiskittel, A.R., Chui, Y.H., Zhang, S.Y., 2009. External knot size and frequency in black spruce trees from an initial spacing trial in Thunder Bay, Ontario. *For. Chron.* 85, 618-624.
- Bergqvist, G. 1999. Stand and wood properties of boreal Norway spruce growing under birch shelter. *Acta Universitatis Agriculturae Sueciae – Silvestria*, Issue: 108, 85 pp.
- Berninger, F., and Nikinmaa, E. 1994. Foliage area – sapwood area relationships of Scots pine (*Pinus sylvestris*) trees in different climates. *Can. J. For. Res.* 24: 2263-2268.
- Berninger, F., Coll, L., Vanninen, P., Mäkelä, A., Palmroth, S., and Nikinmaa, E. 2005. Effects of tree size and position on pipe model ratios in Scots pine. *Can. J. of For. Res.* 35: 1294-1304.
- Boatright, S. W. J. and Garrett, G. G. 1979. The effects of knots on the fracture strength of wood - I. A review of methods of assessment. *Holzforschung* 33-3, pp. 58-72.
- Bokalo, M., Stadt, K.J., Comeau, P.G., Titus, S.J., 2010. Mixedwood Growth Model (MGM) (version MGM2010.xls). University of Alberta, Edmonton, Alberta, Canada. 2010.

Available online: <http://www.rr.ualberta.ca/Research/MixedwoodGrowthModel.aspx>.
(accessed on 7 July 2011).

- Bokalo, M., Stadt, K.J., Comeau, P.G., Titus, S.J., 2013. The Validation of the Mixedwood Growth Model (MGM) for Use in Forest Management Decision Making. *Forests* 4, 1-27.
- Bolker, B.M., Brooks, M.E., Clark, C.J., Geange, S.W., Poulsen, J.R., Stevens, M.H.H., White, J.S., 2009. Generalized linear mixed models: a practical guide for ecology and evolution. *Trends in Ecology & Evolution* 24, 127-135.
- Bond, B.J., 2000. Age-related changes in photosynthesis of woody plants. *Trends in plant science. Reviews*. Vol 5, No. 8: 349-353.
- Briggs, G.E. 1925. Plant yield and the intensity of external factors – Mitscherlich's 'Wirkungsgesetz'. *Annals of Botany*, Vol 39: 475-502
- Bruechert, F., and Gardiner, B. 2006. The effect of wind exposure on the tree aerial architecture and biomechanics of sitka spruce (*Picea sitchensis*, Pinaceae). *Am. J. Bot.* 93: 1512-1521.
- Burnham KP, Anderson DR., 2002. Model selection and multimodel inference: a practical information-theoretic approach. Springer, New York
- Carmean, W. 1972. Site Index Curves for Upland Oaks in Central States. *For. Sci.* 18: 109-120.
- Castéra, P., Faye, C., and El Ouadrani, A. 1996. Previsions of the bending strength of timber with a multivariate statistical approach. *Ann. For. Sci.* 53: 885-896.
- Cave, I.D., and Walker, J.C.F. 1994. Stiffness of wood in fast-grown plantation softwoods - the influence of microfibril angle. *For. Prod. J.* 44: 43-48.

- Ceulemans, R., Stettler, R., Hinckley, T., Iserbrands, J., and Heilman, P. 1990. Crown architecture of *Populus* clones as determined by branch orientation and branch characteristics. *Tree Physiol.* 7: 157-167.
- Colin, F., and Houllier, F. 1991. Branchiness of Norway spruce in North-Eastern France - modeling vertical trends in maximum nodal branch size. *Ann. For. Sci.* 48: 679-693.
- Colin, F., Houllier, F., 1992. Branchiness of Norway Spruce in Northeastern France - predicting the main crown characteristics from usual tree measurements. *Ann. Sci. For.* 49, 511-538.
- Cowdrey, D.R. and Preston, R.D. 1966. Elasticity and microfibrillar angle in the wood of Sitka spruce. *Proceedings from the Royal Society of London. Series B, Biological Sciences.* 66: 245-272
- Cown, D.J., Hebert J., Ball R. 1999. Modelling *Pinus radiata* lumber characteristics. Part 1: mechanical properties of small clears. *NZ J For Sci* 29:203–213.
- Coyea, M.R., and Margolis, H.A. 1992. Factors affecting the relationship between sapwood Area and leaf-area of balsam fir. *Can. J. of For. Res.* 22: 1684-1693.
- Davidson, R.L. 1969. Effect of root/leaf temperature differentials on root/shoot ratios in some pasture grasses and clover. *Annals of Botany* 33: 561-569.
- De Boever, L., Vansteenkiste, D., Van Acker, J., and Stevens, M. 2007. End-use related physical and mechanical properties of selected fast-growing poplar hybrids (*Populus trichocarpa* x *P-deltoides*). *Ann. For. Sci.* 64: 621-630.
- Downes, G.M., Drew, D., Battaglia, M., and Schulze, D. 2009. Measuring and modelling stem growth and wood formation: An overview. *Dendrochronologia* 27: 147-157.

- Duchateau, E., Longuetaud, F., Mothe, F., Ung, C., Auty, D., Achim, A., 2013. Modelling knot morphology as a function of external tree and branch attributes. *Can. J. For. Res.* 43: 266-277.
- Duursma, R.A., Mäkelä, A., Reid, D.E.B., Jokela, E.J., Porte, A.J., and Roberts, S.D. 2010. Self-shading affects allometric scaling in trees. *Funct. Ecol.* 24: 723-730.
- Dyer, M., and Bailey, R. 1987. A test of 6 methods for estimating true heights from stem analysis data. *For. Sci.* 33: 3-13.
- Eckmullner, O., and Sterba, H. 2000. Crown condition, needle mass, and sapwood area relationships of Norway spruce (*Picea abies*). *Can. J. of For. Res.* 30: 1646-1654.
- Evans, R., and Ilic, J. 2001. Rapid prediction of wood stiffness from microfibril, angle and density. *For. Prod. J.* 51: 53-57.
- Forest Products Laboratory. 2010. Wood handbook—Wood as an engineering material. General Technical Report FPL-GTR-190. Madison, WI: U.S. Department of Agriculture, Forest Service, Forest Products Laboratory. 508 p.
- FPInnovations 2009. Wood market statistics including pulp and paper in Alberta. 2009 Edition. Compiled by Rhonda Lindenbach-Gibson and James Poon, for FPInnovations, Point-Claire, QC and Vancouver, BC.
- Garber, S., Maguire, D., 2005. Vertical trends in maximum branch diameter in two mixed-species spacing trials in the central Oregon Cascades. *Can. J. For. Res.* 35: 295-307.

- Gartner, B.L. 1995. Patterns of xylem variation within a tree and their hydraulic and mechanical consequences. In B. L. Gartner, ed. *Plant Stems: Physiology and Functional Morphology*, pp. 125-149. Academic Press, San Diego, CA.
- Gartner, B.L., Lei, H., and Milota, M.R. 1997. Variation in the anatomy and specific gravity of wood within and between trees of red alder (*Alnus rubra* Bong). *Wood Fiber Sci.* 29: 10-20.
- Geron, C.D., and Ruark, G.A. 1988. Comparison of constant and variable allometric ratios for predicting foliar biomass of various Tree genera. *Can. J. of For. Res.* 18: 1298-1304.
- Gilmore, D.W., Seymour, R.S., and Maguire, D.A. 1996. Foliage-sapwood area relationships for *Abies balsamea* in central Maine, USA. *Can. J. of For. Res.* 26: 2071-2079.
- Goudie, J.W., and Parish R., 2008. Modelling the impact of silviculture treatments on the wood quality of interior spruce. http://www.for.gov.bc.ca/hfd/library/FIA/2008/FSP_Y081078a.pdf (5 May 2008) [accessed Aug 26, 2013].
- Groot, A. and Schneider, R. 2011. Predicting maximum branch diameter from crown dimensions, stand characteristics and tree species. *The Forestry Chronicle* 7: 542-551.
- Grossnickle SC. 2000. *Ecophysiology of northern spruce species: the performance of planted seedlings*. Ottawa: NRC Research Press.
- Hargrave, K., Kolb, K., Ewers, F., and Davis, S. 1994. Conduit Diameter and Drought-Induced Embolism in *Salvia-Mellifera* Greene (Labiatae). *New Phytol.* 126: 695-705.

- Heger, L. 1971. Site-index/soil relationships for white spruce in Alberta Mixedwoods. Canadian Forestry Service, Information Report FMR-X-32, Project 31. Forest Management Institute, Ottawa, ON. 15 p.
- Hein, S., Mäkinen, H., Yue, C., Kohnle, U., 2007. Modelling branch characteristics of Norway spruce from wide spacings in Germany. *For. Ecol. Manage.* 242, 155-164.
- Houllier, F., Leban, J.M., and Colin, F. 1995. Linking Growth Modeling to Timber Quality Assessment for Norway Spruce. *For. Ecol. Manage.* 74: 91-102.
- Ilomäki, S., Nikinmaa, E., and Mäkelä, A. 2003. Crown rise due to competition drives biomass allocation in silver birch. *Can. J. of For. Res.* 33: 2395-2404.
- Ishii, H., McDowell, N., 2002. Age-related development of crown structure in coastal Douglas-fir trees. *For. Ecol. Manage.* 169, 257-270.
- Jordan, L., Re, R., Hall, D.B., Clark, Alexander, III, and Daniels, R.F. 2006. Variation in loblolly pine cross-sectional microfibril angle with tree height and physiographic region. *Wood Fiber Sci.* 38: 390-398.
- Kabzems, R., A.L. Nemeč, and C. Farnden. 2007. Growing trembling aspen and white spruce intimate mixtures: Early results (13–17 years) and future projections. *BC Journal of Ecosystems and Management* 8(1):1–14.
- Kaipainen, L.; Hari, P., 1985: Consistencies in the structure of Scots pine. Crop physiology of forest trees. Proceedings of an international conference on managing forest trees as cultivated plants, held in Finland, 23-28 July 1984: 31-37

- Kantola, A., and Mäkelä, A. 2004. Crown development in Norway spruce [*Picea abies* (L.) Karst.]. *Trees-Structure and Function* 18: 408-421.
- Kantola, A., and Mäkelä, A. 2006. Development of biomass proportions in Norway spruce (*Picea abies* [L.] Karst.). *Trees-Structure and Function* 20: 111-121.
- Kantola, A., Mäkinen, H., and Mäkelä, A. 2007. Stem form and branchiness of Norway spruce as a sawn timber - Predicted by a process based model. *For. Ecol. Manage.* 241: 209-222.
- Kliger, I.R., Perstorper, M., and Johansson, G. 1998. Bending properties of Norway spruce timber. Comparison between fast- and slow-grown stands and influence of radial position of sawn timber. *Ann. Sci. For.* 55: 349-358.
- Kojima, M., Yamamoto, H., Yoshida, M., Ojio, Y., and Okumura, K. 2009. Maturation property of fast-growing hardwood plantation species: A view of fiber length. *For. Ecol. Manage.* 257: 15-22.
- Koubaa, A., Hernandez, R.E., Beaudoin, M., and Poliquin, J. 1998. Interclonal, intraclonal, and within-tree variation in fiber length of poplar hybrid clones. *Wood Fiber Sci.* 30: 40-47.
- Kubo, T., and Koyama, M. 1993. Maturation Rate of Tracheid Lengthening in Slow-Grown Young Sugi (*Cryptomeria-Japonica*) Trees. *Iawa Journal* 14: 267-272.
- Lachenbruch, B., Moore, J.R., and Evans, R. 2011. Radial Variation in Wood Structure and Function in Woody Plants, and Hypotheses for Its Occurrence.
- Landsberg, J.J., and Sands, P. 2010. *Physiological Ecology of Forest Production: Principles, Processes and Models*; Academic Press (Elsevier): New York, NY, USA, 2010.

- Leban, J.M., and Haines, D.W. 1999. The modulus of elasticity of hybrid larch predicted by density, rings per centimeter, and age. *Wood Fiber Sci.* 31: 394-402.
- Lehtonen, A. 2005. Estimating foliage biomass in Scots pine (*Pinus sylvestris*) and Norway spruce (*Picea abies*) plots. *Tree Physiol.* 25: 803-811.
- Lenz, P., Cloutier, A., MacKay, J., and Beaulieu, J. 2010. Genetic control of wood properties in *Picea glauca* - an analysis of trends with cambial age. *Can. J. For. Res.* 40: 703-715.
- Liang Shan-qing, and Fu Feng. 2007. Comparative study on three dynamic modulus of elasticity and static modulus of elasticity for Lodgepole pine lumber. *Journal of Forestry Research (Harbin)* 18: 309-312.
- Lieffers, V.J., and Stadt, K.J. 1994. Growth of Understory *Picea-Glauca*, *Calamagrostis-Canadensis*, and *Epilobium-Angustifolium* in Relation to Overstory Light Transmission. *Can. J. of For. Res.* 24: 1193-1198.
- Lundgren, C. 2004. Microfibril angle and density patterns of fertilized and irrigated Norway spruce. *Silva Fenn.* 38: 107-117.
- Lyhykainen, H.T., Mäkinen, H., Mäkelä, A., Pastila, S., Heikkila, A., and Usenius, A. 2009. Predicting lumber grade and by-product yields for Scots pine trees. *For. Ecol. Manage.* 258: 146-158.
- Machado, S.d.A., Rodrigues da Silva, L.C., Figura, M.A., Teo, S.J., and Mendes Nascimento, R.G. 2010. Comparison of methods for estimating heights from complete stem analysis data for *Pinus taeda*. *Ciencia Florestal* 20: 45-55.

- Maguire, D., Moeur, M., Bennett, W., 1994. Models for Describing Basal Diameter and Vertical-Distribution of Primary Branches in Young Douglas-Fir. *For. Ecol. Manage.* 63, 23-55.
- Mäkelä, A. 1986. Implications of the Pipe Model-Theory on Dry-Matter Partitioning and Height Growth in Trees. *J. Theor. Biol.* 123: 103-120.
- Mäkelä, A., and Sievänen, R. 1992. Height Growth Strategies in Open-Grown Trees. *J. Theor. Biol.* 159: 443-467.
- Mäkelä, A. 1997. A carbon balance model of growth and self-pruning in trees based on structural relationships. *For. Sci.* 43: 7-24.
- Mäkelä, A., and Vanninen, P. 1998. Impacts of size and competition on tree form and distribution of aboveground biomass in Scots pine. *Can. J. of For. Res.* 28: 216-227.
- Mäkelä, A., and Vanninen, P. 2001. Vertical structure of Scots pine crowns in different age and size classes. *Trees-Structure and Function* 15: 385-392.
- Mäkelä, A. 2002. Derivation of stem taper from the pipe theory in a carbon balance framework. *Tree Physiol.* 22: 891-905.
- Mäkelä, A., and Mäkinen, H. 2003. Generating 3D sawlogs with a process-based growth model. *For. Ecol. Manage.* 184: 337-354.
- Mäkelä, A., and Valentine, H.T. 2006. Crown ratio influences allometric scaling in trees. *Ecology* 87: 2967-2972.
- Mäkinen, H., Colin, F., 1999. Predicting the number, death, and self-pruning of branches in Scots pine. *Can. J. For. Res.* 29: 1225-1236.

- Mäkinen, H., Saranpää, P., and Linder, S. 2001. Effect of nutrient optimization on branch characteristics in *Picea abies* (L.) Karst. *Scand. J. For. Res.* 16: 354-362.
- Mäkinen, H., Mäkelä, A., and Hynynen, J. 2009. Predicting Wood and Branch Properties of Norway Spruce as a Part of a Stand Growth Simulation System. U S Forest Service Pacific Northwest Research Station General Technical Report PNW-GTR 15-21.
- Manning, G.H., M.R.C. Massie and J. Rudd. 1984. Metric single-tree weight tables for the Yukon Territory. Inf. Rep. BC-X-250. Environment Canada, Canadian Forestry Service, Pacific Forest Research Centre, Victoria, BC, 60 p.
- Matyas, C., and Peszlen, I. 1997. Effect of age on selected wood quality traits of poplar clones. *Silvae Genet.* 46: 64-72.
- McCulloh, K., Sperry, J.S., Lachenbruch, B., Meinzer, F.C., Reich, P.B., and Voelker, S. 2010. Moving water well: comparing hydraulic efficiency in twigs and trunks of coniferous, ring-porous, and diffuse-porous saplings from temperate and tropical forests. *New Phytol.* 186: 439-450.
- McDowell, N., Barnard, H., Bond, B., Hinckley, T., Hubbard, R., Ishii, H., Kostner, B., Magnani, F., Marshall, J., Meinzer, F., Phillips, N., Ryan, M., and Whitehead, D. 2002. The relationship between tree height and leaf area: sapwood area ratio. *Oecologia* 132: 12-20.
- Megraw, RA, Bremer, D, Leaf, G, & Roers, J. 1999. Stiffness in Loblolly Pine as a Function of Ring Position and Height, and its Relationship to Microfibril Angle and Specific Gravity (IUFRO Workshop S5.01.04, La Londe-Les-Meures, pp. 341–349)

- Mencuccini, M., and Grace, J. 1996. Developmental patterns of above-ground hydraulic conductance in a Scots pine (*Pinus sylvestris* L) age sequence. *Plant Cell and Environment* 19: 939-948.
- Mencuccini, M. 2002. Hydraulic constraints in the functional scaling of trees. *Tree Physiol.* 22: 553-565.
- Merrill, R., and Mohn, C. 1985. Heritability and Genetic Correlations for Stem Diameter and Branch Characteristics in White Spruce. *Can. J. For Res.* 15: 494-497.
- Middleton, G. R. and Munro, B. D. 2002. Wood density of Alberta white spruce - Implications for silvicultural practices. Forintek Canada Corp. Vancouver, BC. 66p.
- Mitchell, K. 1975. Dynamics and Simulated Yield of Douglas-Fir. *For. Sci.* 1-39.
- Mochan, S., Connolly, T. and Moore, J. 2009. Using Acoustic Tools in Forestry and the Wood Supply Chain. Edinburgh: Forestry Commission, Sep. 2009. Technical Note. 6 p.
- Natural Regions Committee 2006. Natural Regions and Subregions of Alberta. Compiled by D.J. Downing and W.W. Pettapiece. Government of Alberta. Pub. No. T/852.
- Navratil, S. and Bella, I. E. 1988. Regeneration, development and density management in aspen stands. Northern Forestry Centre, Forestry Canada, 5320 - 122 st., Edmonton, Alberta, T6H 3S5
- Nemec, A.F.L., Parish, R., Goudie, J.W., 2012. Modelling number, vertical distribution, and size of live branches on coniferous tree species in British Columbia. *Can. J. For. Res* 42, 1072-1090.

- Nikinmaa, E. 1992. Analyses of the growth of Scots pine: Matching structure with function. *Acta For. Fenn.* 235: 1-68.
- Niklas, K.J., and Spatz, H. 2010. Worldwide Correlations of Mechanical Properties and Green Wood Density. *Am. J. Bot.* 97: 1587-1594.
- NLGA 2003. Standard grading rules for Canadian lumber. National Lumber Grades Authority, New Westminster, British Columbia, Canada
- Okerblom, P., and Kellomaki, S. 1982. Effect of Angular-Distribution of Foliage on Light-Absorption and Photosynthesis in the Plant Canopy - Theoretical Computations. *Agricultural Meteorology* 26: 105-116.
- Ondro, W.J. 1991. Present trends and future prospects for poplar utilization in Alberta. *For. Chron.* 67: 271-274
- Opio, C., Jacob, N., and Coopersmith, D. 2000. Height to diameter ratio as a competition index for young conifer plantations in northern British Columbia, Canada. *For. Ecol. Manage.* 137: 245-252
- Panshin, A.J., de Zeeuw, C., 1980. *Textbook of Wood Technology*. McGraw-Hill Book Company, New York.
- Park, Y., Weng, Y., and Mansfield, S.D. 2012. Genetic effects on wood quality traits of plantation-grown white spruce (*Picea glauca*) and their relationships with growth. *Tree Genetics & Genomes* 8: 303-311.

- Peng, M., and Stewart, J.D. 2013. Development, validation, and application of a model of intra- and inter-tree variability of wood density for lodgepole pine in western Canada. *Can. J. For. Res.* 43: 1172-1180.
- Perala, D. A. 1990. *Populus tremuloides*. Michx. Quaking aspen. Pp. 555-569, IN: R.M. Burns and B.H. Honkala. *Silvics of North America. Volume 2. Hardwoods.* USDA Forest Service Agric. Handbook 654, Washington, D.C. http://willow.ncfes.umn.edu/silvics_manual/Volume_2/populus/tremuloides.htm Accessed May 2015.
- Peterson, E.B. and Peterson, N.M. 1992. Ecology, management, and use of aspen and balsam poplar in the prairie provinces, Canada. *For. Can., Northwest Reg., North. For. Cent., Edmonton, Alberta. Spec. Rep. 1.*
- Pinheiro, J.C., and Bates, D.M. 2000. *Mixed-effects models in S and S-PLUS.* Statistics and Computing Series, Springer-Verlag, New York.
- Pinheiro, J.C., Bates, D.M., DebRoy, S., Sarkar, D., and the R Development Core Team 2013. nlme: Linear and Nonlinear Mixed Effects Models. R package version 3.1-109. Available from www.R-project.org [accessed May 27, 2013).
- Pinheiro, J., Bates, D., DebRoy, S., Sarkar, D., and R Core Team 2015 nlme: Linear and Nonlinear Mixed Effects Models. R package version 3.1-120.
- Pokharel, B., Dech, J.P., Groot, A., and Pitt, D. 2014. Ecosite-based predictive modeling of black spruce (*Picea mariana*) wood quality attributes in boreal Ontario. *Can. J. For. Res.* 44: 465-475.

- R Core Team. 2012. R: a language and environment for statistical computing. R Foundation for Statistical Computing, Vienna, Austria. ISBN 3-900051-07-0. Available from www.R-project.org [accessed May 27, 2013].
- R Core Team 2013. R: A Language and Environment for Statistical Computing. R Foundation for Statistical Computing, Vienna, Austria. URL: <http://R-project.org>.
- Rais, A., Poschenrieder, W., Pretzsch, H., and van de Kuilen, J.G. 2014. Influence of initial plant density on sawn timber properties for Douglas-fir (*Pseudotsuga menziesii* (Mirb.) Franco). *Ann. For. Sci.* 71: 617-626.
- Reid, D.E.B., Young, S., Tong, Q., Zhang, S.Y., and Morris, D.M. 2009. Lumber grade yield, and value of plantation-grown black spruce from 3 stands in northwestern Ontario. *For. Chron.* 85: 609-617.
- Ricardo, P., Hein, G., and Lima, J.T. 2012. Relationship between microfibril angle, modulus of elasticity and compressive strength in Eucalyptus wood. *Ciencia y tecnologia*, 14: 267-274.
- Robinson, A.P., Duursma, R.A., and Marshall, J.D. 2005. A regression-based equivalence test for model validation: shifting the burden of proof. *Tree Physiol.* 25: 903-913.
- Rosner, S., Klein, A., Muller, U., and Karlsson, B. 2008. Tradeoffs between hydraulic and mechanical stress responses of mature Norway spruce trunk wood. *Tree Physiol.* 28: 1179-1188.
- Ruark, G.A., Martin, G.L., and Bockheim, J.G. 1987. Comparison of Constant and Variable Allometric Ratios for Estimating *Populus Tremuloides* Biomass. *For. Sci.* 33: 294-300.

- Samson, M., and Blanchet, L. 1992. Effect of Knots on the Flatwise Bending Stiffness of Lumber Members. *Holz Als Roh-Und Werkstoff* 50: 148-152.
- Satoo, T. 1962. Notes on Kittredge's method of estimation of amount of leaves of forest stand. *Jour Japanese Forest Soc* 44: 267-272.
- Schneider, R., Zhang, S.Y., Swift, D.E., Begin, J., and Lussier, J. 2008. Predicting selected wood properties of jack pine following commercial thinning. *Can. J. For. Res.* 38: 2030-2043.
- Schneider, R., Berninger, F., Ung, C., Mäkelä, A., Swift, D.E., and Zhang, S.Y. 2011. Within crown variation in the relationship between foliage biomass and sapwood area in jack pine. *Tree Physiol.* 31: 22-29.
- Schoonmaker, A.L., Lieffers, V.J., and Landhaeusser, S.M. 2014. Uniform versus Asymmetric Shading Mediates Crown Recession in Conifers. *PLoS One* 9: e104187.
- Shcherbinina, A. 2012. Validation of the jack pine version of Crobas-Pipequal. Master thesis, University of British Columbia, Vancouver, Canada.
- Shinozaki, K.K., Yoda, K., Hozumi, K., and Kira, T. 1964. A quantitative analysis of plant form — the pipe model theory. 1. Basic analyses. *Jpn. J. Ecol.* 14: 97–105.
- Smith, E.A., Collette, S.B., Boynton, T.A., Lillrose, T., Stevens, M.R., Bekker, M.F., Eggett, D., and St Clair, S.B. 2011. Developmental contributions to phenotypic variation in functional leaf traits within quaking aspen clones. *Tree Physiol.* 31: 68-77.
- Steffenrem, A., Lindland, F., and Skroppa, T. 2008. Genetic and environmental variation of internodal and whorl branch formation in a progeny trial of *Picea abies*. *Scand. J. For. Res.* 23: 290-298.

- Steffenrem, A., Kvaalen, H., Hoibo, O.A., Edvardsen, O.M., and Skroppa, T. 2009. Genetic variation of wood quality traits and relationships with growth in *Picea abies*. *Scand. J. For. Res.* 24: 15-27.
- Sustainable Resource Development (SRD), 2009. Sustainable Forest Management: Current Facts and Statistics. ISBN No. 978-0-7785-8722-4 No. I/398. August 2009.
- Temesgen, H., LeMay, V., Mitchell, S., 2005. Tree crown ratio models for multi-species and multi-layered stands of southeastern British Columbia. *For. Chron.* 81, 133-141.
- Trincado, G., and Burkhart, H.E. 2009. A framework for modeling the dynamics of first-order branches and spatial distribution of knots in loblolly pine trees. *Can. J. For. Res. -Rev. Can. Rech. For.* 39: 566-579.
- Thorpe, H.C., Astrup, R., Trownbridge, A. and Coates, K.D., 2010. Competition and tree crowns: A neighborhood analysis of three boreal tree species. *For. Ecol. and Manage.* 259: 1586-1596.
- Tong, Q., Duchesne, I., Belley, D., Beaudoin, M., Swift, E., 2013. Characterization of Knots in Plantation White Spruce. *Wood Fiber Sci.* 45, 84-97.
- Tyree, M.T., Davis, S.D., and Cochard, H. 1994. Biophysical Perspectives of Xylem Evolution - is there a Tradeoff of Hydraulic Efficiency for Vulnerability to Dysfunction. *Iawa Journal* 15: 335-360.
- Valentine, H.T., Baldwin, V.C., Gregoire, T.G., and Burkhart, H.E. 1994. Surrogates for Foliar Dry-Matter in Loblolly-Pine. *For. Sci.* 40: 576-585.

- Valentine, H.T., and Mäkelä, A. 2005. Bridging process-based and empirical approaches to modeling tree growth. In *Tree Physiology*, JUL, Edited by Anonymous pp. 769-779.
- Van Gelder, H. A., Poorter, L., and Sterck, F.J. 2006. Wood mechanics, allometry, and life-history variation in a tropical rain forest tree community. *New Phytologist* 171: 367-378.
- Venables, W.N. and Ripley, B.D., 2002. *Modern Applied Statistics with S, Fourth Edition*. New York: Springer.
- Waghorn, M.J., Watt, M.S., and Mason, E.G. 2007. Influence of tree morphology, genetics, and initial stand density on outerwood modulus of elasticity of 17-year-old *Pinus radiata* RID C-3813-2009. *For. Ecol. Manage.* 244: 86-92.
- Walker, J.C.F. 2006. *Primary wood processing: principles and practice*.
- Wang, E.I.C., and Micko, M.M. 1984. Wood quality of white spruce from north central Alberta. *Can. J. For. Res.* 14: 181-185.
- Wang, Y., Titus, S.J., and LeMay, V.M. 2000. Relationships between tree slenderness coefficients and tree or stand characteristics for major species in boreal mixedwood forests. *Can. J. For. Res.* 28: 1171-1183.
- Waring, R.H., Schroeder, P.E., and Oren, R. 1982. Application of the Pipe Model-Theory to Predict Canopy Leaf-Area. *Can. J. of For. Res.* 12: 556-560.
- Watt, M.S., and Zoric, B. 2010. Development of a model describing modulus of elasticity across environmental and stand density gradients in plantation-grown *Pinus radiata* within New Zealand. *Can. J. For. Res.* 40: 1558-1566.

- Watt, M.S., Zoric, B., Kimberley, M.O., and Harrington, J. 2011. Influence of stocking on radial and longitudinal variation in modulus of elasticity, microfibril angle, and density in a 24-year-old *Pinus radiata* thinning trial. *Can. J. For. Res.* 41: 1422-1431.
- Wellek, S. 2003. Testing statistical hypotheses of equivalence. Chapman and Hall/CRC. 284 pp.
- Weiskittel, A.R., Maguire, D.A., Monserud, R.A., 2007a. Response of branch growth and mortality to silvicultural treatments in coastal Douglas-fir plantations: Implications for predicting tree growth. *For. Ecol. Manage.* 251, 182-194.
- Weiskittel, A.R., Maguire, D.A., Monserud, R.A., 2007b. Modeling crown structural responses to competing vegetation control, thinning, fertilization, and Swiss needle cast in coastal Douglas-fir of the Pacific Northwest, USA. *For. Ecol. Manage.* 245, 96-109.
- Weiskittel, A.R., Seymour, R.S., Hofmeyer, P.V. and Kershaw, J.A. Jr., 2010. Modelling primary branch frequency and size for five conifer species in Maine, USA. *For. Ecol. and Manage.* 259: 1912-1921.
- Whitehead, D. and P.G. Jarvis. 1981. Coniferous forests and plantations. In *Water Deficits and Plant Growth*. Vol. VI. Ed. T.T. Kozlowski. Academic Press, New York, pp 49–152.
- Whitehead, D., Jarvis, P.G., and Waring, R.H. 1984a. Stomatal Conductance, Transpiration, and Resistance to Water-Uptake in a *Pinus Sylvestris* Spacing Experiment. *Can. J. of For. Res.* 14: 692-700.

- Whitehead, D., Edwards, W.R.N., and Jarvis, P.G. 1984b. Conducting Sapwood Area, Foliage Area, and Permeability in Mature Trees of *Picea-Sitchensis* and *Pinus-Contorta*. *Can. J. of For. Res.* 14: 940-947.
- Whitehead, D., and Gower, S.T. 2001. Photosynthesis and light-use efficiency by plants in a Canadian boreal forest ecosystem. *Tree Physiol.* 21: 925-929.
- Wolcott, M.P., Shepard, R.K., and Shottafer, J.E. 1987. Age and thinning effects on wood properties of red spruce (*Picea rubens* Sarg.). Technical Bulletin - Maine Agricultural Experiment Station iv + 17 pp.-iv + 17 pp.
- Wykoff, W.R., Crookston, N.L., and Stage, A.R., 1982. User's guide to the stand prognosis model. USDA For. Serv. Gen. Tech. Rep. INT-133.
- Wykoff, W.R., 1986. Supplement to the User's Guide for the Stand Prognosis Model – Version 5.0. Gen. Tech. Rep. INT-208. USDA For. Serv., Ogden, UT. 36 p.
- Yamamoto H, Yoshida M, Okuyama T., 2002. Growth stress controls negative gravitropism in woody plant stems. *Planta* 216: 280–292.
- Yu, Q., Zhang, S.Y., Pliura, A., MacKay, J., Bousquet, J., and Perinet, P. 2008. Variation in mechanical properties of selected young poplar hybrid crosses. *For. Sci.* 54: 255-259.
- Zeide, B., and Pfeifer, P. 1991. A Method for Estimation of Fractal Dimension of Tree Crowns. *For. Sci.* 37: 1253-1265.

Zhang, S.Y., Chauret, G., Ren, H.Q.Q., and Desjardins, R. 2002. Impact of initial spacing on plantation black spruce lumber grade yield, bending properties, and MSR yield. *Wood Fiber Sci.* 34: 460-475.

Zimmermann, M.H. 1983. *Xylem structure and the ascent of sap*. Berlin; Springer-Verlag.